

## TOPICAL REVIEW

## Rare region effects at classical, quantum, and nonequilibrium phase transitions

Thomas Vojta

Department of Physics, University of Missouri - Rolla, Rolla, MO 65409, USA

**Abstract.** Rare regions, i.e., rare large spatial disorder fluctuations, can dramatically change the properties of a phase transition in a quenched disordered system. In generic classical equilibrium systems, they lead to an essential singularity, the so-called Griffiths singularity, of the free energy in the vicinity of the phase transition. Stronger effects can be observed at zero-temperature quantum phase transitions, at nonequilibrium phase transitions, and in systems with correlated disorder. In some cases, rare regions can actually completely destroy the sharp phase transition by smearing.

This topical review presents a unifying framework for rare region effects at weakly disordered classical, quantum, and nonequilibrium phase transitions based on the effective dimensionality of the rare regions. Explicit examples include disordered classical Ising and Heisenberg models, insulating and metallic random quantum magnets, and the disordered contact process.

PACS numbers: 05.70.Jk, 05.50.+q, 64.60.Ak, 64.60.Ht

Submitted to: *J. Phys. A: Math. Gen.*

## Contents

<b>1</b>	<b>Preamble</b>	<b>2</b>
<b>2</b>	<b>Phase transitions and critical behavior</b>	<b>4</b>
2.1	Landau theory . . . . .	4
2.2	Scaling and the renormalization group . . . . .	5
2.3	Classical versus quantum phase transitions . . . . .	7
2.4	Finite-size scaling . . . . .	8
<b>3</b>	<b>Quenched disorder effects</b>	<b>9</b>
3.1	Average disorder and Harris criterion . . . . .	10
3.2	Rare regions and Griffiths effects . . . . .	11
3.3	A classification of rare region effects . . . . .	13
3.3.1	Class A: . . . . .	14
3.3.2	Class B: . . . . .	14
3.3.3	Class C: . . . . .	15

<b>4</b>	<b>Classical phase transitions</b>	<b>15</b>
4.1	Randomly diluted Ising model . . . . .	15
4.2	Optimal fluctuation theory . . . . .	17
4.3	Random- $T_c$ Landau-Ginzburg-Wilson theory . . . . .	18
4.4	Dynamic rare region effects . . . . .	19
4.5	Disorder correlations and enhanced rare region effects . . . . .	21
4.6	Smearred phase transition in an Ising model with planar defects . . . . .	23
4.7	Optimal fluctuation theory for smearred phase transition . . . . .	24
4.8	Dynamics at a smearred phase transition . . . . .	27
<b>5</b>	<b>Quantum phase transitions</b>	<b>28</b>
5.1	Random transverse field Ising model . . . . .	28
5.2	Quantum Griffiths singularities: Optimal fluctuation arguments . . . . .	29
5.3	Strong-disorder renormalization group and infinite-randomness critical point in one dimension . . . . .	32
5.4	Higher dimensions and other generalizations . . . . .	35
5.5	Continuous symmetry quantum magnets . . . . .	37
5.6	Itinerant quantum magnets . . . . .	41
5.7	Quantum Griffiths effects in other systems . . . . .	44
<b>6</b>	<b>Nonequilibrium phase transitions</b>	<b>45</b>
6.1	Contact process . . . . .	46
6.2	Contact process with uncorrelated disorder . . . . .	48
6.2.1	Griffiths singularities: Optimal fluctuation arguments. . . . .	48
6.2.2	Strong-disorder renormalization group. . . . .	49
6.2.3	Computer simulations. . . . .	51
6.2.4	Contact process on a randomly diluted lattice. . . . .	52
6.3	Contact process with extended defects . . . . .	53
6.4	Other nonequilibrium systems . . . . .	56
<b>7</b>	<b>Discussion and conclusions</b>	<b>56</b>
7.1	Summary: Classification of rare region effects . . . . .	56
7.2	Experiments . . . . .	59
7.2.1	Classical phase transitions. . . . .	59
7.2.2	Quantum phase transitions. . . . .	60
7.2.3	Nonequilibrium phase transitions. . . . .	61
7.3	Conclusions . . . . .	61

**1. Preamble**

Phase transitions belong to the most fascinating phenomena in nature. The large scale structure of the universe is the result of a series of phase transitions during the early stages of its development. At low temperatures, quantum phase transitions between different ground states lead to unconventional behavior and exotic new phases of matter. Phase transitions also occur between nonequilibrium states, e.g., during growth processes or chemical reactions. Even our everyday life is unimaginable without the never ending transformations of water between ice, liquid and vapor.

Under normal conditions, the phase transitions of water are so-called first-order transitions. At these transitions, the two phases coexist at the transition point, and

a finite amount of heat (the latent heat) is released when going from one phase to the other. Transitions that do not involve phase coexistence and latent heat are called continuous transitions or critical points. They are particularly interesting because the typical length and time scales of fluctuations diverge when approaching the transition point. Understanding the resulting singularities of physical observables, the so-called *critical behavior* has been a prime endeavor in physics, and the concepts established during this process, viz., scaling and the renormalization group, now belong to the central paradigms of modern physics.

Many realistic systems contain a certain amount of quenched (i.e., time-independent or frozen in) disorder. This disorder can take the form of vacancies or impurity atoms in a crystal lattice, or it can consist of extended defects such as dislocations or grain boundaries. The question of how quenched disorder influences phase transitions and critical points is both conceptually very interesting and of fundamental importance for practical applications. It is therefore not surprising that this question has attracted considerable attention over the course of the last thirty years or so. Early work often focused on the average behavior of the disorder on larger and larger length scales.

However, it has become increasingly clear that an important role is played by *rare but large* disorder fluctuations and the *rare spatial regions* where they occur. These regions can lead to a singularity (the so-called Griffiths singularity) in the free energy in an entire parameter region close to the phase transition that is now known as the Griffiths region or Griffiths phase. In generic classical systems, the thermodynamic Griffiths singularity is very weak and probably unobservable in experiment. In recent years, rare region effects have reattracted considerable attention, in particular in connection with nonequilibrium phase transitions and with zero-temperature quantum phase transitions. At these transitions, rare regions can have much stronger effects, ranging from strong power-law singularities in the free energy to a complete destruction of the phase transition.

The goal of this review is to provide a unifying framework for rare region effects on classical, quantum, and nonequilibrium phase transitions with quenched disorder. The core of the discussion will be limited to (order-disorder) phase transitions between conventional phases, i.e., we assume that the bulk phases are not changed qualitatively by the presence of the disorder. The microscopic effect of the impurities and defects then consists in locally favoring one of the two phases over the other. This type of quenched disorder is sometimes referred to as *weak* disorder, or random- $T_c$  disorder (because it changes the local critical temperature at a thermal transition), or, from analogy with quantum field theory, random-mass disorder.

The structure of this review is as follows. In section 2, we collect the basic concepts of phase transitions and critical phenomena necessary for the purpose of this review. In section 3 we give an introduction to the influence of quenched disorder on phase transitions with particular emphasis on rare region effects. We then put forward a general classification of weakly disordered phase transitions according to the effective dimensionality of the rare regions. In the bulk of the review, consisting of sections 4, 5, and 6, we illustrate these general ideas by discussing in detail rare regions effects at several classical, quantum, and nonequilibrium phase transitions, respectively. We conclude in section 7 with a summary and a discussion of experiments and open questions.

## 2. Phase transitions and critical behavior

In this section, we briefly collect the basic theoretical concepts of phase transitions and critical phenomena to the extent necessary for the purpose of this review. More details can be found in textbooks on this topic such as those by Ma [1] or Goldenfeld [2].

### 2.1. Landau theory

Most modern theories of phase transitions are built on the foundation of Landau theory [3–6]. Landau introduced the general concept of an *order parameter*, a thermodynamic quantity that vanishes in one phase (the disordered phase<sup>‡</sup>) and is non-zero in the other phase (the ordered phase). Very often the choice of an order parameter for a particular transition is obvious, e.g., for the ferromagnetic transition where the total magnetization is an order parameter. Sometimes, however, finding an appropriate order parameter is a complicated problem in itself, e.g., for the disorder-driven localization-delocalization transition of non-interacting electrons.

Landau theory can be understood as the unification of earlier mean-field theories such as the van-der-Waals theory of the liquid gas transition [7] or Weiss' molecular field theory of ferromagnetism [8]. It is based on the crucial assumption that the free energy is an analytic function of the order parameter  $m$  and can thus be expanded in a power series,

$$F = F_L(m) = F_0 + r m^2 + v m^3 + u m^4 + O(m^5) . \quad (1)$$

Here  $r, v, u$  are parameters that depend on all degrees of freedom other than the order parameter  $m$ . The physical value of  $m$  is the one that minimizes  $F_L$ . For sufficiently large  $r$ , the minimum free energy is always located at  $m = 0$  (the system is in the disordered phase), while for sufficiently small  $r$ , the minimum is at some  $m \neq 0$  (ordered phase). If  $v \neq 0$ , the transition from  $m = 0$  to  $m \neq 0$  occurs discontinuously, i.e., it is of first order. If  $v = 0$  (as is often the case by symmetry), the theory describes a continuous transition or critical point at  $r = 0$ . Thus,  $r$  is measuring the distance from the critical point,  $r \propto (T - T_c)$  for a thermal transition.

Within Landau theory, the qualitative behavior of all critical points is identical. Specifically, the order parameter vanishes as  $m = (-r/2u)^{1/2}$  when the critical point is approached from the ordered phase. This is an example of the so-called super-universality of Landau theory: The critical exponent  $\beta$  which describes the singularity of the order parameter at the critical point via  $m \propto |r|^\beta$ , is predicted to have the mean-field value  $1/2$  for all critical points. Universality of the critical exponents is actually observed in experiments but it is weaker than the super-universality predicted by Landau theory, and the exponent values are in general different from what Landau theory predicts. Moreover, the exponent values turn out to be dimensionality dependent. For instance, all three-dimensional Ising ferromagnets have a common  $\beta \approx 0.32$  while two-dimensional Ising magnets have  $\beta = 1/8$ . Three-dimensional ferromagnets with  $O(3)$  Heisenberg symmetry also have a common value of  $\beta \approx 0.35$  but it is different from the one in Ising magnets.

The reason for the failure of Landau theory to correctly describe the critical behavior is that it does not adequately include the fluctuations of the order parameter about its average value. The effects of these fluctuations in general decrease with

<sup>‡</sup> Here "disordered phase" refers to a phase without long-range order. This is not to be confused with quenched disorder in the form of impurities and defects.

increasing dimensionality and with increasing number of order parameter components. This explains why the critical behavior of Ising magnets (one order parameter component) deviates more strongly from Landau theory than that of Heisenberg magnets (three components), and why the three-dimensional exponents are closer to the mean-field values than those of two-dimensional systems.

This suggests that Landau theory might actually be correct for systems with sufficiently high dimensionality  $d$ . In fact, the fluctuations lead to two different critical dimensionalities,  $d_c^+$  and  $d_c^-$  for a given phase transition. If the dimensionality  $d$  is larger than the upper critical dimension  $d_c^+$ , fluctuations are unimportant for the leading critical behavior, and Landau theory gives the correct answers. If  $d$  is between the upper and the lower critical dimensions,  $d_c^+ > d > d_c^-$ , a phase transition still exists but the critical behavior is different from mean-field theory. For dimensionalities below the lower critical dimension, fluctuations become so strong that they completely destroy the ordered phase. For the ferromagnetic transition at nonzero temperature,  $d_c^+ = 4$ , and  $d_c^- = 2$  or  $1$  for Heisenberg and Ising symmetries, respectively.

## 2.2. Scaling and the renormalization group

As indicated in the last subsection, below the upper critical dimension  $d_c^+$ , order parameter fluctuations play a crucial role in determining the critical behavior. To include them, one has to generalize the Landau free energy (1) by writing the partition function  $Z$  as a functional integral

$$Z = e^{-F/T} = \int D[\phi] e^{-S[\phi]}, \quad (2)$$

with the action or Landau-Ginzburg-Wilson (LGW) functional  $S$  given by

$$S[\phi] = \frac{1}{T} \int d^d x [c(\nabla\phi(\mathbf{x}))^2 + F_L(\phi(\mathbf{x})) - h\phi(\mathbf{x})]. \quad (3)$$

$\phi$  is a fluctuating field whose average value is equal to the order parameter,  $m = \langle\phi\rangle$ . (Here,  $\langle\dots\rangle$  denotes the average with respect to the statistical weight  $e^{-S[\phi]}$ ). We have also included an external field  $h$  conjugate to the order parameter.

In the disordered phase, away from the critical point, the correlation function of the order parameter fluctuations,  $G(\mathbf{x} - \mathbf{y}) = \langle\phi(\mathbf{x})\phi(\mathbf{y})\rangle$  is generically short-ranged. When the critical point is approached, the correlations become long-ranged. Their typical length scale, the correlation length  $\xi$ , diverges when the distance  $r$  from the critical point vanishes§,

$$\xi \propto |r|^{-\nu}. \quad (4)$$

Here,  $\nu$  is the correlation length critical exponent. Close to the critical point, the correlation length  $\xi$  is the only relevant length scale in the system. Therefore, the physical properties must be unchanged, if we rescale all lengths in the system by a common factor  $b$ , and at the same time adjust the external parameters in such a way that the correlation length retains its old value. This gives rise to the homogeneity relation for the free energy density  $f = -(T/V) \ln Z$ ,

$$f(r, h) = b^{-d} f(r b^{1/\nu}, h b^{y_h}). \quad (5)$$

§ One needs to distinguish between the bare value of  $r$  which appears in the LGW functional (3) and the physical or renormalized value which measures the distance from the true critical point. We will explicitly make this distinction when necessary but otherwise suppress it.

	exponent	definition	conditions
specific heat	$\alpha$	$c \propto  r ^{-\alpha}$	$r \rightarrow 0, h = 0$
order parameter	$\beta$	$m \propto (-r)^\beta$	$r \rightarrow 0-, h = 0$
susceptibility	$\gamma$	$\chi \propto  r ^{-\gamma}$	$r \rightarrow 0, h = 0$
critical isotherm	$\delta$	$h \propto  m ^\delta \text{sign}(m)$	$h \rightarrow 0, r = 0$
correlation length	$\nu$	$\xi \propto  r ^{-\nu}$	$r \rightarrow 0, h = 0$
correlation function	$\eta$	$G(\mathbf{x}) \propto  \mathbf{x} ^{-d+2-\eta}$	$r = 0, h = 0$
dynamical	$z$	$\xi_t \propto \xi^z$	$r \rightarrow 0, h = 0$
activated dynamical	$\psi$	$\ln \xi_t \propto \xi^\psi$	$r \rightarrow 0, h = 0$

**Table 1.** Definitions of the commonly used critical exponents.  $m = \langle \phi \rangle$  is the order parameter, and  $h$  is the conjugate field.  $r$  denotes the distance from the critical point and  $d$  is the space dimensionality. (The exponent  $y_h$  defined in (5) is related to  $\delta$  by  $y_h = d\delta/(1 + \delta)$ .)

The scale factor  $b$  is an arbitrary positive number, and  $y_h$  is another critical exponent. Analogous homogeneity relations for other thermodynamic quantities can be obtained by differentiating  $f$ . These homogeneity laws were first obtained phenomenologically by Widom [9] and are sometimes summarily called the scaling hypothesis. Within the framework of the modern renormalization group theory of phase transitions [10] the scaling laws can be derived from first principles.

In addition to the critical exponents  $\nu$  and  $y_h$  defined above, a number of other exponents is in common use. They describe the dependence of the order parameter and its correlations on the distance from the critical point and on the field conjugate to the order parameter. The definitions of the most commonly used critical exponents are summarized in Table 1. Note that not all the exponents defined in Table 1 are independent from each other. The four thermodynamic exponents  $\alpha, \beta, \gamma, \delta$  can all be obtained from the free energy (5) which contains only two independent exponents. They are therefore connected by the so-called scaling relations

$$2 - \alpha = 2\beta + \gamma, \quad (6)$$

$$2 - \alpha = \beta(\delta + 1). \quad (7)$$

Analogously, the exponents of the correlation length and correlation function are connected by the relations

$$2 - \alpha = d\nu, \quad (8)$$

$$\gamma = (2 - \eta)\nu. \quad (9)$$

Note that scaling relations explicitly involving the dimensionality, the so called hyperscaling relations, only hold below the upper critical dimension  $d_c^+$ . Their breakdown above  $d_c^+$  is caused by dangerously irrelevant variables, see, e.g., Ref. [2].

In addition to the diverging length scale  $\xi$ , a critical point is characterized by a diverging time scale, the correlation time  $\xi_t$ . It leads to the phenomenon of *critical slowing down*, i.e., very slow relaxation towards equilibrium near a critical point. At generic critical points, the divergence of the correlation time follows a power law  $\xi_t \propto \xi^z$  where  $z$  is the dynamical critical exponent. At some transitions, in particular in the presence of quenched disorder, the divergence can be exponential,  $\ln \xi_t \propto \xi^\psi$ . The latter case is referred to as activated dynamical scaling in contrast to the generic power-law dynamical scaling.

As mentioned above, the critical exponents display the remarkable phenomenon of universality, i.e., they are the same for entire classes of phase transitions which may occur in very different physical systems. These classes, the so-called universality classes, are determined only by the symmetries of the Hamiltonian and the spatial dimensionality of the system. The physical mechanism behind universality is the divergence of the correlation length. Close to the critical point the system effectively averages over large volumes rendering the microscopic details of the Hamiltonian unimportant.

### 2.3. Classical versus quantum phase transitions

In classical statistical mechanics, statics and dynamics decouple. This can be seen by considering a classical Hamiltonian  $H(p_i, q_i) = H_{\text{kin}}(p_i) + H_{\text{pot}}(q_i)$  consisting of a kinetic part  $H_{\text{kin}}$  that only depends on the momenta  $p_i$  and a potential part  $H_{\text{pot}}$  that only depends on the coordinates  $q_i$ . The classical partition function of such a system,

$$Z = \int \prod dp_i e^{-H_{\text{kin}}/T} \int \prod dq_i e^{-H_{\text{pot}}/T} = Z_{\text{kin}} Z_{\text{pot}}, \quad (10)$$

factorizes in kinetic and potential parts which are completely independent from each other. The kinetic contribution to the free energy density will usually not display any singularities, since it derives from a product of simple Gaussian integrals. Therefore one can study the *thermodynamic* critical behavior in classical systems using time-independent theories like the Landau-Ginzburg-Wilson theory discussed in the last subsection. As a result of this decoupling, the dynamical critical exponent is completely independent from the thermodynamic ones.

In quantum statistical mechanics, the situation is different. The Hamiltonian  $H$  and its parts  $H_{\text{kin}}$  and  $H_{\text{pot}}$  are now operators, and  $H_{\text{kin}}$  and  $H_{\text{pot}}$  in general do not commute. Consequently, the partition function  $Z = \text{Tr} e^{-H/T}$  does not factorize, and one must solve for the dynamics together with the thermodynamics. Quantum mechanical analogs of the Landau-Ginzburg-Wilson theory (3) therefore need to be formulated in terms of space and time dependent fields; they can be derived, e.g., via a functional integral representation of the partition function. The simplest example of such a quantum Landau-Ginzburg-Wilson functional takes the form

$$S[\phi] = \int_0^{1/T} d\tau \int d^d x [a(\partial_\tau \phi(\mathbf{x}, \tau))^2 + c(\nabla \phi(\mathbf{x}, \tau))^2 + F_L(\phi(\mathbf{x}, \tau)) - h\phi(\mathbf{x}, \tau)] \quad (11)$$

with  $\tau$  being the imaginary time. This functional also illustrates another remarkable feature of quantum statistical mechanics. The imaginary time variable  $\tau$  effectively acts as an additional coordinate. For nonzero temperatures,  $1/T < \infty$ , the extra dimension extends only over a finite interval. If one is sufficiently close to the critical point so that the condition  $\xi_t > 1/T$  is fulfilled, the extra dimension will not affect the leading critical behavior. We thus conclude that the asymptotic critical behavior at any transition with a nonzero critical temperature is purely classical. However, a quantum phase transition at  $T = 0$  is described by a theory that effectively is in a different (higher) dimension. Therefore, it will be in a different universality class. At finite temperatures and in the vicinity of a quantum phase transition, the interplay between classical and quantum fluctuations leads to nontrivial crossover phenomena [11–14].

Using the equivalence between imaginary time and an additional dimension, the homogeneity law for the free energy can be easily generalized to the quantum case (see, e.g., [12]). For conventional power law dynamical scaling it takes the form

$$f(r, h, T) = b^{-(d+z)} f(r b^{1/\nu}, h b^{y_h}, T b^z) . \quad (12)$$

This relation implies that the scaling behavior of a zero-temperature quantum phase transition in  $d$  dimensions can be mapped onto that of some classical transition in  $d + z$  spatial dimensions. If space and time enter the theory symmetrically the dynamical exponent is  $z = 1$ , but in general, it can take any positive value. Note that this quantum to classical mapping is valid for the thermodynamics only. Other properties like the real time dynamics at finite temperatures require more careful considerations [12]. Moreover, some quantum phase transitions, such as the metal-insulator transition, do not have a classical counterpart and thus the quantum to classical mapping does not directly apply.

Let us also emphasize that the entire concept of a Landau-Ginzburg-Wilson theory in terms of the order parameter field relies on the order parameter fluctuations being the only soft or gapless mode in the system. If there are other soft modes, e.g., due to conservation laws or broken continuous symmetries, they lead to long-range power-law correlations of various quantities even *away from the critical point*. This phenomenon is called generic scale invariance [15–17]. If one insists on deriving a Landau-Ginzburg-Wilson theory for a phase transition in the presence of generic scale invariance, the additional soft modes lead to coefficients that are singular functions of space and time, severely limiting the usefulness of the theory [18–20]. In such a situation one should instead work with a coupled theory that keeps all soft modes at the same footing. This question has been explored in detail in Ref. [14]. In practise, complications due to generic scale invariance are more common for quantum phase transitions than for classical ones because (i) there are more soft modes at  $T = 0$  than at  $T > 0$ , and (ii) phenomena that classically only affect the dynamics influence the static critical behavior of a quantum phase transition as well. In addition to this mechanism, there are other reasons for a quantum phase transition being more complicated than one might naively expect, including topological effects. In many of these cases, a description of the transition in terms of a Landau-Ginzburg-Wilson theory is not possible.

#### 2.4. Finite-size scaling

We now turn to the question of how a finite system size influences the behavior at a critical point, a question that will be very important later on for our discussion of rare region effects. In general, a sharp phase transition can only exist in the thermodynamic limit, i.e., in an infinite system. A finite system size results in a rounding and shifting of the critical singularities. If the extension of the system is finite only in some directions and infinite in others, a sharp phase transition can still exist, but the critical point will be shifted compared to the bulk value. Moreover, the universality class will change.

The behavior of finite size systems in the vicinity of a critical point is described by finite-size scaling theory [21–23]. Finite-size scaling starts from the observation that the inverse system size acts as an additional parameter that takes the system away from the critical point. Because the correlation length of the infinite system  $\xi_\infty$  is the only relevant length scale close to the critical point, finite-size effects in a system of linear size  $L$  must be controlled by the ratio  $L/\xi_\infty$  only. We can therefore generalize



the classical homogeneity relation (5) for the free energy density by including the system size

$$f(r, h, L) = b^{-d} f(r b^{1/\nu}, h b^{y_h}, L b^{-1}). \quad (13)$$

The quantum version (12) of the homogeneity law can be generalized in the same way:

$$f(r, h, T, L) = b^{-(d+z)} f(r b^{1/\nu}, h b^{y_h}, T b^z, L b^{-1}). \quad (14)$$

We note in passing that the temperature scaling in the quantum homogeneity law can be viewed as finite-size scaling in imaginary time direction with the inverse temperature playing the role of the system size.

The shift of the critical temperature or critical coupling as a function of  $L$  for geometries that still allow a sharp phase transition at finite  $L$  follows directly from (13). Setting  $b = L$ ,  $h = 0$ , we obtain

$$f(r, L) = L^d F(r L^{1/\nu}) \quad (15)$$

where  $F(x)$  is a dimensionless scaling function. The quantum case can be treated analogously. The finite- $L$  phase transition corresponds to a singularity in the scaling function at some nonzero argument  $x_c$ . The transition thus occurs at  $r_c L^{1/\nu} = x_c$ , and the transition temperature  $T_c(L)$  of the finite-size system is shifted from the bulk value  $T_c^0$  by

$$T_c(L) - T_c^0 \sim r_c = x_c L^{-1/\nu}. \quad (16)$$

Note that the simple form of finite-size scaling summarized above is only valid below the upper critical dimension  $d_c^+$  of the phase transition. Finite-size scaling can be generalized to dimensions above  $d_c^+$ , but this requires taking dangerously irrelevant variables into account. One important consequence is that the shift of the critical temperature,  $T_c(L) - T_c^0 \sim L^{-\phi}$ , is controlled by an exponent  $\phi$  which in general is different from  $1/\nu$ .

### 3. Quenched disorder effects

In this section, we give a brief introduction into the effects of quenched disorder on phase transitions and critical points. We focus on what is arguably the simplest and most benign type of disorder, viz., impurities and defects that lead to spatial variations of the coupling strength (i.e., spatial variations in the tendency towards the ordered phase) but not to frustration or random external fields. This also implies that the two bulk phases (that are separated by the transition) are not changed qualitatively by the presence of the quenched disorder. This type of quenched disorder is sometimes referred to as weak disorder, random- $T_c$  disorder, or, in analogy to quantum field theory, random-mass disorder.

In ferromagnetic materials, random- $T_c$  disorder can be achieved, e.g., by diluting the lattice, i.e., by replacing magnetic atoms with nonmagnetic ones. Within a Landau-Ginzburg-Wilson theory such as (3) or (11), random- $T_c$  disorder can be modelled by making the bare distance from the critical point a random function of spatial position,  $r \rightarrow r + \delta r(\mathbf{x})$ . In this representation, the character of the impurities and defects is encoded in the statistical properties of the random- $T_c$  term  $\delta r(\mathbf{x})$ . Point-like impurities correspond to short-range correlations of  $\delta r(\mathbf{x})$  in all directions while linear and planar defects lead to perfect correlations of  $\delta r(\mathbf{x})$  in one and two dimensions, respectively. Let us also briefly comment on the disorder probability distribution  $P(\delta r)$ . As long as the physics is dominated by long-wavelength

properties and the average behavior of the disorder, the details of the probability distribution should not play an important role. In theoretical investigations a realistic distribution is often replaced by a Gaussian because the latter can be easily handled mathematically. We emphasize, however, that in some cases the dominating physics occurs in the tail of the probability distribution. In these cases, the form of the tail is important, and more careful considerations are required.

Adding weak, random- $T_c$ , quenched disorder to a system undergoing a continuous phase transition naturally leads to the following questions:

- Will the phase transition remain sharp in the presence of quenched disorder?
- If so, will the critical behavior change quantitatively (different universality class with new exponents) or even qualitatively (exotic non-power-law scaling)?
- Will only the transition itself be influenced or also the behavior in its vicinity?

### 3.1. Average disorder and Harris criterion

The question of how quenched disorder influences phase transitions has a long history. Initially it was suspected that disorder destroys any critical point because in the presence of defects, the system divides itself up into spatial regions which independently undergo the phase transition at different temperatures (see Ref. [24] and references therein). However, subsequently it became clear that generically a phase transition remains sharp in the presence of defects, at least for classical systems with short-range disorder correlations.

Harris [25] derived a criterion for the perturbative stability of a clean critical point against weak disorder. Harris considered the effective local critical temperature in blocks of linear size  $\xi$  which is given by an average of  $r + \delta r(\mathbf{x})$  over the volume  $V = \xi^d$ . He observed that a sharp phase transition can only occur if the variation  $\Delta r$  of these local critical temperatures from block to block is smaller than the global distance from the critical point  $r$ . For short-range correlated disorder, the central limit theorem yields  $\Delta r \propto \xi^{-d/2} \propto r^{d\nu/2}$ . Thus, a clean critical point is perturbatively stable, if the clean critical exponents fulfill the inequality  $r^{d\nu/2} < r$  for  $r \rightarrow 0$ . This implies the exponent inequality

$$d\nu > 2 \tag{17}$$

which is called the Harris criterion. Note that the Harris criterion is a necessary condition for the stability of a clean fixed point, not a sufficient one. It only deals with the average behavior of the disorder at large length scales. However, effects due to qualitatively new physics at finite length scales (and finite disorder strength) are not covered by the Harris criterion.

The Harris criterion can be used as the basis for a classification of critical points with quenched disorder, based on the behavior of the average disorder strength with increasing length scale, i.e., under coarse graining. Three classes of critical points can be distinguished [26].

(i) The first class contains systems whose clean critical points fulfill the Harris criterion  $d\nu > 2$ . At these phase transitions, the disorder strength *decreases* under coarse graining, and the system becomes asymptotically homogeneous at large length scales. Consequently, the quenched disorder is asymptotically unimportant, and the critical behavior of the dirty system is identical to that of the clean system. Technically, this means the disorder is renormalization group irrelevant at the clean

critical fixed point. In this class of systems, the macroscopic observables are self-averaging at the critical point, i.e., the relative width of their probability distributions vanishes in the thermodynamic limit [27, 28]. A prototypical example in this class is the three-dimensional classical Heisenberg model whose clean correlation length exponent is  $\nu \approx 0.698$  (see, e.g., [29]), fulfilling the Harris criterion.

If a clean critical point violates the Harris criterion, it is destabilized by weak quenched disorder, and the behavior must change. Nonetheless, a sharp critical point can still exist in the presence of the disorder, but it must fall into one of the two following classes.

(ii) In the second class, the system remains inhomogeneous at all length scales with the relative strength of the inhomogeneities approaching a finite value for large length scales. The resulting critical point still displays conventional power-law scaling but with new critical exponents which differ from those of the clean system (and fulfill the inequality  $d\nu > 2$ ). These transitions are controlled by renormalization group fixed points with a nonzero value of the disorder strength. Macroscopic observables are not self-averaging, but in the thermodynamic limit, the relative width of their probability distributions approaches a size-independent constant [27, 28]. An example in this class is the classical three-dimensional Ising model. Its clean correlation length exponent,  $\nu \approx 0.627$  (see, e.g. [30]) does not fulfill the Harris criterion. Introduction of quenched disorder, e.g., via dilution, thus leads to a new critical point with an exponent of  $\nu \approx 0.684$  [31].

(iii) At critical points in the third class, the relative magnitude of the inhomogeneities *increases* without limit under coarse graining. The corresponding renormalization group fixed points are characterized by infinite disorder strength. At these infinite-randomness critical points, the power-law scaling is replaced by activated (exponential) scaling. The probability distributions of macroscopic variables become very broad (even on a logarithmic scale) with the width diverging with system size. Consequently, their averages are often dominated by rare events, e.g., spatial regions with atypical disorder configurations. This type of behavior was first found in the McCoy-Wu model, a two-dimensional Ising model with bond disorder perfectly correlated in one dimension [32, 33]. However, it was fully understood only when Fisher [34, 35] solved the one-dimensional random transverse field Ising model by a version of the Ma-Dasgupta-Hu real space renormalization group [36]. Since then, several infinite-randomness critical points have been identified, mainly at quantum phase transitions since the disorder, being perfectly correlated in (imaginary) time, has a stronger effect on quantum phase transitions than on thermal ones. Examples include one-dimensional random quantum spin chains as well as one-dimensional and two-dimensional random quantum Ising models [26, 37–40]. Very recently, a similar infinite-randomness fixed point has been found in the disordered one-dimensional contact process [41–43].

### 3.2. Rare regions and Griffiths effects

In the last subsection we have discussed scaling scenarios for phase transitions with quenched disorder based on the *global, i.e., average*, behavior of the disorder strength under coarse graining. In this subsection, we turn to the main topic of this review, viz., the effects of *rare* strong spatial disorder fluctuations.

Let us start by considering the example of a diluted classical ferromagnet as sketched in figure 1. The dilution reduces the tendency towards magnetic long-range

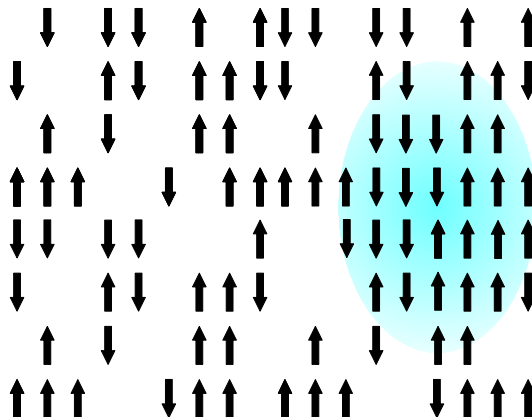


**Figure 1.** Sketch of a diluted magnet. The shaded region is devoid of impurities and therefore acts as a piece of the clean bulk system

order and thus reduces  $T_c$  from its clean bulk value  $T_c^0$ . However, in an infinite system one can find arbitrarily large spatial regions that are devoid of impurities. For temperatures between  $T_c^0$  and  $T_c$ , these regions will show local magnetic order even though the bulk system is globally in the paramagnetic phase. These spatial regions are known as *rare regions* and the order parameter fluctuations induced by them belong to a class of excitations known as *local moments*; sometimes they are also referred to as *instantons*. The dynamics of the rare regions is very slow because flipping them requires a coherent change of the order parameter over a large volume. Griffiths [44] was the first to show that these rare regions can lead to a singularity in the free energy, the Griffiths singularity, in the entire temperature region  $T_c < T < T_c^0$  which is now known as the Griffiths region or the Griffiths phase [45]. Analogous singularities also exist on the ordered side of the phase transition.

The probability  $w$  for finding a rare region is exponentially small in its volume  $V_{RR}$  and in the impurity concentration  $p$ ; up to pre-exponential factors it is given by  $w \sim \exp(-pV_{RR})$ . Rare regions are thus nonperturbative degrees of freedom that are not accounted for in conventional approaches to phase transitions and critical points that are based on perturbation theory and the perturbative renormalization group. They can be viewed as examples of a broader class of rare event phenomena that range from the well known Lifshitz tails in the density of states of disordered semiconductors [46, 47] to the slowing down of computer algorithms in combinatorial optimization [48].

In classical systems with uncorrelated or short-range correlated disorder, thermodynamic Griffiths effects are very weak because the singularity in the free energy is only an essential one [49–51]. To the best of our knowledge, classical thermodynamic Griffiths singularities have therefore not been verified in experiment (see also [52]). In contrast, the long-time *dynamics* inside the Griffiths phase is dominated by the rare regions, as is signified by a non-exponential time-dependence of the spin autocorrelation function [45, 53–56].

Long-range disorder correlations can increase the rare region effects qualitatively. In particular, if the disorder is perfectly correlated in some spatial directions, or – in the case of a zero-temperature quantum phase transition – in imaginary time, the rare regions are extended objects which are infinite in the correlated space or imaginary

time directions. This makes their dynamics even slower and so increases their effects. This enhancement of rare region effects was first observed in the abovementioned McCoy-Wu model [32,33], a two-dimensional classical Ising model with linear defects. More recently, it has been studied in great detail in various disordered quantum systems: In one-dimensional and two-dimensional random transverse field Ising models, the singularity of the free energy in the Griffiths phase takes a power-law form with nonuniversal continuously varying exponents. Several thermodynamic observables including the average susceptibility actually diverge in a finite region of the disordered phase [26,34,35,39,40] rather than only at the critical point. Similar phenomena have also been found in quantum Ising spin glasses [57–59]. In addition, power-law Griffiths effects, sometimes also called Griffiths-McCoy effects, were also found at the nonequilibrium phase transition in a disordered one-dimensional contact process [41–43].

Recently, it has been shown that rare region effects can become strong enough to completely destroy the sharp phase transition. This happens, if the dynamics of the rare regions stops completely, i.e., if a static order parameter develops on an isolated rare region independent of the bulk system. The global phase transition is then smeared or rounded, as was found in itinerant quantum magnets [60] where the overdamping of the magnetic excitations by the electronic degrees of freedom suppresses the dynamics of sufficiently large rare regions [61,62]. Later, analogous smeared transitions been found in a variety of systems, ranging from classical Ising magnets with planar defects [63,64] to nonequilibrium spreading transitions in the contact process [65,66].

### 3.3. A classification of rare region effects

In the last subsection, we have seen that the influence of rare regions on continuous phase transitions can range from exponentially weak free energy contributions to a complete destruction of the sharp phase transition by smearing. It would clearly be very desirable to determine what conditions lead to which type of rare region effects. Recently, a general classification of rare region effects at order-disorder phase transitions in systems with weak, random-mass disorder has been suggested [67]. This classification is based on the following idea. The probability  $w$  for finding a large spatial region of volume  $V_{\text{RR}} \sim L_{\text{RR}}^d$  devoid of impurities decreases exponentially with its volume,  $w(L_{\text{RR}}) \sim \exp(-pV_{\text{RR}})$ . The importance of large rare regions thus depends on how rapidly the contribution of a *single* region to observable quantities *increases* with its size. It turns out that this question is controlled by the effective dimensionality  $d_{\text{RR}}$  of the rare regions, or more precisely, by the relation between  $d_{\text{RR}}$  and the lower critical dimension  $d_c^-$  of the phase transition under consideration.||

To understand this, let us consider a single isolated region of linear size  $L_{\text{RR}}$  that is locally in the ordered phase, i.e., the bulk distance from the critical point is negative,  $r = r(\infty) < 0$ . We now ask: How does the renormalized distance from the critical point,  $r(L_{\text{RR}})$ , (or equivalently, the energy gap) of the finite size rare region depend on its linear size  $L_{\text{RR}}$ ? Three cases can be distinguished (a summary is given in table 2).

|| When counting the *effective* dimensionalities for quantum phase transitions we include the imaginary time direction as one of the dimensions.

Class	RR dimension	Griffiths effects	Dirty critical point	Critical scaling
A	$d_{\text{RR}} < d_c^-$	weak exponential	conventional	power law
B	$d_{\text{RR}} = d_c^-$	strong power-law	infinite randomness	activated
C	$d_{\text{RR}} > d_c^-$	RR become static	smearred transition	no scaling

**Table 2.** Classification of rare region (RR) effects at critical points in the presence of weak quenched disorder according to the effective dimensionality  $d_{\text{RR}}$  of the rare regions. For details see text.

*3.3.1. Class A:* If the effective dimensionality  $d_{\text{RR}}$  of the rare regions is *below* the lower critical dimensionality  $d_c^-$  of the problem, an isolated rare region cannot undergo the phase transition by itself. The renormalized  $r(L_{\text{RR}})$  is therefore positive, but it decreases with  $L_{\text{RR}}$  following a power law. The leading contributions of a rare region to thermodynamic quantities are controlled by  $r(L_{\text{RR}})$ , e.g., the order parameter susceptibility  $\chi$  is proportional to  $r^{-1}(L_{\text{RR}})$ . The contributions of a rare region to observables can therefore at most grow as a power of its linear size  $L_{\text{RR}}$ . (In the case of a classical magnet,  $\chi \sim S_{\text{eff}}^2 \sim L_{\text{RR}}^{2d}$ ). This power-law increase cannot overcome the exponential drop in the rare region density  $w(L_{\text{RR}})$ .

As a result, for transitions in this class, thermodynamic rare region effects are exponentially weak and characterized by an essential singularity in the free energy [44, 49–51]. Right at the dirty critical point, the rare region effects are subleading, and the critical behavior is of conventional power-law type. Examples for critical points in class A can be found in generic classical equilibrium systems with point defects (where the rare regions are finite in all directions and thus  $d_{\text{RR}} = 0$ ) but also at some quantum phase transitions such as the transition in the diluted bilayer Heisenberg quantum antiferromagnet [68–70] (here  $d_{\text{RR}} = 1$  but  $d_c^- = 2$  so that the condition for class A is fulfilled).

*3.3.2. Class B:* In this class, the rare regions are exactly *at* the lower critical dimension,  $d_{\text{RR}} = d_c^-$ . They still cannot undergo the phase transition independently, but the renormalized distance from the critical point (or equivalently, the energy gap) decreases *exponentially* with the rare region volume  $V_{\text{RR}}$ . Therefore, the rare region contribution to observables such as the susceptibility increases exponentially with size and can potentially overcome the exponential decrease of the rare region density.

Generically, this results in a power-law low-energy density of states leading to strong power-law Griffiths singularities with a nonuniversal continuously varying exponents. The scaling behavior at the dirty critical point itself is dominated by the rare regions resulting in exotic activated (exponential) scaling instead of conventional power-law scaling. Class B is realized, e.g., in a classical Ising model with linear defects, i.e., disorder perfectly correlated in one direction (McCoy-Wu model [32, 33]), in percolation with linear defects [71], and in random quantum Ising models (where the disorder correlations are in imaginary time direction) [26, 34, 35, 39, 40]. In all these systems,  $d_{\text{RR}} = d_c^- = 1$ . Several thermodynamic observables including the average susceptibility actually diverge in a finite region of the disordered phase rather than just at the critical point. Class B rare region effects also occur at the nonequilibrium phase transition of the contact process with point defects. Including the time dimension, this transition also has  $d_{\text{RR}} = d_c^- = 1$ .

*3.3.3. Class C:* Finally, in class C, the rare regions can undergo the phase transition independently from the bulk system, i.e., they are effectively *above* the lower critical dimension of the problem,  $d_{\text{RR}} > d_c^-$ . In this case, the dynamics of the locally ordered rare regions completely freezes, and they develop a truly static order parameter. As a result, the global phase transition is destroyed by smearing [60] because different spatial parts of the system order at different values of the control parameter. In the tail of the smeared transition, the order parameter is extremely inhomogeneous, with statically ordered islands or droplets coexisting with the disordered bulk of the system. This behavior was identified in itinerant quantum Ising magnets [60–62] where the damping due to the electronic degrees of freedom leads to an effective long-range ( $1/\tau^2$ ) interaction in time direction. At this transition  $d_{\text{RR}} = 1$  and  $d_c^- = 1$  but it nonetheless belongs to class C because the rare region can undergo a Kosterlitz-Thouless type phase transition to the ordered phase. Smeared transitions can also be found in classical magnets with planar defects [63, 64] ( $d_{\text{RR}} = 2 > d_c^- = 1$ ), in nonequilibrium spreading transitions with extended (linear or planar defects) [65, 66] where  $d_{\text{RR}} > 1$  but  $d_c^- = 1$  (including the time dimension) or in stratified percolation [72] ( $d_{\text{RR}} = 2, d_c^- = 1$ ).

This classification is expected to apply to all continuous order-disorder transitions between conventional phases that can be described by Landau-Ginzburg-Wilson type theories with random-mass disorder and short-range interactions. It also relies on the assumption that the interaction between the rare regions can be neglected if their density is sufficiently low (i.e., sufficiently far away from the true disordered critical point, if any). While this seems a reasonable assumption in the case of short-range spatial interactions, long-range interactions will likely modify the rare region effects. In the case of itinerant quantum Heisenberg magnets, it has been argued that the interaction between the rare regions due to the long-range RKKY interaction strongly enhances the rare region effects, leading to a smeared transition even though a single rare region would not independently undergo the phase transition [73].

The classification of rare region effects provides a general framework for a variety of existing results, and it helps organizing the search for new phenomena. In the following sections of this review we will discuss in detail several examples of rare region effects at classical, quantum, and nonequilibrium phase transitions with quenched disorder and relate them to the above classification.

## 4. Classical phase transitions

This section is devoted to rare region effects at classical equilibrium phase transitions in systems with random- $T_c$  type disorder. We first consider the case of uncorrelated disorder (point-like defects) which leads to exponentially weak “classical” Griffiths effects. We then show that disorder correlation enhance the rare region effects by discussing systems with linear and planar defects.

### 4.1. Randomly diluted Ising model

For definiteness, let us consider a randomly site-diluted classical Ising magnet on a  $d$ -dimensional hypercubic lattice of  $N = L^d$  sites. The Hamiltonian is given by

$$H = -J \sum_{\langle i,j \rangle} \epsilon_i \epsilon_j S_i S_j - h \sum_i \epsilon_i S_i \quad (18)$$

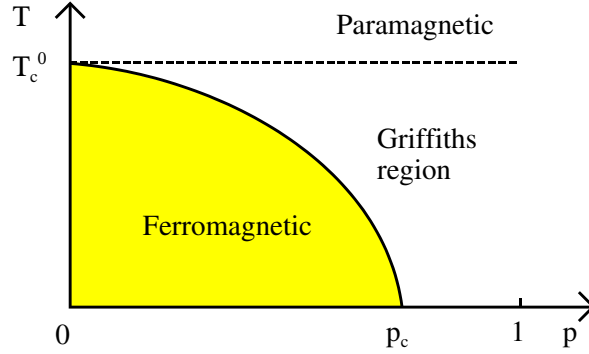


**Figure 2.** Schematic phase diagram of a randomly diluted Ising model as function of temperature  $T$  and impurity concentration  $p$ .  $p_c$  is the geometric percolation threshold of the lattice, and  $T_c^0$  is the clean critical temperature

Here,  $S_i = \pm 1$  is the Ising spin at lattice site  $i$ ,  $h$  is the external magnetic field,  $J > 0$  is the exchange interaction, and  $\langle i, j \rangle$  indicates that the sum is over pairs of nearest neighbor sites only. The site dilution is introduced by the quenched random variables  $\epsilon_i$  with  $\epsilon_i = 1$  representing an occupied site and  $\epsilon_i = 0$  corresponding to a vacancy. In our case of point defects, the  $\epsilon_i$  are statistically independent with a probability density

$$P(\epsilon) = (1 - p)\delta(\epsilon - 1) + p\delta(\epsilon) , \quad (19)$$

i.e.,  $p$  is the probability for finding a vacancy at a particular site. A schematic phase diagram of this system as function of  $p$  and temperature  $T$  is shown in figure 2. At zero temperature, magnetic long-range order survives for all concentrations  $p \leq p_c$ , where  $p_c$  is the geometric percolation threshold of the lattice. If  $p > p_c$ , no long-range order is possible as the system is decomposed into independent finite-size clusters. For  $p < p_c$ , magnetic order survives up to a nonzero temperature  $T_c(p)$ ; but at  $p_c$ , it is destroyed immediately by thermal fluctuations<sup>¶</sup>,  $T_c(p_c) = 0$  [74–76].

In a seminal paper, Griffiths [44] showed that in the thermodynamic limit, the magnetization (per site),  $m = \frac{1}{N}M = \frac{1}{N} \sum_i \epsilon_i S_i$ , is a singular function of the magnetic field  $h$  at  $h = 0$  for any temperature  $T$  below the transition temperature  $T_c^0$  of the clean system (below the dashed line in figure 2) independent of  $p$ . Conventional paramagnetic behavior only appears above  $T_c^0$ . This singularity and the corresponding singularities in other thermodynamic quantities are now known as the Griffiths singularities and the temperature region over which they occur is called the Griffiths region or the Griffiths phase [45]. Griffiths' proof of the singular dependence of the magnetization on the field relied on an application of the theorem of Yang and Lee on the complex zeros of the partition function [77, 78], and it did not immediately give the functional form of the predicted singularity. However, after some controversy it was soon established that the Griffiths singularity is a weak essential singularity with the magnetization remaining infinitely differentiable at  $h = 0$  [49, 50, 52].

<sup>¶</sup> For Ising symmetry, this appears counterintuitive as the fractal dimension of the critical percolation cluster is larger than the lower critical dimension  $d_c^- = 1$ . However, for fractals, topological factors like ramification are important for magnetic ordering [74].



## 4.2. Optimal fluctuation theory

The leading singularities in the thermodynamic quantities in the Griffiths region can be easily estimated using optimal fluctuation theory arguments similar to those employed in the study of band tails of doped semiconductors [79, 80].

In the site diluted Ising model (18), the probability  $w(L_{\text{RR}})$  for finding a region of volume  $L_{\text{RR}}^d$  devoid of vacancies is (to exponential accuracy)

$$w(L_{\text{RR}}) \sim (1-p)^{L_{\text{RR}}^d} = \exp(-\tilde{p}L_{\text{RR}}^d) \quad (20)$$

with  $\tilde{p} = -\ln(1-p)$ . Let us now consider a temperature  $T$  in the paramagnetic Griffiths region,  $T_c(p) < T < T_c^0$ , or equivalently  $r_0 = (T - T_c^0)/T_c^0 < 0$ . The bare distance  $r(L_{\text{RR}})$  from the local critical point for a rare region of size  $L_{\text{RR}}$  is shifted by finite size effects because the rare region acts as a finite-size piece of the clean system. If  $r_0$  is not too close to zero (in the Gaussian fluctuation region), the shift can be determined by finite size scaling (16) with the mean-field value  $\nu = 1/2$ , leading to

$$r(L_{\text{RR}}) = r_0 + A/L_{\text{RR}}^2 \quad (21)$$

where  $A$  is a constant.

If  $r(L_{\text{RR}}) < 0$ , the rare region is locally in the ordered phase. Thus, at a given  $r_0$ , only rare regions larger than  $L_{\text{min}}(r_0) = |r_0/A|^{-1/2}$  will show local order. Since they are of finite size, the locally ordered rare regions do not undergo a true transition but coherently fluctuate due to thermal fluctuations. To estimate their contribution  $F_{\text{RR}}$  to the free energy, we note that the contribution of a single region varies at most like a power of its size. To leading exponential accuracy, the free energy of the rare regions can therefore be estimated by summing their probabilities,

$$F_{\text{RR}} \sim \int_{L_{\text{min}}}^{\infty} dL_{\text{RR}} w(L_{\text{RR}}) \sim \exp(-\tilde{p}|r_0/A|^{-d/2}). \quad (22)$$

Close to the bulk critical point  $r_0 = 0$ , i.e., in the clean bulk critical region, the mean field relation for the finite-size shift of  $r$  is not valid anymore and has to be replaced by finite size scaling with the shift exponent  $\phi = 1/\nu$  where  $\nu$  is the clean bulk correlation length exponent. The behavior of the free energy then crosses over to  $F_{\text{RR}} \sim \exp(-\tilde{p}|r_0/A|^{-d\nu})$ .

The response to a small external magnetic field can be derived in a similar way: In the Griffiths region, an isolated, locally ordered rare region essentially acts as a single big Ising spin of magnitude  $S_{\text{eff}} \sim L_{\text{RR}}^d$ . Thus its magnetization in an external field  $h$  is given by

$$M(L_{\text{RR}}) = S_{\text{eff}} \tanh(hS_{\text{eff}}/T) \sim \begin{cases} hL_{\text{RR}}^{2d} & (L_{\text{RR}} < bh^{-1/d}) \\ L_{\text{RR}}^d & (L_{\text{RR}} > bh^{-1/d}) \end{cases} \quad (23)$$

where  $b$  is a constant that depends on  $r_0$ . The singularity in the magnetization-field relation arises from the large rare regions whose magnetization is saturated by the field  $h$ . To exponential accuracy, the singular rare region contribution to the total magnetization is therefore given by

$$M_{\text{RR}} = \int_{bh^{-1/d}}^{\infty} dL_{\text{RR}} w(L_{\text{RR}}) \sim \exp(-\tilde{p}b^d/h) \quad (24)$$

in agreement with references [50, 52]. More recently, many of the properties of Griffiths phases have been proven rigorously in the mathematical physics literature, see e.g., [81–83] and references therein.

At this point, it is important to emphasize that the Griffiths singularities do *not* display the same degree of universality as the critical singularities right at a continuous phase transition. This is caused by the fact the rare regions are phenomena at *finite* length scales in the *tail* of the disorder probability distribution. Therefore, the functional form of the Griffiths singularities can depend on the specifics of the disorder distribution. We will now illustrate this non-universality by comparing the results (22) and (24) for the randomly diluted Ising model with those of a Landau-Ginzburg-Wilson theory with Gaussian disorder.

#### 4.3. Random- $T_c$ Landau-Ginzburg-Wilson theory

In this subsection, we consider rare region effects in a classical Landau-Ginzburg-Wilson (LGW) theory with random- $T_c$  disorder. From a critical phenomena point of view, the phase transition in this model belongs to the same universality class as the transition in the randomly site diluted Ising model considered above. Nonetheless, the functional form of the Griffiths singularities will turn out to be different from (22) and (24).

Let us start from a  $d$ -dimensional LGW theory of the form [see equations (1) and (3)]

$$S[\phi] = \int d^d x [(\nabla\phi(\mathbf{x}))^2 + (r_0 + \delta r(\mathbf{x}))\phi^2(\mathbf{x}) + u\phi^4(\mathbf{x}) - h\phi(\mathbf{x})]. \quad (25)$$

The disorder is modelled by the random contribution  $\delta r(\mathbf{x})$  to the distance to the critical point. The distribution of  $\delta r(\mathbf{x})$  is usually chosen to be a Gaussian

$$P[\delta r(\mathbf{x})] \propto \exp \left[ -\frac{1}{2\Delta} \int d^d x \delta^2 r(\mathbf{x}) \right]. \quad (26)$$

In this model, a rare region is a large spatial region in which the typical value of  $r_0 + \delta r(\mathbf{x})$  is negative while the bulk distance  $r_0$  from the critical point is positive. One qualitative difference to the randomly diluted Ising model case is immediately obvious: Because the Gaussian disorder is unbounded, locally ordered rare regions can exist for any value of the bulk distance  $r_0$  from the critical point. This means, there is no conventional paramagnetic phase, and the Griffiths region covers the entire high-temperature part of the phase diagram.

The contribution of these rare regions to the free energy can be estimated using optimal fluctuation arguments [84] similar to those in the subsection 4.2. The probability for finding a large region of linear size  $L_{\text{RR}}$  and a typical value  $\delta r_{\text{typ}} = -r_0 - s$  of the disorder variable is exponentially small,

$$w(L_{\text{RR}}, s) \sim \exp \left[ -\frac{1}{2\Delta} L_{\text{RR}}^d (s + r_0)^2 \right]. \quad (27)$$

Treating the finite-size corrections in mean-field theory (valid outside the asymptotic bulk critical region) as before, the bare distance from the critical point for such a rare region is given by

$$r(L_{\text{RR}}, s) = r_0 + \delta r_{\text{typ}} + A/L_{\text{RR}}^2 = -s + A/L_{\text{RR}}^2. \quad (28)$$

If  $r(L_{\text{RR}}, s) < 0$ , the rare region is locally in the ordered phase. Thus, the minimum size permitting local order is  $L_{\text{min}} = (A/s)^{1/2}$ . To leading exponential accuracy,

the contribution of the locally ordered rare regions to the free energy can again be estimated by summing their probabilities,

$$F_{\text{RR}} \sim \int_0^\infty ds \int_{L_{\text{min}}}^\infty dL_{\text{RR}} w(L_{\text{RR}}, s) \sim \int_0^\infty ds \exp[-Cs^{-d/2}(s+r_0)^2]. \quad (29)$$

where  $C$  is a constant. The second equality arises because the integral over  $L$  is dominated by its lower bound. The integral over  $s$  can be estimated using the saddle point method. The leading contribution comes from  $s_{\text{SP}} = r_0 d / (4 - d)$ . This implies that with increasing  $r_0$ , i.e., with increasing distance from the true transition, the dominating rare region contribution to the free energy comes from *smaller* and *deeper* disorder fluctuations. This is qualitatively different from the case of the randomly diluted Ising model where with increasing  $r_0$  larger and larger islands dominate. Inserting the saddle point value into the equation for  $F_{\text{RR}}$  gives

$$F_{\text{RR}} \sim \exp[-C' r_0^{(4-d)/2}]. \quad (30)$$

where  $C'$  is another constant. This result has also been derived more rigorously by considering replica instanton solutions of the replicated and disorder averaged Landau-Ginzburg-Wilson theory [84, 85].

Comparing the Griffiths singularities of the randomly diluted Ising model (22) and the LGW theory with Gaussian disorder (30), we find them both exponentially weak. However, the functional form of the singularity is *not* universal, it does depend on the specifics of the microscopic disorder distribution. Dotsenko [84] also calculated the rare region contribution to the free energy in a nonzero magnetic field for the LGW theory with Gaussian disorder. He found  $\delta F_{\text{RR}}(h) \sim \exp[-Eh^{-d/3}]$  with  $E$  a constant. To exponential accuracy, the same singularity should also govern the magnetization. As in the zero-field case, the functional form of the Griffiths singularity is different from that of the randomly site diluted Ising model, equation (24).

#### 4.4. Dynamic rare region effects

So far, we have focussed on the effects of the rare regions on *thermodynamic* properties, and we have found them to be exponentially weak in generic classical systems with short-range correlated disorder. In contrast, rare region effects on the dynamics are much more dramatic, as will be discussed in this subsection.

For definiteness, let us again consider the dilute ferromagnet (18). The dynamics is assumed to be purely relaxational, corresponding to model A in the classification of Hohenberg and Halperin [86]. Microscopically, this type of dynamics can be realized, e.g., via the Glauber [87] or Metropolis [88] algorithms. Because the rare region effects are local in space, their dynamic properties can be characterized in terms of the average spin *autocorrelation* function  $C(t)$  defined by

$$C(t) = \frac{1}{N} \sum_i \langle S_i(t) S_i(0) \rangle \quad (31)$$

where  $S_i(t)$  is the value of the spin at time  $t$  and  $\langle \cdot \rangle$  denotes the thermodynamic average. In the conventional paramagnetic phase  $T > T_c^0$  (see figure 2), the average autocorrelation function decays exponentially fast because none of the rare regions is locally ordered. In contrast, in the Griffiths region  $T_c(p) < T < T_c^0$ , we expect the rare regions to display slow dynamics. Following arguments first made by Dhar [53] and later refined by Randeria et al. [45] and Bray [56, 89], the rare region

part of the autocorrelation function can be estimated as the sum of independent contributions from each of the rare regions

$$C_{\text{RR}}(t) \sim \int_0^\infty dL_{\text{RR}} w(L_{\text{RR}}) \exp[-t/\xi_t(L_{\text{RR}}, r_0)] . \quad (32)$$

Here  $w(L_{\text{RR}})$  is the probability for finding a rare region of size  $L_{\text{RR}}$  as given in (20) and  $\xi_t(L_{\text{RR}}, r_0)$  is the relaxation time of such a rare region at reduced temperature  $r_0$ . Depending on  $r_0$ , equation (32) predicts different long time behavior of the autocorrelation function.

(i) In the conventional paramagnetic phase,  $T > T_c^0$  ( $r_0 > 0$ ), the relaxation time remains finite even for the largest islands. Close to  $T_c^0$  it behaves as  $\xi_t(L_{\text{RR}}, r_0) \sim \xi^z \sim r_0^{-z\nu}$  for sufficiently large islands ( $L_{\text{RR}} > \xi$ ). Here  $\xi$  is the clean bulk correlation length and  $z$  and  $\nu$  are the clean bulk critical exponents. The asymptotic time dependence of  $C(t)$  in this regime is a simple exponential.

$$\ln C(t) \sim -t/\xi^z . \quad (33)$$

(ii) At the clean critical temperature  $T = T_c^0$  ( $r_0 = 0$ ), i.e., at the boundary of the Griffiths region, the relaxation time of the large rare regions is given by finite-size scaling [22]. It diverges as  $\xi_t(L_{\text{RR}}) \sim L_{\text{RR}}^z$ . After inserting this into (32), the integral over  $L_{\text{RR}}$  can be estimated using the saddle-point method. The asymptotic time dependence of  $C(t)$  is a stretched exponential

$$\ln C(t) \sim -\tilde{p}^{z/(d+z)} t^{d/(d+z)} . \quad (34)$$

(iii) Inside the Griffiths region,  $T_c(p) < T < T_c^0$ , the relaxation time is limited by the time taken to coherently reverse the entire rare region. Such a reversal requires creating a domain wall whose free energy is  $\sigma L_{\text{RR}}^{d-1}$ . Therefore, the relaxation time of an island of linear size  $L_{\text{RR}}$  is given by  $\xi_t(L_{\text{RR}}) \sim \tau_0 \exp[\sigma L_{\text{RR}}^{d-1}]$ . The factor  $1/T$  in the Arrhenius behavior has been absorbed into the surface tension  $\sigma$ , and  $\tau_0$  is a microscopic time scale. For large  $t$ , the integral (32) can be calculated using the saddle point method leading to an even slower time dependence of the form

$$\ln C(t) \sim -(\ln t)^{d/(d-1)} . \quad (35)$$

More recently, this asymptotic decay of the autocorrelation function was established rigorously for disordered discrete lattice spin systems with *bounded* disorder distributions [90, 91]. It should be noted however, that in Monte-Carlo simulations [92–95] the time dependence of  $C(t)$  seems to follow a stretched exponential form  $\ln C(t) \sim -t^x$  rather than the asymptotic form (35). This suggests that the asymptotic regime is only reached after a very long transient time interval. We also point out that (35) is universally valid only for bounded disorder distributions; unbounded distributions can lead to asymptotic forms different from (35) as was shown in Ref. [96].

So far our discussion of dynamic rare region effects has focused on Ising systems. For continuous spin symmetry, the behavior of the autocorrelation function at and above the clean critical temperature  $t_c^0$  remains to be given by relations (33) and (34). However, in the Griffiths region,  $T_c(p) < T < T_c^0$ , the behavior changes. The relaxation time of a rare region is much shorter than for Ising spins since there is no free energy barrier hindering relaxation. Rather, the relaxation occurs by diffusion of the order parameter, driven by thermal noise. Following Bray [56], the relaxation time can be estimated as follows: The change of cluster magnetization during some small time interval  $\delta t$  is  $\delta \mathbf{M} \sim L_{\text{RR}}^{d/2}$  since the noise at different sites adds incoherently. Since several of such steps also act incoherently, the change of magnetization after

time  $t$  is  $\delta\mathbf{M}(t) \sim t^{1/2}L_{\text{RR}}^{d/2}$ . Complete relaxation has occurred for  $\delta\mathbf{M}(t) \sim \mathbf{M} \sim L_{\text{RR}}^d$  giving  $\xi_t \sim L_{\text{RR}}^d$ . Putting this into (32) and evaluating the integral by the saddle point method gives

$$\ln C(t) \sim -t^{1/2}, \quad (36)$$

a much faster decay than the corresponding equation (35) for the Ising case. The same result has also been derived in the large- $N$  limit (where  $N$  refers to the number of spin components) [55]. In contrast to the Ising case, Monte-Carlo simulations of a diluted Heisenberg magnet [93] are in good agreement with (36) suggesting that the asymptotic regime is reached much faster in the Heisenberg case than in the Ising case.

#### 4.5. Disorder correlations and enhanced rare region effects

In addition to localized defects such as impurity atoms or vacancies, many realistic systems also contain extended defects such as dislocations or grain boundaries. They can be modelled by quenched disorder that is perfectly correlated in one (linear defects) or two (planar defects) dimensions.

It is interesting to ask whether such disorder correlations increase or decrease the influence of the defects. Naively, one might expect that disorder which is perfectly correlated in  $d_{\text{cor}}$  dimensions but uncorrelated in the remaining  $d_{\text{ran}} = d - d_{\text{cor}}$  dimensions is weaker than uncorrelated disorder because the system is “random only in some of the directions”. However, this naive assumption turns out to be incorrect. In fact, the opposite is true: Long-range disorder correlations enhance the influence of the defects because “it is harder to average out an extended fluctuation than a local one”.

The first systematic study of a phase transition in the presence of extended defects was carried out more than 30 years ago by McCoy and Wu. In a series of papers [32, 33, 97–100], these authors studied a disordered two-dimensional Ising model, now known as McCoy-Wu model, in which all horizontal bonds are identical while all vertical bonds in each row are the same. However, the vertical bonds vary from row to row as independent random variables. Thus, the disorder is perfectly correlated in one dimension (the horizontal direction) but uncorrelated in the other (the vertical direction). This implies  $d_{\text{cor}} = d_{\text{ran}} = 1$ .

The McCoy-Wu model in zero magnetic field is partially exactly solvable with transfer-matrix type methods (see also [101]). McCoy and Wu [33] analyzed the free energy and found that there is only an essential singularity at the critical temperature. No exact results could be obtained for the spontaneous magnetization, but McCoy [98, 99] calculated the properties of the spins on the surface of a half-plane cut perpendicular to the random direction. Because of Griffiths’ theorem [102], magnetization and susceptibility of these boundary spins provide lower bounds for the corresponding bulk values. McCoy found the surprising result that the susceptibility is infinite for an entire range of temperatures above the critical temperature  $T_c$ . He also found that there is an even larger range of temperatures in which the susceptibility exists but the magnetization is still a nonanalytic function of the field. These unusual results initially gave rise to some confusion as to whether the phase transition in the McCoy-Wu model is sharp or smeared.

By now, it has become clear that the transition is actually sharp, i.e., the spontaneous magnetization develops as a collective effect of the whole system at the

critical temperature  $T_c$  which is also the (only) temperature at which the spatial correlation length becomes infinite. The unusual behavior of the susceptibility in the vicinity of the critical temperature is a rare region effect that can be understood as follows: For simplicity, let us assume that the random vertical bonds in the McCoy-Wu model have a binary probability distribution

$$P(J) = (1 - p)\delta(J - J_0) + p\delta(J - cJ_0) \quad (37)$$

with  $c < 1$ . Thus,  $p$  is the probability of a vertical bond being weak. In an infinite sample, one can find arbitrarily large “stacks” of rows with only strong vertical bonds. The probability for finding such a rare region of width  $L_{\text{RR}}$  is given by

$$w(L_{\text{RR}}) \sim (1 - p)^{L_{\text{RR}}} \sim \exp(-\tilde{p}L_{\text{RR}}) \quad (38)$$

with  $\tilde{p} = -\ln(1 - p)$ . In the Griffiths region below the transition temperature  $T_c^0$  of the clean system with only strong vertical bonds, these rare regions are locally in the ordered phase. Since each rare region is infinite in the horizontal direction and of finite width  $L_{\text{RR}}$  in the vertical direction, it is equivalent to a one-dimensional Ising model with an effective interaction proportional to  $L_{\text{RR}}$ . As such, it cannot undergo a phase transition by itself but its susceptibility increases exponentially with its width,

$$\chi(L_{\text{RR}}) \sim \frac{1}{T} \exp(aL_{\text{RR}}) \quad (39)$$

where the constant  $a$  vanishes at the clean critical temperature  $T_c^0$  and increases with decreasing temperature (see, e.g., [2]).

The rare region contribution to the total susceptibility can be obtained by summing over all rare regions,

$$\chi_{\text{RR}} \sim \int dL_{\text{RR}} w(L_{\text{RR}}) \chi(L_{\text{RR}}). \quad (40)$$

This integral diverges when  $a > \tilde{p}$  before the true critical point of the dirty system is reached (the divergence does *not* require coherence between the rare regions). Thus, in the Griffiths region of the McCoy-Wu model, the exponential rarity of large rare regions is overcome by an exponential increase of a rare region’s susceptibility with its size. The probability distribution  $w_\chi$  of local susceptibilities  $\chi_l$  can be obtained by combining (38) and (39), leading to

$$w_\chi(\chi_l) \sim \chi_l^{-1/z'-1} \quad (41)$$

where  $z' = a/\tilde{p}$  is an exponent that varies continuously throughout the Griffiths region. In contrast, the corresponding probability distribution for the case of uncorrelated disorder decreases exponentially for large  $\chi_l$  because the susceptibility of a rare region only increases like a power of  $L_{\text{RR}}$ , see equation (23). The perfect disorder correlations in the McCoy-Wu model therefore enhance the rare region effects from exponentially weak classical Griffiths singularities to much stronger power-law singularities that are sometimes called Griffiths-McCoy singularities.

Let us emphasize that none of the peculiar properties of McCoy and Wu’s exact solution are reflected in the standard perturbative renormalization group approach to the problem. Early renormalization group work [103] based on a single expansion in  $\epsilon = 4 - d$  did not produce a critical fixed point. This was interpreted as a smeared transition or a first order one [104,105]. An alternative approach, the double- $\epsilon$  expansion in powers of  $\epsilon = 4 - d$  and the number  $d_{\text{cor}}$  of correlated dimensions [106–108] gave rise to a critical fixed point with a conventional power-law singularity in the

free energy rather than the essential singularity found in McCoy and Wu's solution. However, the general arguments on the importance of rare regions made in section 3.3 point to a qualitative difference between  $d_{\text{cor}} = 1$  in the McCoy-Wu model and  $d_{\text{cor}} \ll 1$  assumed in the double- $\epsilon$  expansion. For  $d_{\text{cor}} = 1$ , the rare regions (whose effective dimension  $d_{\text{RR}} = d_{\text{cor}}$ ) are at the lower critical dimension  $d_c^-$ , leading to the exponential size dependence (39) of the susceptibility. In contrast, for  $d_{\text{cor}} < 1$ , the rare regions are below  $d_c^-$ . Thus, the susceptibility depends on the rare region size via a power law, and the Griffiths effects in the double- $\epsilon$  expansion are exponentially small. Therefore it is not surprising that the double- $\epsilon$  expansion approach cannot capture the physics of the McCoy-Wu model.

The partition function of the McCoy-Wu model written in terms of the transfer matrix in horizontal direction is essentially equivalent to the partition function of a quantum mechanical random transverse-field Ising model [12, 101]. Much insight can therefore be obtained by studying this quantum Ising model. In fact, the behavior of the McCoy-Wu model remained incompletely understood until Fisher [34, 35] applied a version of the Ma-Dasgupta-Hu [36] real-space renormalization group to the random transverse-field Ising model. We will discuss these developments in more detail in sections 5.1 to 5.3.

#### 4.6. Smearing phase transition in an Ising model with planar defects

In the last subsections we have seen that perfect disorder correlations in one direction greatly enhance the rare region effects. In this subsection, we consider planar defects, i.e., disorder perfectly correlated in two dimensions. Recently, it has been shown [63, 64] that they have even more dramatic consequences: They completely destroy the sharp Ising phase transition by smearing.

Most of our arguments below will be rather general. If necessary for definiteness, we focus on a three-dimensional Ising model with nearest-neighbor interactions on a cubic lattice. In the clean system, all interactions are identical and have the value  $J_0$ . The defects are modelled via 'weak' bonds randomly distributed in one dimension (uncorrelated direction). The bonds in the remaining two dimensions (correlated directions) remain equal to  $J_0$ . The system effectively consists of blocks separated by parallel planes of weak bonds. Thus,  $d_{\text{ran}} = 1$  and  $d_{\text{cor}} = 2$ . The Hamiltonian of the system is given by:

$$H = - \sum_{\substack{i=1, \dots, L_{\text{ran}} \\ j, k=1, \dots, L_{\text{cor}}}} J_i S_{i,j,k} S_{i+1,j,k} - \sum_{\substack{i=1, \dots, L_{\text{ran}} \\ j, k=1, \dots, L_{\text{cor}}}} J_0 (S_{i,j,k} S_{i,j+1,k} + S_{i,j,k} S_{i,j,k+1}), \quad (42)$$

where  $L_{\text{ran}}(L_{\text{cor}})$  is the length in the uncorrelated (correlated) direction,  $i$ ,  $j$  and  $k$  are integers counting the sites of the cubic lattice, and  $J_i$  is the random coupling constant in the uncorrelated direction. The  $J_i$  are drawn from a binary distribution:

$$P(J) = (1 - p) \delta(J - J_0) + p \delta(J - cJ_0) \quad (43)$$

characterized by the concentration  $p$  and the relative strength  $c$  of the weak bonds ( $0 < c \leq 1$ ).

Let us now consider rare regions in this system which consist of "thick slabs" containing only strong bonds in the uncorrelated direction. As in the case of point or linear defects, for temperatures below the clean critical temperature  $T_c^0$ , these rare regions are locally in the ordered phase even if bulk system is still in the disordered (paramagnetic) phase. However, the behavior of locally ordered planar rare regions

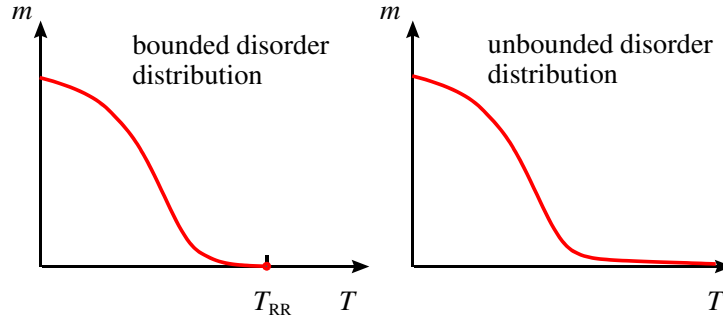


**Figure 3.** Schematic behavior of the magnetization in the tail of a smeared phase transition for bounded and unbounded disorder distributions. For details see text.

differs *qualitatively* of that of localized or linear rare regions. Each planar rare region is infinite in the two correlated dimensions but finite in the uncorrelated direction. Thus, it is equivalent to a two dimensional Ising model that can undergo a real phase transition independently of the rest of the system. Thus, each rare region can independently develop true static order with a non-zero static value of the local magnetization. (Griffiths theorem [102] ensures that the interaction of the rare region with the paramagnetic bulk system can only *increase* its magnetization over that of a completely isolated “slab”.) Once static order has developed, the magnetizations of different rare regions can be aligned by an infinitesimally small interaction or external field. The resulting phase transition will thus be markedly different from a conventional continuous phase transition. At a conventional transition, a non-zero order parameter develops as a collective effect of the entire system which is signified by a diverging correlation length of the order parameter fluctuations at the critical point. In contrast, in a system with planar defects, different parts of the system (in the uncorrelated direction) will order independently, at different temperatures. Therefore the global order will develop inhomogeneously and the correlation length in the uncorrelated direction will remain finite at all temperatures. This defines a *smeared* or *rounded* phase transition.

Note that similar to the Griffiths effects discussed in the proceeding sections, the properties of the smeared transition depend on whether or not the disorder distribution is bounded (see figure 3). If the disorder distribution is bounded like the binary distribution (43), there is a true paramagnetic phase with zero total order parameter at high temperatures. At some temperature  $T_{RR}$  (identical to the clean critical temperature  $T_c^0$  for the distribution (43)), a non-zero order parameter starts to develop on the rare regions, accompanied by an essential singularity in the free energy density (which stems from the probability for finding a rare region). In contrast, for distributions that are unbounded in the sense that they permit rare regions with a local  $T_c = \infty$  (e.g., a Gaussian distribution), the total order parameter is non-zero for *all* temperatures, and the free energy density is analytic.

#### 4.7. Optimal fluctuation theory for smeared phase transition

The leading thermodynamic behavior in the tail of the smeared transition can be determined using optimal fluctuation theory similar to section 4.2. Following [63],



we develop this theory for the general case of  $d_{\text{cor}} \geq 2$  correlated dimensions and  $d_{\text{ran}} = d - d_{\text{cor}}$  uncorrelated dimensions. We first consider bounded disorder distributions like the binary distribution (43) and later briefly describe the differences for Gaussian disorder.

The probability  $w$  of finding a thick slab of width  $L_{\text{RR}}$  devoid of any weak bonds is, up to pre-exponential factors, given by

$$w(L_{\text{RR}}) \sim \exp(-\tilde{p}L_{\text{RR}}^{d_{\text{ran}}}) . \quad (44)$$

with  $\tilde{p} = -\ln(1-p)$ . Such a rare region develops static long-range order at some temperature  $T_c(L_{\text{RR}})$  below the clean critical point  $T_c^0$ . The value of  $T_c(L_{\text{RR}})$  varies with the size of the region: The largest islands develop long-range order closest to the clean critical point. As discussed in section 2.4, finite size scaling for the clean system (because the rare regions are free of defects) yields

$$T_c^0 - T_c(L_{\text{RR}}) = |r_c(L_{\text{RR}})| = A L_{\text{RR}}^{-\phi} \quad (45)$$

where  $\phi$  is the finite-size scaling shift exponent and  $A$  is the amplitude for the crossover from  $d$  dimensions to a slab geometry infinite in  $d_{\text{cor}}$  dimensions but finite in  $d_{\text{ran}} = d - d_{\text{cor}}$  dimensions. If the total dimensionality  $d$  is below the upper critical dimension  $d_c^+ = 4$ , hyperscaling is valid and the shift exponent  $\phi = 1/\nu$ . The reduced temperature  $r = T - T_c^0$  measures the distance from the *clean* critical point. Combining (44) and (45) we obtain the probability for finding a rare region which becomes critical at  $r_c$  as

$$w(r_c) \sim \exp(-B |r_c|^{-d_{\text{ran}}/\phi}) \quad (\text{for } r \rightarrow 0-) \quad (46)$$

where the constant  $B$  is given by  $B = \tilde{p} A^{d_{\text{ran}}/\phi}$ . The total (or average) order parameter  $m$  is obtained by integrating over all rare regions having  $r_c(L_{\text{RR}}) > r$ . Since the functional dependence on  $r$  of the order parameter on a given island is of power-law type it only enters the pre-exponential factors. Therefore we obtain to exponential accuracy

$$m(r) \sim \exp(-B |r|^{-d_{\text{ran}}/\phi}) \quad (\text{for } r \rightarrow 0-) . \quad (47)$$

Once a nonzero density of ordered and aligned rare regions exist, the Ising symmetry is spontaneously globally broken. The rare regions produce an effective background magnetic field everywhere in space which cuts off any possible further singularities.

The spatial magnetization distribution in the tail of the smeared transition is very inhomogeneous. On the already ordered islands, the local order parameter  $m(\mathbf{x})$  is of the same order of magnitude as in the clean system. Away from these islands it decays exponentially with the distance from the nearest island. The *typical* local order parameter  $m_{\text{typ}}$  can be estimated via the typical distance of any point from the nearest ordered island. From (46) we obtain

$$x_{\text{typ}} \sim \exp(B |r|^{-d_{\text{ran}}/\phi}/d_{\text{ran}}) . \quad (48)$$

At this distance from an ordered island, the local order parameter has decayed to

$$m_{\text{typ}} \sim e^{-x_{\text{typ}}/\xi_0} \sim \exp\left[-C \exp(B |r|^{-d_{\text{ran}}/\phi}/d_{\text{ran}})\right] \quad (49)$$

where  $\xi_0$  is the bulk correlation length (which is finite and changes slowly throughout the tail region of the smeared transition) and  $C$  is constant. A comparison with (47) gives the relation between  $m_{\text{typ}}$  and the thermodynamic order parameter  $m$ ,

$$|\log m_{\text{typ}}| \sim m^{-1/d_{\text{ran}}} . \quad (50)$$

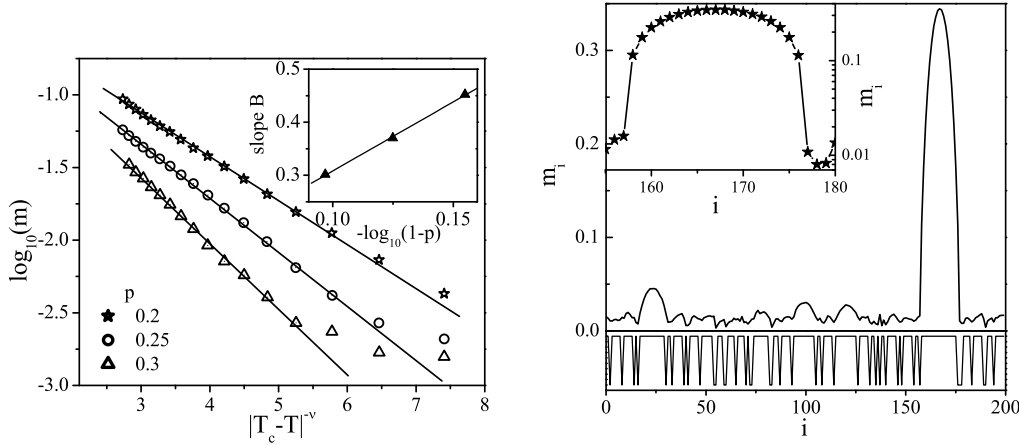


**Figure 4.** Left: Logarithm of the magnetization  $m$  as a function of  $|T_c^0 - T|^{-\nu}$  ( $\nu = 0.627$ ) for impurity concentrations  $p = 0.2, 0.25, 0.3$  and strength  $c = 0.1$ . Inset: Decay slope  $B$  as a function of  $-\log(1-p)$ . Right: Local magnetization  $m_i$  as function of position  $i$  in the uncorrelated direction at temperature  $T = 4.425$  (one particular disorder realization). Lower panel: Coupling constant  $J_i$  in the uncorrelated direction as a function of position  $i$ . Inset: Log-linear plot of the region in the vicinity of the largest ordered island (from [64]).

Thus,  $m_{\text{typ}}$  decays exponentially with  $m$  indicating an extremely broad distribution of the local order parameter  $m_{\mathbf{x}} = \langle S_{\mathbf{x}} \rangle$ . Its functional form has been determined in reference [63], it reads

$$P[\log(m_{\mathbf{x}})] \sim |\log(m_{\mathbf{x}})|^{d_{\text{ran}}-1} \quad (\text{for } m_{\mathbf{x}} \ll 1). \quad (51)$$

These predictions of the optimal fluctuation theory have been tested by large scale computer simulations. A model with infinite-range interactions in the correlated directions was studied in reference [63]. This mean-field type calculation permitted large system sizes of up to  $L_{\text{ran}} = 10^6$  making it very suitable for identifying effects of rare events. The results were in excellent agreement with the theoretical predictions. Note that a similar mean-field model had been investigated earlier [109] but for much smaller sizes of up to  $L_{\text{ran}} = 1000$ . The raw data in this paper are very similar to reference [63], but they were interpreted in terms of power-law critical behavior with an unusually large order parameter exponent  $\beta \approx 3.6$ . This may be partially due to an unfortunate choice of parameters (in particular, a higher impurity concentration of  $p = 0.5$ ) which makes it hard to extract the functional form of the magnetization tail.

Recently, the short-range Ising model with planar defects (42) has been studied by large scale Monte-Carlo simulations [64] using the Wolff cluster algorithm [110]. The results confirm the smeared transition scenario and the predictions of optimal fluctuation theory for a realistic model. A typical result for the magnetization in the tail of the smeared transition below  $T_c^0 \approx 4.511$  is presented in the left panel of figure 4. It shows the logarithm of the total magnetization vs.  $|T_c^0 - T|^{-\nu}$  averaged over 240 samples for system size  $L_{\text{ran}} = 200$ ,  $L_{\text{cor}} = 280$  and three disorder concentrations  $p = \{0.2, 0.25, 0.3\}$ . Here,  $\nu = 0.627$  is the three-dimensional clean critical Ising exponent. For all three concentrations the data follow (47) over more than an order of magnitude in  $m$ . The deviation from the straight line for small  $m$  is due to the

conventional finite size effects. In the inset we show that the decay constant  $B$  depends linearly on  $\tilde{p} = -\log(1-p)$ .

The right panel of figure 4 illustrates the very inhomogeneous character of the local magnetization in the tail of the smeared transition. It displays the local magnetization  $m_i$  of a particular disorder realization as a function of the position  $i$  in the uncorrelated direction for the size  $L_{\text{ran}} = 200$ ,  $L_{\text{cor}} = 200$  at a temperature  $T = 4.425$  in the tail of the smeared transition. The lower panel shows the local coupling constant  $J_i$  as a function of  $i$ . The figure shows that a sizable magnetization has developed on the longest island only (around position  $i = 160$ ). One can also observe that order starts to emerge on the next longest island located close to  $i = 25$ . Far from these islands the system is still in its disordered phase.

As discussed in the last subsection, the functional form of the tail of the smeared transition is nonuniversal. In particular, for unbounded disorder distributions, it differs from (47). In the case of Gaussian disorder, the magnetization for large  $r$  behaves as  $m \sim \exp(-Br^{2-d_{\text{ran}}/\phi})$ , i.e., the magnetization tail reaches all the way to  $T = \infty$  [63].

#### 4.8. Dynamics at a smeared phase transition

The static magnetic order on the rare regions in an Ising model with planar defects also modifies the dynamics. The leading long-time behavior can be determined by generalizing the approach of section 4.4 to the case of extended defects, as was done in reference [111]. The behavior above and at the clean critical temperature  $T_c^0$  turns out to be identical to the conventional dynamic Griffiths effects discussed in section 4.4. This is not surprising because above  $T_c^0$  there is no difference between the Griffiths and the smearing scenarios: All rare regions are locally still in the disordered phase. Specifically, the asymptotic time dependence of the spin autocorrelation function  $C(t)$  right at the clean critical temperature is given by

$$\ln C(t) \sim -\tilde{p}^{z/(d_{\text{ran}}+z)} t^{d_{\text{ran}}/(d_{\text{ran}}+z)} \quad (52)$$

where  $z$  is the clean critical exponent of the  $d$ -dimensional system. For temperatures below  $T_c^0$ , the behavior at a smeared transition differs from the dynamic Griffiths effects of section 4.4. Here, at short times before a crossover time  $t_x$ , the decay of  $C(t)$  is still given by the stretched exponential (52). For  $t > t_x$ , the system realizes that some of the rare regions have developed static order and contribute to a non-zero equilibrium value  $C(\infty)$  of the autocorrelation function  $C(t)$ . The approach of  $C(t)$  to this equilibrium value follows a nonuniversal power law

$$C(t) - C(\infty) \sim t^{-\psi} . \quad (53)$$

The value of  $\psi$  could not be found since it depends on the pre-exponential factors neglected in the optimal fluctuation theory.

Reference [111] also discussed the rare region contribution to the nonequilibrium relaxation of the magnetization in the tail of the smeared transition. It turned out to be controlled by decay laws with the same functional form as those of the autocorrelation function. These results were confirmed by computer simulations of a infinite-range model similar to that in reference [63]. Figure 5 shows a typical result of these simulations. The left panel shows the time evolution of the magnetization of a large system of  $L_{\text{ran}} = 10^5$  sites, averaged over 25 disorder realizations, for several temperatures from  $T = 2.8$  to  $3.25$  in the vicinity of the clean critical point which is  $T_c^0 = 3$  for the infinite-range model. The behavior at  $T_c^0$  follows the stretched

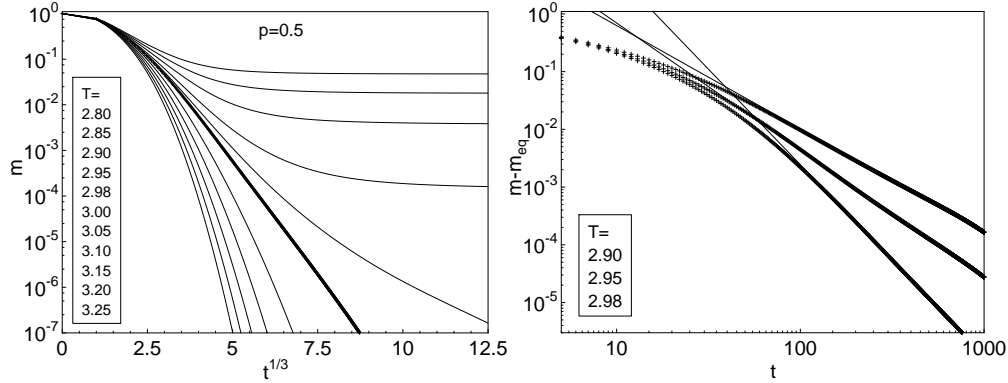


**Figure 5.** Left: Time evolution of the magnetization for several temperatures from  $T = 2.8$  to  $3.25$  (top to bottom) in the vicinity of the clean critical point  $T_c^0 = 3$ . The impurity concentration is  $p = 0.5$  their strength is  $c = 0.2$ . The runs start from a fully polarized state at  $t_0 = 0$  and go to  $t_{max} = 2000$ . Right: Double-logarithmic plot of the approach of the magnetization to the equilibrium value for  $T = 2.90, 2.95$  and  $2.98$  (top to bottom). The straight lines are fits to power laws yielding exponents of 1.78, 2.20, and 3.31, respectively (from [111]).

exponential  $\ln m(t) \sim -t^{1/3}$  as expected from the analog of (52) because the mean-field value of the clean dynamical exponent is  $z = 2$ , and  $d_{\text{ran}} = 1$ . For  $T > T_c^0$ , the magnetization decay is faster, and a detailed analysis [111] shows it to be simple exponential. For  $T < T_c^0$ , the magnetization approaches a nonzero equilibrium value  $m_{eq}$ . The approach to this equilibrium value is analyzed in the right panel of figure 5. The difference  $m(t) - m_{eq}$  follows a nonuniversal power law  $m(t) - m_{eq} \sim t^{-\psi}$ .

## 5. Quantum phase transitions

In section 4, we have seen that rare region effects in classical systems with generic short-range-correlated disorder are exponentially weak and that stronger effects require long-range disorder correlations. In this section, we discuss quantum phase transitions which occur at zero temperature and thus require the inclusion of the imaginary time direction, as discussed in section 2. Quenched impurities are time independent, the disorder is therefore always correlated in at least one of the relevant dimensions, and we generically expect rare region effects at a quantum phase transition to be stronger than at a classical transition.

The main focus of this section will again be on order-disorder transitions between conventional phases that can be described by Landau-Ginzburg-Wilson theories. However, the concept of quantum rare region effects or quantum Griffiths singularities is much broader, and in section 5.7, we will briefly discuss other examples.

### 5.1. Random transverse field Ising model

One of the prototypical models (if not *the* prototypical model) displaying a quantum phase transition is the transverse field Ising model. Its Hamiltonian

$$H = - \sum_{\langle i,j \rangle} J_{ij} \hat{S}_i^z \hat{S}_j^z - \sum_i h_i^x \hat{S}_i^x \quad (54)$$

consists of two noncommuting parts, the first being the exchange interaction between the  $z$ -components of the spin- $\frac{1}{2}$  operators  $\hat{S}_i$  on nearest neighbor sites of a hypercubic lattice in  $d$  space dimensions. The second part describes the interaction of  $x$ -components of the spins with a magnetic field in transverse ( $x$ -) direction.

Let us first briefly consider the clean model with all  $J_{ij} \equiv J$  and all  $h_i^x \equiv h^x$ . It can be viewed, e.g., as a model for the magnetic behavior of LiHoF<sub>4</sub> in a transverse field [112].<sup>+</sup> Without the field, the exchange interaction favors parallel spins pointing in positive or negative  $z$ -direction. Thus, for  $h^x = 0$ , the ground state is ferromagnetic. The transverse magnetic field  $h^x$  induces spin flips between the “up” and “down” states ( $2\hat{S}^x = \hat{S}^+ + \hat{S}^-$ ) and reduces the magnetization in  $z$ -direction. For sufficiently strong transverse field  $h^x > h_c^x$ , this destroys the magnetic long-range order. The quantum critical point at  $h_c^x$  was indeed observed experimentally [112]. The partition function of the transverse field Ising model (54) in  $d$  space dimensions is equivalent to that of a classical Ising model in  $d + 1$  space dimensions [12, 113] with imaginary time playing the role of the extra dimension. This is an example of the quantum-classical mapping discussed in section 2.3. The quantum phase transition of the  $d$ -dimensional clean transverse-field Ising model is therefore in the  $d + 1$  dimensional classical Ising universality class.

Quenched disorder can be introduced into the transverse field Ising model by making the interaction  $J_{ij}$  and/or the transverse field  $h_i^x$  a random function of position. We will only consider the case where all  $J_{ij}$  remain positive. (Introducing negative, i.e., antiferromagnetic bonds introduces frustration that can lead to qualitatively new physics such as spin glass behavior [114, 115].) Applying the above-mentioned quantum-classical mapping now leads to a disordered classical Ising model. However, because the disorder in the quantum model is time-independent, the disorder in the equivalent classical model is perfectly correlated in one of the dimensions, viz., the one representing the imaginary time direction. Specifically, the one-dimensional random transverse-field Ising model (the random transverse Ising chain) maps onto the classical McCoy-Wu model [32, 33] discussed in section 4.5 when only the interactions  $J_{ij}$  are random, or on its generalization by Shankar and Murthy [101] when both  $J_{ij}$  and  $h_i^x$  are random.

Even though the free energy of the random transverse field Ising chain can be obtained exactly using transfer matrix methods analogous to those applied to the McCoy-Wu model [33, 101], many other properties including the spontaneous magnetization and the average spin correlations could not be obtained this way. A better understanding of this model was achieved in the early and mid 1990s by two methods: (i) a phenomenological optimal fluctuation theory of rare region effects [57] and (ii) an asymptotically exact real space renormalization group [34, 35]. We will discuss these approaches in the next two subsections.

## 5.2. Quantum Griffiths singularities: Optimal fluctuation arguments

In this subsection we develop optimal fluctuation arguments for the rare region effects in the random transverse field Ising model. These arguments, which were introduced by Thill and Huse [57] and applied to both quantum Ising spin glasses [58, 59] and the random transverse field Ising model [39, 116], can be viewed as quantum version of the

<sup>+</sup> The actual interaction in LiHoF<sub>4</sub> is of long-range dipolar nature, so the nearest-neighbor interaction in the model Hamiltonian (54) constitutes an approximation.

arguments given in section 4.5 for the McCoy-Wu model (for an early brief review see also reference [117]).

For definiteness, we consider a situation with random interactions  $J_{ij}$  but a homogeneous transverse field  $h^x$ . The probability distribution of the interactions is assumed to be binary,  $P(J) = (1-p)\delta(J-J_0) + p\delta(J-cJ_0)$  with  $0 < c < 1$ . Generalizations to other distributions and randomness in the transverse fields are straight forward. Consider a rare strongly-coupled spatial region of linear size  $L_{\text{RR}}$  having only strong bonds. The probability for finding such a region is exponentially small in its volume

$$w(L_{\text{RR}}) \sim \exp(-\tilde{p}L_{\text{RR}}^d). \quad (55)$$

where  $\tilde{p} = -\ln(1-p)$  as before. We are interested in the Griffiths region of the disordered phase where the applied transverse field  $h^x > h_c^x$  but  $h^x < h_{c,\text{clean}}^x$  such that the rare region is locally ordered. The energy levels of a locally ordered cluster can be described as follows [118]. The two lowest states correspond to the states of a single effective Ising spin with magnet moment  $\sim L_{\text{RR}}^d$  in an effective transverse field  $h_{\text{eff}}(L_{\text{RR}})$ . It can be estimated to be  $h_{\text{eff}}(L_{\text{RR}}) \sim h^x \exp[-aL_{\text{RR}}^d]$  since the ‘‘up’’ and ‘‘down’’ states of the effective spin are coupled in perturbation theory of order  $L^d$  in  $h^x$ . The constant  $a$  increases continuously with the difference between  $h_{c,\text{clean}}^x$  and  $h_c^x$ . The energy gap of a rare region of linear size  $L_{\text{RR}}$  thus decreases exponentially with its volume

$$\epsilon(L_{\text{RR}}) \sim \exp(-aL_{\text{RR}}^d). \quad (56)$$

An analogous result can be obtained by employing the quantum-classical mapping and representing the rare region as a one-dimensional classical Ising model [57, 59]. The exchange interaction in the time-like direction is then proportional to the spatial volume of the rare region,  $J_{\text{eff}} \sim L_{\text{RR}}^d$ . Together with the fact that the gap in the one-dimensional Ising model depends exponentially on the interaction, this leads to (56), see also section 4.5.

Combining equations (55) and (56) leads to a power-law density of states for the low-energy excitations of the rare regions,

$$\rho(\epsilon) \sim \epsilon^{\tilde{p}/a-1} = \epsilon^{d/z'-1} \quad (57)$$

where the second equality defines the customarily used dynamical exponent  $z'$  [116]. It continuously varies with disorder concentration or distance from the clean critical point. The power-law density of states (57) is obtained here because the exponentially small probability for finding a rare region is compensated by the exponential dependence of its energy gap on its volume. In contrast, in generic classical systems, such as the disordered Ising models of sections 4.1 to 4.3, the gap depends on the volume via a power law, and the resulting rare region density of states is exponentially small.

Many results follow from the power-law density of states (57). For instance, a region with a local energy gap  $\epsilon$  has a local spin susceptibility that decays exponentially in imaginary time,  $\chi_{\text{loc}}(\tau \rightarrow \infty) \propto \exp(-\epsilon\tau)$ . Averaging by means of  $\rho$  yields

$$\chi_{\text{loc}}^{\text{av}}(\tau \rightarrow \infty) \propto \tau^{-d/z'}. \quad (58)$$

The temperature dependence of the static average susceptibility is then

$$\chi_{\text{loc}}^{\text{av}}(T) = \int_0^{1/T} d\tau \chi_{\text{loc}}^{\text{av}}(\tau) \propto T^{d/z'-1}. \quad (59)$$

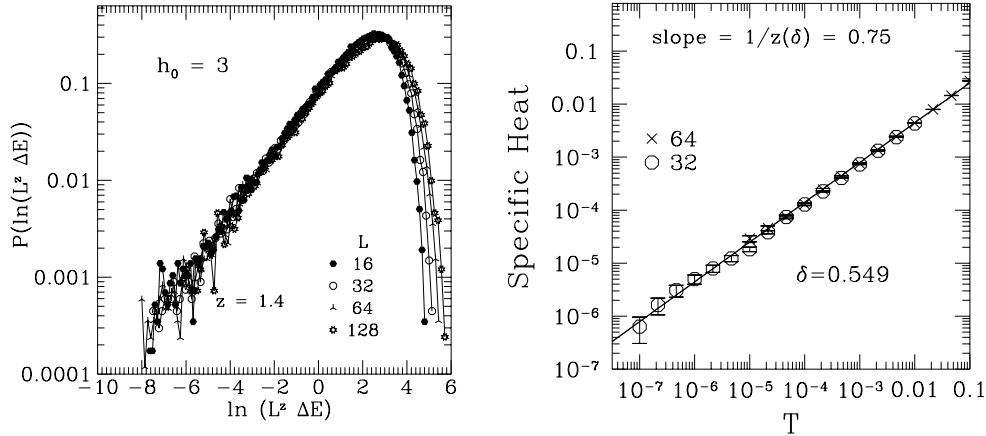


**Figure 6.** Left: Scaled probability distribution of the energy gap for a one-dimensional random transverse Ising model in the Griffiths region ( $h_0 > h_c^x = 1$ ) for different system sizes  $L$ . A fit of the low-energy tail to (57) gives  $z' \approx 1.4$  (from [39]). Right: Specific heat as a function of temperature for the same system. A fit to  $\Delta C \propto T^{d/z'}$  gives  $1/z' \approx 0.75$  (from [116])

If  $d < z'$ , the local zero-temperature susceptibility diverges, even though the system is globally still in the disordered phase. The contribution of the rare regions to the specific heat  $C$  can be obtained from

$$\Delta E = \int d\epsilon \rho(\epsilon) \epsilon e^{-\epsilon/T} / (1 + e^{-\epsilon/T}) \propto T^{d/z'+1} \quad (60)$$

which gives  $\Delta C \propto T^{d/z'}$ . To determine the zero temperature magnetization in a small ordering field  $H$  in  $z$ -direction we note that all rare regions with  $\epsilon < H$  are (almost) fully polarized while the rare regions with  $\epsilon > H$  have a very small magnetization. Thus,

$$m(H) \sim \int_0^H d\epsilon \rho(\epsilon) \sim H^{d/z'} . \quad (61)$$

Other observables can be determined in a similar fashion. The power-law density of states (57) in the Griffiths region of a random transverse field Ising magnet and the resulting power-law singularities (58), (59), (60), (61) are called the quantum Griffiths singularities or the Griffiths-McCoy singularities.

The power-law quantum Griffiths singularities predicted by the optimal fluctuation arguments above have been verified in numerical simulations. Young and Rieger [39] mapped the one-dimensional random transverse field Ising chain onto a system of non-interacting fermions which was then solved numerically. An example of the resulting density of states in the Griffiths region is shown in the left panel of figure 6. The low-energy tail of this distribution shows power-law behavior. A fit to the predicted form (57) gives  $z' \approx 1.4$  for the parameter set studied. The right panel of figure 6 shows the temperature dependence of the specific heat for the same system as calculated by Young [116]. As predicted after (60), this dependence is of power-law type, and a fit gives the exponent  $z' \approx 4/3$  in good agreement with the value from

the density of states. These numerical simulations have later been extended to surface quantities and to the ferromagnetic phase [119] as well as to nonlinear susceptibility, higher excitations, and the energy autocorrelation function [120].

### 5.3. Strong-disorder renormalization group and infinite-randomness critical point in one dimension

While the optimal fluctuation arguments presented in the last subsection provide a simple qualitative understanding of the behavior of random transverse field Ising model in the Griffiths region, they do not give quantitative results and they also cannot be applied to the quantum critical point itself. The behavior of the random transverse field Ising model was therefore not fully understood before Fisher [34, 35] applied a novel real-space or rather energy-space renormalization group method to the problem. This method which is now often called the “strong-disorder renormalization group” has recently been reviewed in detail by Iglói and Monthus [121]. Therefore we will only briefly explain its basic idea and then discuss the results.

The strong-disorder renormalization group was introduced by Ma, Dasgupta and Hu [36] for the random antiferromagnetic spin chain. Since then it has been used extensively for various disorder problems including random quantum spin chains [38, 122–133] and ladders [134–137] as well as random walks [138–140] and other nonequilibrium systems [41, 42, 141, 142]. The main idea of the strong-disorder renormalization group is to take the strongest coupling in the system and find the ground state of the corresponding part of the Hamiltonian exactly. The coupling to the rest of the system is treated perturbatively. One then neglects the excited states involving the strong coupling and derives a new effective Hamiltonian with the number of degrees of freedom reduced. This basic renormalization group step is repeated ad infimum.

We now follow reference [35] and apply this idea to the random transverse field Ising model (54) in one dimension. We choose first the largest of the set of couplings,  $\Omega = \max(h_i^x, J_{ij})$ . If the largest coupling is a field, say  $h_2^x$ , the unperturbed Hamiltonian is  $-h_2^x \hat{S}_2^x$  with ground state  $|\rightarrow_2\rangle$  and excited state  $|\leftarrow_2\rangle$  separated by a gap  $h_2^x$ . The coupling of  $\hat{S}_2$  to the rest of the system  $-J_{12} \hat{S}_1^z \hat{S}_2^z - J_{23} \hat{S}_2^z \hat{S}_3^z$  is treated in second order perturbation theory. This yields an effective interaction of the form  $-\bar{J}_{13} \hat{S}_1^z \hat{S}_3^z$  with the effective exchange constant

$$\bar{J}_{13} \approx J_{12} J_{23} / h_2^x . \quad (62)$$

We now throw out  $\hat{S}_2$  completely by neglecting its excited state. This leads to a new spin chain with one less spin and a new coupling  $\bar{J}_{13} < \Omega$ . If the largest coupling is a bond, say,  $J_{23}$ , the corresponding unperturbed Hamiltonian is  $-J_{23} \hat{S}_2^z \hat{S}_3^z$  with two degenerate ground states  $|\uparrow\uparrow\rangle$  and  $|\downarrow\downarrow\rangle$ . The transverse fields  $h_2^x$  and  $h_3^x$  can now be treated perturbatively yielding an effective field

$$\bar{h}_2^x \approx h_2^x h_3^x / J_{23} \quad (63)$$

inducing coherent flips of the cluster  $\hat{S}_2 + \hat{S}_3$ . We now throw away the excited (antiparallel) states of this cluster and treat the cluster as an effective spin whose moment is the sum of the moments of  $\hat{S}_2$  and  $\hat{S}_3$ . Again, we have a new spin chain with one less spin degree of freedom and all couplings smaller than  $\Omega$ .

The repeated application of this basic renormalization group step constitutes a aggregation and annihilation process of spin clusters. When the strongest coupling is



a field, the corresponding cluster is annihilated, and when it is a bond, the clusters that it connects are aggregated into one cluster. At each renormalization group step, the clusters represent sets of original spins that are correlated at the current cutoff energy  $\Omega$ . In the paramagnetic phase, annihilation dominates for  $\Omega \rightarrow 0$ , and no large clusters are generated. In the ferromagnetic phase, the aggregation dominates for  $\Omega \rightarrow 0$  generating arbitrarily large clusters until, at  $\Omega = 0$  an infinite cluster will have formed. The quantum critical point is the point where such an infinite cluster first appears [26, 126]. The multiplicative structure of the recursion relations (62) and (63) is very important because it establishes an exponential relationship between the length scale and the energy scale: In each RG step, the lengths of clusters or bonds are *added* while their couplings are *multiplied* to determine the effective renormalized values. Thus, the length scale  $L$  of the clusters and effective bonds scales with the logarithm of the energy scale

$$L^\psi \sim \ln(\Omega_0/\Omega) \quad (64)$$

where  $\Omega_0$  is a microscopic energy scale and the critical exponent  $\psi$  turns out to be  $\psi = 1/2$ . Analogously, the typical magnetic moment of a cluster increases as

$$\mu \sim (\ln(\Omega_0/\Omega))^\phi \quad (65)$$

with the exponent  $\phi = (1 + \sqrt{5})/2$  equal to the golden mean. Thus, the random transverse field Ising model displays activated dynamical scaling rather than conventional power-law scaling.

Using this approach, Fisher [34, 35], derived renormalization group equations for the probability distributions of the logarithms of the couplings,  $\ln J$  and  $\ln h^x$ . The resulting renormalization group flow displays very interesting and unusual properties. At the critical point which occurs at  $[\ln J]_{\text{av}} = [\ln h^x]_{\text{av}}$  where  $[\dots]_{\text{av}}$  is the disorder average [101], the probability distributions of  $\ln J$  and  $\ln h^x$  broaden without limit with decreasing energy scale  $\Omega$ . This broadening is crucial for the renormalization group to work: In the limit of infinitely broad distributions, the recursion relations (62) and (63) become asymptotically exact for  $\Omega \rightarrow 0$ , since in each renormalization group step the ratio between the dominating coupling and those treated perturbatively diverges. Because of the diverging widths of the probability distributions of  $\ln J$  and  $\ln h^x$ , the critical fixed point in the random transverse field Ising model is also called an infinite randomness fixed point.

Off criticality, the distance from the critical point can be conveniently defined as

$$r = \frac{[\ln h^x]_{\text{av}} - [\ln J]_{\text{av}}}{\text{var}(\ln h^x) + \text{var}(\ln J)} \quad (66)$$

where  $\text{var}(x)$  is the variance of the probability distribution of  $x$ . The so defined  $r$  is invariant under renormalization. In the disordered (paramagnetic) phase, there will be a length scale  $\xi$  at which the renormalization flow qualitatively changes. On scales larger than  $\xi$  almost all effective fields are larger than the effective couplings. Upon further renormalization, only fields will be decimated, leading to longer and weaker bonds but not to longer clusters. Thus,  $\xi$  is the correlation length. It is found to scale like

$$\xi \sim r^{-\nu} \quad (67)$$

where the exponent  $\nu = 2$  saturates the Harris criterion  $d\nu \geq 2$  [25]. Analogously, in the ordered (ferromagnetic) phase for  $r$  small and negative, there will be a length scale  $\xi \sim |r|^{-\nu}$  beyond which (almost) all interactions are larger than the fields. Upon further renormalization, all clusters will be joined together to form the infinite cluster

at  $\Omega = 0$ . Thus, excitations from the ferromagnetic state exist only up to the length scale  $\xi$  which is thus the (connected) correlation length in the ordered phase. The three exponents  $\phi, \psi$  and  $\nu$  completely determine the properties of the infinite-randomness critical point.

The unusual renormalization group flows lead to correspondingly unusual scaling behavior of observables at the quantum phase transition. At zero temperature, the magnetization in a small ordering magnetic field  $H$  in  $z$ -direction can be determined by stopping the renormalization at an energy scale  $\Omega_H = H$  and analyzing the cluster distribution at that scale.\* This leads to the scaling form

$$m(r, \ln(H_0/H)) = b^{\phi\psi-d} m\left(rb^{1/\nu}, \ln(H_0/H)b^{-\psi}\right) \quad (68)$$

where  $b$  is an arbitrary scale factor, and  $H_0$  is a nonuniversal constant. This equation again reflects the activated nature of the dynamical scaling; the energy scale set by  $H$  enters the scaling relations in logarithmic form rather than in power-law form. At criticality,  $r = 0$ , we can set  $b = [\ln(H_0/H)]^{1/\psi}$  and obtain

$$m(H) \sim [\ln(H_0/H)]^{\phi-d/\psi} \quad (69)$$

The exponent evaluates to  $\phi - d/\psi = \phi - 2 = (\sqrt{5} - 3)/2$ . Setting  $H = 0$  and  $b = r^{-\nu}$  we can obtain the spontaneous magnetization in the ordered phase ( $r < 0$ )

$$m(r) \sim |r|^\beta \quad (70)$$

with  $\beta = (d - \phi\psi)\nu = 2 - \phi = (3 - \sqrt{5})/2$ . Temperature dependent quantities can be determined in a similar fashion. At criticality and zero ordering field  $H$ , the magnetic susceptibility behaves as

$$\chi \sim \frac{1}{T} [\ln(T_0/T)]^{2\phi-d/\psi} \quad (71)$$

where  $T_0$  is a nonuniversal constant, and the specific heat is given by

$$c_v \sim [\ln(T_0/T)]^{-(1+d/\psi)} . \quad (72)$$

The infinite-randomness character of the critical point also has interesting consequences for the behavior of the spin-spin correlation function  $C(x) = \langle S_i^z S_{i+x}^z \rangle$ . Because the coupling constant distributions broaden without limit under renormalization,  $C(x)$  is also very broadly distributed. As a result *typical* and *average* correlations behave very differently. At the critical point, typical spin pairs are never in the same renormalization cluster and thus have only weak correlations that fall off as a stretched exponential

$$\ln C_{\text{typ}}(x) \sim -x^\psi . \quad (73)$$

In contrast, the average correlation function is dominated by rare spin pairs on the same cluster that have atypically large correlations of order unity. It is thus much larger than the typical one and falls off as a power law

$$C_{\text{av}}(x) \sim x^{-2(d-\phi\psi)} . \quad (74)$$

This discrepancy between typical and average properties is one of the main characteristics of an infinite-randomness critical point. Fisher and Young [143] numerically studied the end-to-end correlations in an open one-dimensional random

\* More precisely, the field energy scale is  $H\mu$  where  $\mu$  is the typical cluster moment at scale  $\Omega_H$ . This introduces an extra logarithmic correction.

transverse-field Ising model and found good agreement with the prediction of the strong-disorder renormalization group.

The strong-disorder renormalization group can also be used to analyze thermodynamic observables and correlation functions off criticality. In the Griffiths region of the disordered phase, Fisher [35] found strong power-law quantum Griffiths singularities of the form predicted by the optimal fluctuation arguments presented in the last subsection. Moreover, he found an explicit expression for the nonuniversal dynamical exponent  $z'$ . Close to the true quantum critical point, i.e. for  $r \ll 1$  it is given by  $z' = 1/|2r|$ . The discrepancy between typical and average correlations persists in the Griffiths region. Typical correlations fall off exponentially with a correlation length  $\xi_{\text{typ}}$  that diverges as  $\xi_{\text{typ}} \sim |r|^{-\nu_{\text{typ}}}$  with  $\nu_{\text{typ}} = 1$ . In contrast, the average correlations decay with the much larger true correlation length  $\xi \sim |r|^{-\nu}$  with  $\nu = 2$ . An analogous Griffiths region with power-law singularities was also identified in the ordered phase.

Igloi et al. [144, 145] extended Fishers analytical solution into the off-critical region and obtained asymptotically exact results for dynamical quantities including the dynamical exponent  $z'$ . Static quantities or spatial correlations, however, cannot be obtained exactly off criticality because the coupling constant distributions do *not* broaden without limit under renormalization. Rieger and Igloi [146] studied the influence of power-law spatial correlations of the random couplings on the transition. They found the infinite-randomness scenario still valid, but sufficiently long-ranged correlations yield new exponents that enhance both the critical and the quantum Griffiths singularities.

#### 5.4. Higher dimensions and other generalizations

The discovery of an infinite-randomness critical point in the one-dimensional random transverse-field Ising model lead to a surge of activity in this area starting in the mid 1990's. Early on, an important question was whether or not the infinite-randomness critical point is special to one dimension, or whether it also occurs in higher-dimensional systems. Senthil and Sachdev [118] considered a bond-diluted transverse field Ising model in  $d \geq 2$ . A sketch of the phase diagram of a general diluted quantum magnet is shown in figure 7. The diluted transverse field Ising model has two quantum phase transitions, separated by a multicritical point at the lattice percolation threshold  $p_c$  and a transverse field  $h^x = h^*$ . The transition at dilutions  $p < p_c$  (transition “a” in figure 7) is expected to be in the universality class of the generic random transverse-field Ising model. Senthil and Sachdev focused on the transition “b” across the percolation threshold of the lattice. Using the well known properties of critical percolation clusters [147], they showed that this quantum phase transition shares many properties with the infinite-randomness critical point in the one-dimensional random transverse Ising model. Specifically, the dynamical scaling is activated and the magnetization in a small ordering field obeys the scaling form (68) with  $\psi = D_f$ ,  $\phi = 1$  and  $\nu = \nu_c$  where  $D_f$  is the fractal dimension of the critical percolation cluster and  $\nu_c$  is the correlation length exponent of the lattice percolation problem. The transition is accompanied by strong power-law quantum Griffiths singularities both above and below  $p_c$ . All these predictions were verified by quantum Monte-Carlo results of Ikegami et al. [148].

To study the generic random transverse field Ising transition in dimensions  $d \geq 2$ , Motrunich et al. [26] applied a strong-disorder renormalization group to the two-

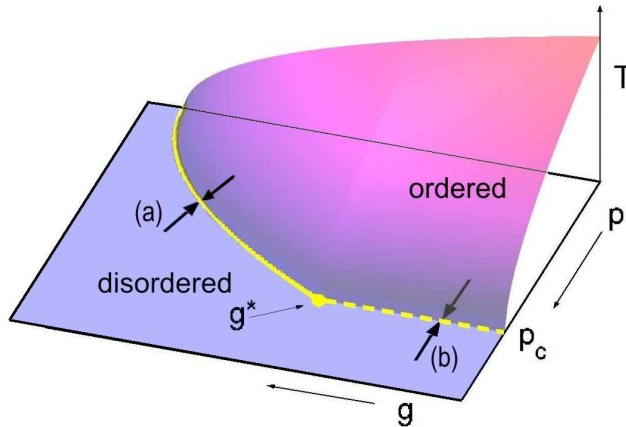


**Figure 7.** Schematic phase diagram of a general diluted quantum magnet with impurity concentration  $p$ , temperature  $T$ , and quantum fluctuation strength  $g$  (for the transverse-field Ising model  $g \sim h^z$ ). There is a quantum multicritical point (big dot) at  $(p_c, g^*)$ .

dimensional random transverse-field Ising model. In dimensions larger than one, the renormalization group calculation cannot be carried out analytically because the renormalization group does not preserve the lattice structure but generates longer and longer ranged couplings. Therefore, Motrunich et al. [26], implemented the renormalization procedure numerically. For two dimensions, they found that the renormalization group flow for stronger disorder is indeed towards even stronger disorder, i.e., towards an infinite-randomness fixed point, as in one dimension. As a result, the same scaling scenario as outlined in section 5.3 also applies to the two-dimensional case, but with different exponent values. Motrunich et al. estimated  $\psi \approx 0.42$ ,  $\phi \approx 2.5$ , and  $\nu \approx 1.1$ . Other numerical implementations [149, 150] of the strong disorder renormalization group found similar values. Preliminary results for three dimensions point to the same scenario, but reliable estimates for the exponents have not yet been obtained. The results of the numerically implemented strong-disorder renormalization group are in very good agreement with Monte-Carlo simulations of a two-dimensional random transverse field Ising model [40, 151].

The infinite-randomness critical fixed points found in the random transverse field Ising model control more than just Ising ferromagnetic quantum phase transitions. As was first pointed out by Senthil and Majumdar [152], Potts models or any random quantum systems with continuous quantum phase transitions at which a discrete symmetry of a non-conserved order parameter is broken, will have the same critical behavior as the Ising case. This applies even to systems that are frustrated on microscopic length scales, such as quantum Ising spin glasses. Because the coupling constant distributions become infinitely broad at the infinite-randomness fixed point, in any frustrated loop the weakest interaction will be infinitely weaker than the others and can thus be neglected. Thus, for Ising symmetry, frustration becomes irrelevant at the infinite-randomness critical point.

## 5.5. Continuous symmetry quantum magnets

In the last subsections we have seen that the qualitative zero-temperature behavior of random quantum Ising systems does not depend much on dimensionality: There is an infinite-randomness critical point separating a conventional paramagnetic phase from a phase with long-range order (of course, the critical exponent values at this critical point do depend on dimensionality).

For continuous-symmetry quantum spin systems such as quantum Heisenberg or XY magnets, the situation is drastically different. In one space dimension, these systems do not show magnetic long-range order. Instead they can be in a variety of exotic phases that will be briefly discussed in section 5.7. In staying with the main topic of this review, the present subsection is focussed on transitions between a disordered and a long-range ordered phase that can occur in continuous symmetry quantum magnets for  $d \geq 2$ .

Let us start by considering a two-dimensional  $S = 1/2$  Heisenberg quantum antiferromagnet with random site dilution. This problem is of direct relevance for antiferromagnetic layered cuprates with nonmagnetic impurities [153–156]. In the clean limit, the ground state of this system displays magnetic long-range order. However, the zero-point quantum fluctuations reduce the staggered magnetization by about 40% compared to the classical value (see, e.g., [157]). Upon randomly removing sites (or bonds) with probability  $p$ , the tendency towards magnetic order decreases, but the location and character of the phase transition were initially controversial. Early theoretical investigations [158–161] suggested that magnetic long-range order is destroyed before the impurity concentration  $p$  reaches the classical (geometric) percolation threshold  $p_c \approx 0.407$  [147] of the lattice. Kato et al. [162] found evidence of the critical dilution coinciding with percolation threshold  $p_c$  but argued that the infinite percolation cluster is quantum critical, with power-law spin correlations. However, using extensive quantum Monte-Carlo simulations, Sandvik [163,164] showed that the infinite percolating cluster at  $p_c$  displays long-range order. The transition at  $p_c$  is thus of percolation type. If the quantum fluctuations are enhanced to induce a quantum phase transition at impurity concentrations  $p < p_c$ , the zero-temperature phase diagram takes the general form shown in figure 7. However, at finite temperatures, no long-range order exists because of the Mermin-Wagner theorem [165].

An obvious and experimentally relevant way to increase the quantum fluctuations is via an interlayer coupling in a bilayer Heisenberg quantum antiferromagnet as depicted in the inset of figure 8. The spins in each 2d layer interact via nearest neighbor exchange  $J_{\parallel}$ , and the interplane coupling is  $J_{\perp}$  with the ratio  $g \sim J_{\perp}/J_{\parallel}$  controlling the strength of the quantum fluctuations. The clean version of this model has been studied extensively [166–169]. For  $J_{\perp} \gg J_{\parallel}$ , neighboring spins from the two layers form singlets, and the ground state is paramagnetic. In contrast, for  $J_{\parallel} \gg J_{\perp}$  the system develops Néel order. Both phases are separated by a quantum phase transition at  $J_{\perp}/J_{\parallel} \approx 2.525$ .

Quenched disorder can be introduced by randomly removing spins. We emphasize that in order to achieve random-mass type disorder, *pairs* (dimers) of adjacent spins, one from each layer have to be removed. In this way, no random Berry phases arise, because the Berry phase contributions from the two spins of each unit cell exactly cancel [12, 170]. In contrast, for site dilution, the physics would completely change: The random Berry phases (which have no classical analogue) are equivalent to impurity-induced moments [171], and those become weakly coupled via bulk

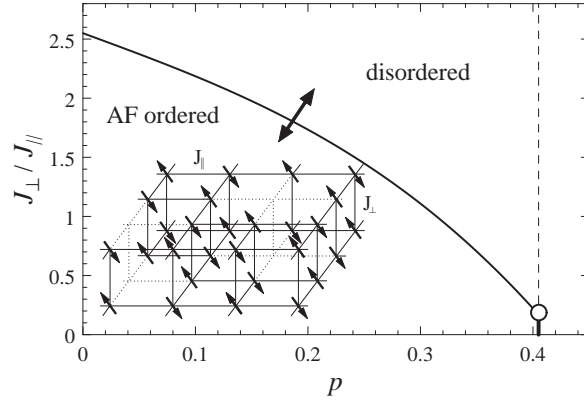


**Figure 8.** Phase diagram [68, 69] of the diluted bilayer Heisenberg antiferromagnet, as function of  $J_{\perp}/J_{\parallel}$  and dilution  $p$ . The dashed line is the percolation threshold, the open dot is the multicritical point. Inset: The model: Quantum spins (arrows) reside on the two parallel square lattices. The spins in each plane interact with the coupling strength  $J_{\parallel}$ . Interplane coupling is  $J_{\perp}$ . Dilution is done by removing dimers (from [70]).

excitations. For all  $p < p_p$  the ground state of the system shows long-range order, independent of  $J_{\perp}/J_{\parallel}$ ! Thus, site dilution actually changes the bulk phases, i.e., it introduces disorder effects more complicated than random-mass disorder. These are beyond the scope of this review.

The Hamiltonian of the dimer-diluted bilayer Heisenberg model is:

$$H = J_{\parallel} \sum_{\substack{\langle i,j \rangle \\ a=1,2}} \epsilon_i \epsilon_j \hat{\mathbf{S}}_{i,a} \cdot \hat{\mathbf{S}}_{j,a} + J_{\perp} \sum_i \epsilon_i \hat{\mathbf{S}}_{i,1} \cdot \hat{\mathbf{S}}_{i,2}, \quad (75)$$

and  $\epsilon_i=0$  ( $\epsilon_i=1$ ) with probability  $p$  ( $1-p$ ). The zero-temperature phase diagram of this model has been studied in detail by Sandvik [68] and Vajk and Greven [69]; it is shown in Fig. 8. For small  $J_{\perp}$ , magnetic order survives up to the percolation threshold  $p_p \approx 0.4072$ , and a multicritical point exists at  $p = p_p$  and  $J_{\perp}/J_{\parallel} \approx 0.16$ . Thus, the dimer-diluted bilayer Heisenberg antiferromagnet has two quantum phase transitions, the generic transition for  $p < p_c$  (corresponding to transition “a” in the generic phase diagram, figure 7) and a quantum percolation transition at  $p = p_c, J_{\perp} < 0.16J_{\parallel}$  (corresponding to transition “b” in figure 7).

The low-energy properties of bilayer quantum antiferromagnets are represented by a (2+1)-dimensional  $O(3)$  quantum rotor model with the rotor coordinate  $\hat{\mathbf{n}}_i$  corresponding to  $\hat{\mathbf{S}}_{i,1} - \hat{\mathbf{S}}_{i,2}$  and the angular momentum  $\hat{\mathbf{L}}_i$  representing  $\hat{\mathbf{S}}_{i,1} + \hat{\mathbf{S}}_{i,2}$  [12,170]. This quantum rotor model in turn maps onto a 3d classical Heisenberg model in which the disorder is perfectly correlated in the imaginary time direction. At zero temperature, the rare regions are thus equivalent to classical Heisenberg magnets that are infinite in the time-like direction but finite in the two space directions.

A first qualitative understanding of the rare region effects can again be obtained from optimal fluctuation arguments similar to that used in section 5.2. The probability for finding a rare region of linear size  $L_{RR}$  is exponentially small in its volume,  $w(L_{RR}) \sim \exp(-\tilde{p}L_{RR}^d)$  with  $d = 2$ . However, the energy gap of a locally ordered rare region depends on its *spatial* volume via a power law (rather than exponentially as in the Ising case) as can be obtained from a renormalization group analysis of the

(0+1) dimensional Heisenberg model at its strong coupling fixed point or by an explicit large- $N$  calculation [67]. These arguments thus predict the rare region effects in the Heisenberg case to be exponentially weak and the critical point to be conventional with power-law dynamical scaling.

Sknepnek, Vojta and Vojta [70] performed large scale Monte-Carlo simulations of a classical three-dimensional Heisenberg model with linear defects to test these predictions. They focused on the generic transition for  $p < p_c$  and analyzed the scaling behavior of the so-called Binder ratio of the order parameter moments, given by

$$g_{av} = \left[ 1 - \frac{\langle |\mathbf{m}|^4 \rangle}{3 \langle |\mathbf{m}|^2 \rangle^2} \right]_{av}, \quad (76)$$

where  $[\dots]_{av}$  denotes the disorder average and  $\langle \dots \rangle$  is the Monte-Carlo average for each sample. This quantity has scale dimension 0. Thus, its finite-size scaling form is given by

$$g_{av} = \tilde{g}_C(rL^{1/\nu}, L_\tau/L^z) \quad \text{or} \quad (77)$$

$$g_{av} = \tilde{g}_A(rL^{1/\nu}, \log(L_\tau)/L^\psi) \quad (78)$$

for conventional scaling or for activated scaling, respectively. Here  $L$  and  $L_\tau$  are the linear system sizes in the space and time-like directions. Two important characteristics immediately follow from these scaling forms: (i) For fixed  $L$ ,  $g_{av}$  has a peak as a function of  $L_\tau$ . The peak position  $L_\tau^{\max}$  marks the *optimal* sample shape, where the ratio  $L_\tau/L$  roughly behaves like the corresponding ratio of the correlation lengths in time and space directions,  $\xi_\tau/\xi$ . At the critical temperature  $T_c$ , the peak value  $g_{av}^{\max}$  is independent of  $L$ . Thus, for power law scaling, plotting  $g_{av}$  vs.  $L_\tau/L_\tau^{\max}$  at  $T_c$  should collapse the data, without the need for a value of  $z$ . In contrast, for activated scaling the  $g_{av}$  data should collapse when plotted as a function of  $\log(L_\tau)/\log(L_\tau^{\max})$ . (ii) For samples of the optimal shape ( $L_\tau = L_\tau^{\max}$ ), plots of  $g_{av}$  vs. temperature for different  $L$  cross at  $T_c$ .

A typical result of these calculations is presented in figure 9. This figure shows the Binder ratio at the critical point for a system with impurity concentration  $p = 1/5$  and various system sizes  $L$  and  $L_\tau$ . As can be seen in the main panel, the data scale very well when analyzed according to conventional power-law scaling while the inset shows that they do not scale at all when plotted according to activated scaling. Analogous data were obtained for impurity concentrations  $1/8$ ,  $2/7$ , and  $1/3$ . Sknepnek et al. [70] thus concluded that the quantum critical point in the dimer-diluted bilayer Heisenberg antiferromagnet exhibits conventional power-law scaling with exponentially weak rare region effects, in agreement with the optimal fluctuation arguments above. They also determined the critical exponents at this quantum critical point and found universal (i.e., disorder-independent) values of  $z = 1.310(6)$ ,  $\nu = 1.16(3)$ ,  $\beta/\nu = 0.56(5)$ , and  $\gamma/\nu = 2.15(10)$ .

Sandvik [68] and Vajk and Greven [69] studied the scaling behavior at the multicritical point at  $p = p_p$  and  $J_\perp/J_\parallel \approx 0.16$ . They found that this point also exhibits conventional power-law scaling. Their value of the dynamical exponent  $z \approx 1.3$  agrees within the error bars with that of the generic transition discussed above. Whether or not the dynamic exponents at the generic transition and at the multicritical point are indeed identical and whether or not this agreement is accidental is not resolved so far.

More recently, Vojta and Schmalian [172] considered the quantum phase transition across the percolation threshold (transition “b” in the generic phase

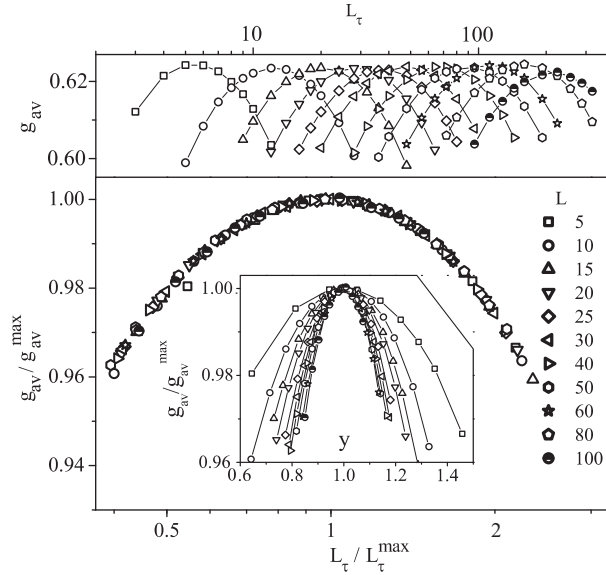


**Figure 9.** Upper panel: Binder ratio  $g_{av}$  as a function of  $L_\tau$  for various  $L$  ( $p = \frac{1}{5}$ ). Lower panel: Power-law scaling plot  $g_{av}/g_{av}^{max}$  vs.  $L_\tau/L_\tau^{max}$ . Inset: Activated scaling plot  $g_{av}/g_{av}^{max}$  vs.  $y = \log(L_\tau)/\log(L_\tau^{max})$  (from [70]).

diagram, figure 7). Combining the well known properties of the lattice percolation transition [147] with a scaling analysis of finite-size quantum Heisenberg clusters at the *stable* low-energy fixed point, they derived a complete scaling theory of this transition. In contrast to the corresponding quantum Ising case [118], the critical behavior is of power-law type. The dynamical exponent is identical to fractal dimension of the percolation cluster,  $z = D_f$ , and the correlation length exponent is identical to that of the lattice percolation problem,  $\nu = \nu_c$ . In fact, these results apply not only to the dimer-diluted bilayer model but general diluted Heisenberg quantum antiferromagnets. The conclusion  $z = D_f$  has been confirmed by Monte Carlo simulations of single-layer [173] and bilayer [68] models.

We can thus conclude that all quantum phase transitions of the dimer-diluted bilayer quantum Heisenberg antiferromagnet (the generic transition for  $p < p_c$ , the percolation transition at  $p_c$  and the multicritical point) exhibit conventional power-law scaling and exponentially weak rare region effects in agreement with the simple extremal statistics arguments. This conclusion is also supported by preliminary results of a strong-disorder renormalization group calculation for the Heisenberg case [26] that show that the infinite-randomness fixed point is unstable and the renormalization group flow is towards smaller disorder strength. Lin et al. [174] used the strong-disorder renormalization group to study the stable low-energy (as opposed to critical) fixed points of random Heisenberg models in two and three dimensions. They found conventional power-law scaling and no infinite randomness behavior. This result has recently been confirmed by quantum Monte-Carlo simulations and exact numerical diagonalizations [175].



## 5.6. Itinerant quantum magnets

In this subsection, we turn from systems of localized spins to quantum phase transitions in itinerant (metallic) spin systems. This field was pioneered by Hertz [176]. Starting from a microscopic theory of interacting electrons, he derived Landau-Ginzburg-Wilson order parameter field theories for the ferromagnetic and antiferromagnetic quantum phase transitions of both clean and dirty metals. He then studied these Landau-Ginzburg-Wilson theories using renormalization group methods. Later, Millis [177] worked out the experimentally important finite-temperature behavior in the vicinity of the quantum critical point. In the case of the ferromagnetic transition, the specific conclusions of the Hertz-Millis theory turned out to be incorrect because generic scale invariance in the of form additional fermionic soft modes invalidates the Landau-Ginzburg-Wilson approach [14, 18–20]. This was briefly discussed at the end of section 2.3. The effective long-range interactions created by the additional soft modes will likely modify the rare region effects, too. However, these extra complications at the dirty ferromagnetic transition are presently not fully understood, and therefore we will not discuss them in detail.

Physically, a crucial difference between itinerant magnets and systems of localized spins is that magnetic excitations are damped in the former while they are undamped in the latter. This is caused by the coupling between the magnetic modes and the gapless particle-hole excitations in the metal. Technically, it is reflected in the frequency dependence of the Gaussian term of the Landau-Ginzburg-Wilson theory. For definiteness, let us consider the itinerant antiferromagnetic transition. The Landau-Ginzburg-Wilson free energy functional of the clean transition reads [176]‡

$$S = \int d^d x d^d y d\tau d\tau' \phi(\mathbf{x}, \tau) \Gamma(\mathbf{x}, \tau, \mathbf{y}, \tau') \phi(\mathbf{y}, \tau') + u \int d^d x d\tau \phi^4(\mathbf{x}, \tau) . \quad (79)$$

Here,  $\Gamma(\mathbf{x}, \tau, \mathbf{y}, \tau')$  is the bare two-point vertex whose Fourier transformation is

$$\Gamma(\mathbf{q}, \omega_n) = r + \mathbf{q}^2 + |\omega_n| \quad (80)$$

with  $r$  being the (bare) distance from criticality and  $\omega_n$  bosonic Matsubara frequencies. We have suppressed constant prefactors. The nonanalytic frequency dependence proportional to  $|\omega_n|$  in the dynamical part of  $\Gamma$  reflects the overdamping of the dynamics due to the coupling of the order parameter to fermionic particle-hole excitations. In contrast, undamped dynamics would lead to an  $\omega_n^2$  term (see also equation (11)).

Weak, random-mass disorder can be introduced by making  $r$  a random function of position,  $r \rightarrow r + \delta r(\mathbf{x})$  [176, 179]. The rare regions in this system are large spatial regions where the local  $r$  is smaller than its average value. Let us consider a single such region that is locally in the ordered phase, while the bulk is still in the disordered phase. The order parameter on such a region is correlated in space, i.e., it behaves coherently over the whole island. The crucial difference between itinerant magnets and the localized spin systems considered in previous sections is in the dynamics of the rare region. Without damping, the order parameter slowly fluctuates giving rise to the quantum Griffiths effects discussed in section 5.2. Damping or dissipation will potentially hinder the dynamics of the rare region. To study this phenomenon, Millis, Morr and Schmalian [61, 62] explicitly calculated the tunneling rate of a locally ordered rare region in an itinerant Ising magnet. They found that for sufficiently large rare

‡ This simple bosonic Landau-Ginzburg Wilson theory only applies for dimensions  $d > 2$ . In two dimensions, fermionic soft modes lead to singular vertices even for the antiferromagnet [178].

regions, the tunneling rate vanishes. This means, these rare regions completely stop to tunnel, and their order parameter becomes static. The same result can also be obtained from quantum-to-classical mapping [60]. In the equivalent classical system, a rare region corresponds to a quasi-one-dimensional Ising model which is of finite size in the space directions but infinite in the time-like direction. The linear frequency dependence in the two-point vertex  $\Gamma$  is equivalent to a long-range interaction in imaginary time of the form  $(\tau - \tau')^{-2}$ . Each rare region is thus equivalent to an one-dimensional Ising model with a  $1/r^2$  interaction. This model is known to have a phase transition [180, 181]. Thus, true static order can develop on those rare regions which are locally in the ordered phase. § Very recently, Schehr and Rieger [182] analyzed a related problem, viz. a random transverse field Ising model coupled to an Ohmic dissipative bath, by a version of the strong-disorder renormalization group. They arrive at an analogous conclusion: Sufficiently large, locally ordered clusters freeze, and develop a static order parameter.

As a result, the phenomenology of rare region effects in an itinerant Ising magnet is very different from that of a localized magnet. Because the large rare regions do not fluctuate the low-energy behavior does not display power-law quantum Griffiths effects, contrary to earlier predictions that did not correctly take into account the dissipation [183]. Instead, the global phase transition is smeared [60] by the same mechanism as the transition in a classical Ising model with planar defects discussed in section 4.6: Once static order has developed on a few isolated rare regions, an infinitesimally small interaction or an infinitesimally small symmetry-breaking field are sufficient to align them. Consequently, a macroscopic order parameter develops inhomogeneously, with different spatial part of the system ordering at different values of the control parameter.

The leading zero-temperature behavior in the tail of the smeared quantum phase transition can be determined by optimal fluctuation arguments similar to section 4.7. Here, we just summarize the results for dilution-type (Poisson) disorder, i.e.,  $\delta r(\mathbf{x}) = 0$  everywhere except on randomly distributed finite-size islands (impurities) of spatial density  $\tilde{p}$  where  $\delta r(\mathbf{x}) = W > 0$ . More details can be found in reference [60]. The probability  $w$  for finding a region of linear size  $L_{\text{RR}}$  devoid of any impurities is given by  $w \sim \exp(-\tilde{p}L_{\text{RR}}^d)$  (up to pre-exponential factors). Such a rare region develops static order at a distance  $r_c(L_{\text{RR}}) < 0$  from the *clean* critical point. Finite size scaling yields  $|r_c(L_{\text{RR}})| \sim L_{\text{RR}}^{-\phi}$  where  $\phi$  is the finite-size scaling shift exponent of the clean system. Thus, the probability for finding a rare region which becomes critical at  $r_c$  is given by  $w(r_c) \sim \exp(-B|r_c|^{-d/\phi})$  for  $r \rightarrow 0-$ . The total order parameter  $m$  is obtained by integrating over all rare regions which are ordered at  $r$ , i.e., all rare regions having  $t_c > t$ . This leads to an exponential tail of  $m$  as a function of the distance  $r$  from the *clean* critical point:

$$m(r) \sim \exp(-B|r|^{-d/\phi}) \quad (\text{for } r \rightarrow 0-). \quad (81)$$

This is identical to the classical result (47) if one replaces the number of uncorrelated dimensions  $d_{\text{ran}}$  by the space dimensionality  $d$ .

We now turn to the experimentally important finite-temperature behavior in the vicinity of the smeared quantum phase transition. A schematic phase diagram is shown in figure 10. At any finite temperature, the static order on the rare regions

§ At the first glance, this result seems to contradict basic statistical mechanics that tells us that spontaneous symmetry breaking cannot occur in a finite-size system. The resolution lies in the fact that the damping is caused by the underlying electronic system which must be infinite to be gapless.

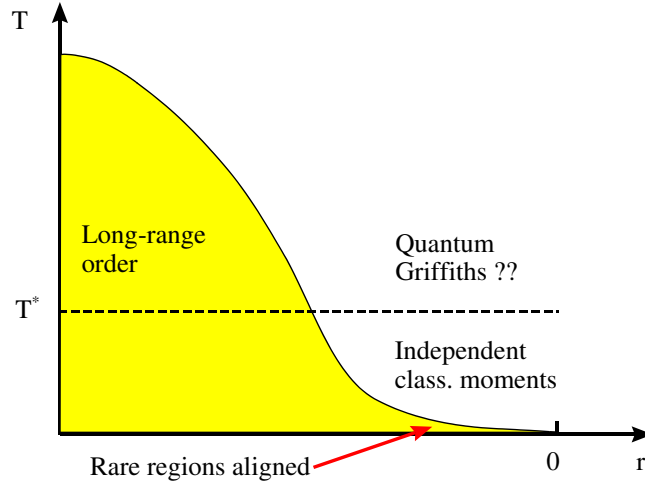


**Figure 10.** Schematic phase diagram in the vicinity of a smeared quantum phase transition. For details see text.

is destroyed, and a finite interaction of the order of the temperature is necessary to align them. This means a sharp phase transition is recovered. To estimate the transition temperature we note that the interaction between two rare regions depends exponentially on their (typical) spatial distance  $|\mathbf{x}|$  which itself depends exponentially on  $r$ . This leads to a double-exponential dependence of the critical temperature on  $r$

$$\log(-a \log T_c) \sim |r|^{-d/\phi} . \quad (82)$$

In other words, the long-range ordered phase develops an double-exponential tail towards to clean quantum critical point at  $r = 0$ . (Note that the inclusion of a long-range spatial interaction such as the RKKY interaction would transform this into a simple stretched exponential. Moreover, weak competing interactions not contained in the model (79) may induce spin glass order in the tail region.) Above this very low temperature different rare regions are not aligned anymore but act as independent classical moments leading to super-paramagnetic behavior with a Curie-type susceptibility [62].

What happens at even higher temperatures depends on nonuniversal microscopic parameters and is subject of an ongoing debate. If the damping of the magnetic modes by the electrons is weak, i.e., if the prefactor of the  $|\omega_n|$ -term in the Gaussian vertex (80) is parametrically small compared to other scales, a subleading  $\omega_n^2$  term (which describes undamped dynamics) becomes dominating at higher energies. This gives rise to a crossover temperature  $T^*$ . Power-law quantum Griffiths behavior can occur in a transient temperature window *above*  $T^*$  but below a microscopic cutoff scale (like the Fermi temperature). However, if the damping is not weak,  $T^*$  should roughly coincide with the microscopic cutoff, and quantum Griffiths effects should not be observable. For more details see the discussion on experiments in section 7.2.

So far, our exploration of itinerant quantum magnets has focused on the case of Ising symmetry where we found a smeared phase transition and static (frozen) rare regions. For continuous spin symmetry, the results are markedly different, as can be readily understood from quantum-to-classical mapping arguments [67]. A rare region in an itinerant magnet with continuous spin symmetry is equivalent to a quasi-

one-dimensional classical  $O(N)$  model ( $N \geq 2$ ). The interaction in the time-like direction has the form  $(\tau - \tau')^{-2}$  as in the Ising case. One-dimensional continuous-symmetry  $O(N)$  models with  $1/\mathbf{x}^2$  interaction do not have a phase transition, but they are exactly *at* their lower critical dimension [184–186]. Therefore, in the quantum problem, an isolated rare region of linear size  $L_{\text{RR}}$  cannot independently undergo a phase transition. Its energy gap depends exponentially on its volume,  $\epsilon(L_{\text{RR}}) \sim \exp(-aL_{\text{RR}}^d)$ . Equivalently, the susceptibility of such a region diverges exponentially with its volume. Combining this exponential law for the gap with an the exponentially small probability for finding a rare region leads to exactly the same power-law quantum Griffiths singularities as in the random transverse field Ising model [67]. Loh et al. [187] studied a related problem, viz., a single spin- $S$  impurity with XY rotational symmetry in a metal. Their results are completely compatible with the quantum Griffiths scenario outlined above.

This scenario is correct as long as different rare regions are effectively independent. Dobrosavljevic and Miranda [73] pointed out that in realistic metallic systems the long-range RKKY interaction leads to an additional damping of the rare regions that destabilizes the quantum Griffiths behavior and leads to static frozen rare regions even in the Heisenberg case. However, in contrast to the Ising case, the freezing requires an interaction between the rare regions and is therefore expected to occur at extremely low temperatures only.

### 5.7. Quantum Griffiths effects in other systems

In accordance with the main theme of this review, our discussion of quantum Griffiths effects so far has been restricted to order-disorder quantum phase transitions between conventional phases, i.e., we have assumed that the phases themselves are not qualitatively changed by the quenched disorder. In the present subsection we will briefly mention, without any pretense of completeness, other examples of quantum rare region effects.

One-dimensional Heisenberg quantum antiferromagnets do not display long-range order even at zero temperature. The behavior of the clean chain depends on the spin value [188, 189]: For integer spin, there is a Haldane gap for magnetic excitations and short-range magnetic order. In the case of half-integer spin, there is quasi long-range spin order with algebraically decaying correlations and no gap. This suggests that the half-integer chains are more susceptible towards weak disorder. Indeed, the ground state of the random antiferromagnetic spin-1/2 chain is a random-singlet state, that is controlled by an infinite-disorder fixed point [38]. Numerical simulations mostly agree with this prediction [190, 191]. In contrast, the dimerized spin-1/2 chain has a gap in the absence of quenched disorder. As a result, the dimerized chain is stable against disorder [123] and the spin correlations remain short-ranged (random dimer phase). For strong disorder or weak dimerization, the random dimer phase is gapless, with a susceptibility that diverges as some nonuniversal inverse power of temperature. This phase can be understood as a Griffiths phase belonging to the critical point at zero dimerization.

The clean antiferromagnetic spin-1 chain has a Haldane gap. Consequently, it is stable against weak disorder. Strong-disorder renormalization group studies [124, 126, 127, 129] predict a random-singlet phase for sufficiently strong disorder. It is separated from the gaped phase by a gapless region of Griffiths singularities, the so-called gapless Haldane phase. While the numerical simulations [192–196] support

the overall structure of the phase diagram, they give somewhat conflicting results on what phases can be reached for which bare disorder distribution and on the location of the critical points. For the spin-3/2 chain, even the question of the phase diagram has not yet been settled. A strong disorder renormalization group study by Refael et al. [130] gave two random singlet phases with different effective spins ( $S_{\text{eff}} = 3/2$  for strong disorder and  $S_{\text{eff}} = 1/2$  for weak disorder). A different implementation of the renormalization group by Saguia et al. [131] gives a random singlet phase only for strong disorder. Weak disorder is an irrelevant perturbation. The latter result also agrees with recent numerical simulations [197]. In addition to spin chains, disordered spin ladder systems also display random singlet, Griffiths and other exotic phases [132, 134–137].

Interesting quantum Griffiths effects have also been identified in inhomogeneously diluted quantum antiferromagnets. As was discussed in section 5.5, in a (homogeneously) diluted two-dimensional Heisenberg quantum antiferromagnet, the ordered phase persists to the classical percolation threshold of the lattice, and the quantum phase transition that eventually destroys the long-range order is of percolation type. Yu et al. [173, 198] introduced *inhomogeneous* bond dilution by using different occupation probabilities for different types of bonds (“dimer” and “ladder” bonds). In this way, they increase the quantum fluctuations and the local tendency towards valence-bond solid order. If the two occupation probabilities are sufficiently different, magnetic long-range order is destroyed before the classical percolation threshold is reached. In the resulting quantum disordered phase, the low-temperature susceptibility diverges algebraically with a non-universal exponent. This phase can be understood as a quantum Griffiths phase.

Dobrosavljevic, Miranda and coworkers [199–201] introduced the concept of an *electronic* Griffiths phase, a phase that occurs in strongly correlated electron systems in the vicinity of a disorder-driven metal insulator transition. These systems possess localized magnetic moments, that are either present from the outset (localized  $f$ -electrons in heavy fermion materials) or are self-generated due to the interplay between disorder and correlations. The electronic Griffiths phase is characterized by a power-law distribution of the Kondo temperatures  $T_K$  of these moments. Integrating over this distribution leads to power-law singularities in many observables including specific heat and magnetic susceptibility. More details can be found in the recent review [202].

Other rare region effects in quantum systems include the Lifshitz tails in the density of states in doped semiconductors [46, 47]. They are probably the oldest known rare region effects but not directly related to a phase transition. Analogous effects were also found in dirty superconductors [203–206]. Motrunich et al. [207] investigated Griffiths effects and quantum critical points in dirty one-dimensional superconductors; and Vafeek et al. [208] discussed rare region effects at the flux-driven superconductor-metal transition in ultrasmall cylinders (see also reference [209]). Finally, Mildenerger et al. [210] identified a Griffiths phase in the thermal quantum Hall effect.

## 6. Nonequilibrium phase transitions

The nonequilibrium behavior of many-particle systems has attracted considerable attention in recent years. Of particular interest are continuous phase transitions between different nonequilibrium states. These transitions are characterized by large scale fluctuations and collective behavior over large distances and times very similar to the behavior at equilibrium critical points. Examples of nonequilibrium transitions can

be found in population dynamics and epidemics, chemical reactions, growing surfaces, and in granular flow and traffic jams (for recent reviews see, e.g., references [211–217]). In this section we demonstrate that quenched spatial disorder at such nonequilibrium phase transitions leads to rare region effects that are analogous to those at equilibrium classical and quantum phase transitions.

### 6.1. Contact process

A prominent class of nonequilibrium phase transitions separates active fluctuating states from inactive, absorbing states where fluctuations cease entirely. Recently, much effort has been devoted to classifying possible universality classes of these absorbing state phase transitions [215, 216]. The generic universality class is directed percolation (DP) [218]. According to a conjecture by Janssen and Grassberger [219, 220], all absorbing state transitions with a scalar order parameter, short-range interactions, and no extra symmetries or conservation laws belong to this class. Examples include transitions in catalytic reactions [221], interface growth [222], or turbulence [223]. In the presence of conservation laws or additional symmetries, other universality classes can occur, e.g., the parity conserving class [224–226] or the  $Z_2$ -symmetric directed percolation (DP2) class [227–230].

The contact process [231] is a prototypical system in the directed percolation universality class. It can be interpreted, e.g., as a model for the spreading of a disease. The contact process is defined on a  $d$ -dimensional hypercubic lattice. Each lattice site  $\mathbf{x}$  can be active (occupied by a particle) or inactive (empty). In the course of the time evolution, active sites can infect their neighbors, or they can spontaneously become inactive. Specifically, the dynamics is given by a continuous-time Markov process during which particles are created at empty sites at a rate  $\lambda n/(2d)$  where  $n$  is the number of active nearest neighbor sites. Particles are annihilated at rate  $\mu$ . The ratio of the rates  $\lambda$  and  $\mu$  controls the behavior of the system. Without loss of generality we will set the annihilation rate  $\mu$  to unity, unless noted otherwise.

For small birth (infection) rate  $\lambda$ , annihilation dominates, and the absorbing state without any particles is the only steady state (inactive phase). For large  $\lambda$ , there is a steady state with finite particle density (active phase). The two phases are separated by a nonequilibrium phase transition in the directed percolation universality class at some critical value  $\lambda_c^0$ . The central quantity in the contact process is the average density of active sites at time  $t$

$$\rho(t) = \frac{1}{L^d} \sum_{\mathbf{x}} \langle n_{\mathbf{x}}(t) \rangle \quad (83)$$

where  $n_{\mathbf{x}}(t)$  is the particle number at site  $\mathbf{x}$  and time  $t$ ,  $L$  is the linear system size, and  $\langle \dots \rangle$  denotes the average over all realizations of the Markov process. The longtime limit of this density (i.e., the steady state density)

$$\rho_{\text{stat}} = \lim_{t \rightarrow \infty} \rho(t) \quad (84)$$

is the order parameter of the nonequilibrium phase transition.

Close to the nonequilibrium phase transition, the density shows scaling behavior very similar to that of equilibrium transitions discussed in section 2.2. Specifically, the order parameter  $\rho_{\text{stat}}$  varies according to the power law

$$\rho_{\text{stat}} \sim (\lambda - \lambda_c)^{\beta} \sim r^{\beta} \quad (85)$$

where  $r = (\lambda - \lambda_c)/\lambda_c$  is the dimensionless distance from the critical point, and  $\beta$  is the critical exponent of the particle density. In addition to the average density, we also need to characterize the length and time scales of the density fluctuations. Close to the transition, correlation length  $\xi_\perp$  and correlation time  $\xi_t$  diverge as

$$\xi_\perp \sim |r|^{-\nu_\perp}, \quad \xi_t \sim \xi_\perp^z, \quad (86)$$

i.e., the dynamical scaling is of power-law form with dynamical exponent  $z$ .<sup>||</sup> Consequently the scaling form of the density as a function of  $r$ , the time  $t$  and the linear system size  $L$  reads

$$\rho(r, t, L) = b^{-\beta/\nu_\perp} \rho(rb^{1/\nu_\perp}, tb^{-z}, Lb^{-1}). \quad (87)$$

Here,  $b$  is an arbitrary dimensionless scaling factor.

Two important quantities arise from initial conditions consisting of a single active site in an otherwise empty lattice. The survival probability  $P_s$  describes the probability that an active cluster survives when starting from such a single-site seed. For directed percolation, the survival probability scales exactly like the density

$$P_s(r, t, L) = b^{-\beta/\nu_\perp} P_s(rb^{1/\nu_\perp}, tb^{-z}, Lb^{-1}). \quad (88)$$

Thus, for directed percolation, the three critical exponents  $\beta$ ,  $\nu_\perp$  and  $z$  completely characterize the critical point.<sup>¶</sup> The pair connectedness function  $C(\mathbf{x}', t', \mathbf{x}, t) = \langle n_{\mathbf{x}'}(t') n_{\mathbf{x}}(t) \rangle$  describes the probability that site  $\mathbf{x}'$  is active at time  $t'$  when starting from an initial condition with a single active site at  $\mathbf{x}$  and time  $t$ . For a clean system, the pair connectedness is translationally invariant in space and time. Thus, it only depends on two arguments  $C(\mathbf{x}, t', \mathbf{x}, t) = C(\mathbf{x}' - \mathbf{x}, t - t')$ . Because  $C$  involves a product of two densities, its scale dimension is  $2\beta/\nu_\perp$ , and the full scaling form reads (as long as hyperscaling is valid)

$$C(r, \mathbf{x}, t, L) = b^{-2\beta/\nu_\perp} C(rb^{1/\nu_\perp}, \mathbf{x}b^{-1}, tb^{-z}, Lb^{-1}). \quad (89)$$

The total number of particles  $N$  when starting from a single seed site can be obtained by integrating the pair connectedness function  $C$  over all space. This leads to the scaling form

$$N(r, t, L) = b^{-2\beta/\nu_\perp + d} N(rb^{1/\nu_\perp}, tb^{-z}, Lb^{-1}). \quad (90)$$

At the critical point,  $r = 0$ , and in the thermodynamic limit,  $L \rightarrow \infty$ , the above scaling relations lead to the following predictions for the time dependencies of observables: The density and the survival probability asymptotically decay like  $\rho(t) \sim t^{-\delta}$  and  $P_s(t) \sim t^{-\delta}$  with  $\delta = \beta/(\nu_\perp z)$ . In contrast, the number of particles in a cluster starting from a single seed site increases like  $N(t) \sim t^\Theta$  where  $\Theta = d/z - 2\beta/(\nu_\perp z)$  is the so-called critical initial slip exponent. Highly precise estimates of the critical exponents for clean one-dimensional directed percolation have been obtained by series expansions [232]:  $\beta = 0.276486$ ,  $\nu_\perp = 1.096854$ ,  $z = 1.580745$ ,  $\delta = 0.159464$ , and  $\Theta = 0.313686$ .

<sup>||</sup> Following the convention in the literature on the contact process, we denote the spatial correlation length and its critical exponent with a subscript  $\perp$ .

<sup>¶</sup> At more general absorbing state transitions, e.g., with several absorbing states, the survival probability scales with an exponent  $\beta'$  which may be different from  $\beta$  (see, e.g., [215])

## 6.2. Contact process with uncorrelated disorder

Quenched spatial disorder can be introduced into the contact process by making the birth rate  $\lambda$  or/and the death rate  $\mu$  random functions of the lattice site  $\mathbf{x}$ . In this subsection, we discuss point defects, i.e., spatially uncorrelated disorder.

The investigation of disorder effects on spreading transitions in the directed percolation universality class actually has a long history, but a coherent picture has been slow to emerge. According to the Harris criterion [25], directed percolation is unstable against weak disorder because the clean spatial correlation length critical exponent  $\nu_{\perp}$  violates the inequality  $d\nu_{\perp} > 2$  in all dimensions  $d > 4$ . (The exponent values are  $\nu_{\perp} \approx 1.097$  (1D), 0.73 (2D), and 0.58 (3D) [215]). A field-theoretic renormalization group study [233] confirmed the instability of the directed percolation critical fixed point. Moreover, no new critical fixed point was found. Instead the renormalization group displays runaway flow towards large disorder, indicating unconventional behavior. Early Monte-Carlo simulations [234] showed significant changes in the critical exponents while later studies [235, 236] of the two-dimensional contact process with dilution found logarithmically slow dynamics in violation of power-law scaling. In addition, slow dynamics was found in whole parameter regions in the vicinity of the phase transition [234, 237–240].

*6.2.1. Griffiths singularities: Optimal fluctuation arguments.* A first qualitative understanding of disorder and rare region effects in the disordered contact process can be gained by optimal fluctuation arguments similar to that in section 4.2. For definiteness, we assume the infection rate depends on the source site only and its probability distribution is binary,

$$P[\lambda(\mathbf{x})] = (1-p)\delta[\lambda(\mathbf{x}) - \lambda] + p\delta[\lambda(\mathbf{x}) - c\lambda]. \quad (91)$$

The impurity density  $p$  and their strength  $c$  are constants between 0 and 1. The impurities locally *reduce* the birth rate; the nonequilibrium transition will therefore occur at a value  $\lambda_c$  that is larger than the clean critical birth rate  $\lambda_c^0$ .

The inactive phase,  $\lambda < \lambda_c$ , can be divided into two regions. For birth rates below the clean critical point,  $\lambda < \lambda_c^0$ , the behavior is conventional because non of the rare regions are locally in the active phase. The system approaches the absorbing state exponentially fast in time. The decay time increases with  $\lambda$  and diverges as  $|\lambda - \lambda_c^0|^{-z\nu_{\perp}}$  where  $z$  and  $\nu_{\perp}$  are the exponents of the clean critical point [56, 66]. In contrast, in the Griffiths region, i.e., for birth rates between the clean and the dirty critical points,  $\lambda_c^0 < \lambda < \lambda_c$ , rare spatial regions devoid of impurities are locally in the active phase. Because they are of finite size, they cannot support a non-zero steady state density but their decay is very slow because it requires a rare, exceptionally large density fluctuation.

Following Noest [234, 237], the contribution of these rare regions to the time evolution of the total density can be estimated as follows. The probability  $w$  for finding a rare region of linear size  $L_{\text{RR}}$  devoid of impurities is given by  $w(L_{\text{RR}}) \sim \exp(-\tilde{p}L_{\text{RR}}^d)$  where  $\tilde{p} = -\ln(1-p)$  is a nonuniversal constant. The long-time decay of the density is dominated by these rare regions. To exponential accuracy, the rare region contribution to the density can be written as

$$\rho(t) \sim \int dL_{\text{RR}} L_{\text{RR}}^d w(L_{\text{RR}}) \exp[-t/\tau(L_{\text{RR}})] \quad (92)$$



where  $\tau(L_{\text{RR}})$  is the decay time of a rare region of size  $L_{\text{RR}}$ . Let us first discuss the behavior at the clean critical point,  $\lambda_c^0$ , i.e., at the boundary between the conventional inactive phase and the Griffiths region. At this point, the decay time of a single, impurity-free rare region of size  $L_{\text{RR}}$  scales as  $\tau(L_{\text{RR}}) \sim L_{\text{RR}}^z$  as follows from finite size scaling [22]. Here,  $z$  is the clean dynamical exponent. A saddle-point analysis leads to a stretched exponential time dependence,

$$\ln \rho(t) \sim -\tilde{p}^{z/(d+z)} t^{d/(d+z)}, \quad (93)$$

in contrast to the simple exponential decay as for  $\lambda < \lambda_c^0$ . Inside the Griffiths region, i.e., for  $\lambda_c^0 < \lambda < \lambda_c$ , the decay time of a single rare region depends exponentially on its volume  $\tau(L_{\text{RR}}) \sim \exp(aL_{\text{RR}}^d)$  because a coordinated fluctuation of the entire rare region is required to take it to the absorbing state [234,241]. The constant  $a$  vanishes at the clean critical point  $\lambda_c^0$  and increases with increasing  $\lambda$ . Repeating the saddle point analysis of the integral (92) for this case, we obtain a power-law decay of the density

$$\rho(t) \sim t^{-\tilde{p}/a} = t^{-d/z'} \quad (94)$$

where  $z' = da/\tilde{p}$  is a customarily used nonuniversal dynamical exponent in the Griffiths region. Thus, the optimal fluctuation arguments predict strong power-law Griffiths effects for the disordered contact process. The reason is the exponential increase of the decay time  $\tau(L_{\text{RR}})$  with the size of the rare region that compensates for their exponential rarity.

*6.2.2. Strong-disorder renormalization group.* An important step towards understanding spatial disorder effects on the directed percolation transition has recently been made by Hooyberghs et al. [41,42]. These authors used the Hamiltonian formalism [242] to map the one-dimensional disordered contact process onto a random quantum spin chain. They then applied a version of the Ma-Dasgupta-Hu strong-disorder renormalization group [36] discussed in section 5.3 and showed that the transition is controlled by an infinite-randomness critical point, at least for sufficiently strong disorder. The basic ingredients of this analysis can be explained by directly discussing the birth and death rates without reference to the equivalent quantum system.

Let us consider a one-dimensional contact process where both the annihilation rate  $\mu_i$  at site  $i$  and the infection rate  $\lambda_{ij}$  between neighboring sites  $i$  and  $j$  are random functions of the lattice sites with broad probability distributions. Following the strong-disorder renormalization group approach, we identify the largest rate in the system  $\Omega = \max(\mu_i, \lambda_{ij})$ . If the largest rate is an annihilation rate, say  $\mu_2$ , site 2 is almost always empty and can be decimated out. However, “virtual occupations” of site 2 generate a renormalized infection rate between sites 1 and 3 that can be estimated as follows: To propagate the infection from site 1 to site 3, first it has to propagate from site 1 to site 2 which happens with rate  $\lambda_{12}$ . However, site 3 can only be reached, if the infection propagates from site 2 to site 3 *before* site 2 decays. Since the probability distributions are broad,  $\mu_2 \gg \lambda_{23}$ , and the probability for this to happen is  $\lambda_{23}/\mu_2$ . Thus, the renormalized infection rate between sites 1 and 3 is

$$\bar{\lambda}_{13} = \lambda_{12}\lambda_{23}/\mu_2. \quad (95)$$

If the largest rate is an infection rate, say  $\lambda_{23}$ , which connects sites 2 and 3, the two sites will (almost) always be in the same state, either both active or both inactive. They can therefore be replaced by a new single site with twice the weight (moment).

To estimate the renormalized annihilation rate, we note that total annihilation of the cluster can occur via two processes: (i) site 2 decays (with rate  $\mu_2$ ), then site 3 decays *before* site 2 gets reinfected. Since  $\lambda_{23} \gg \mu_3$ , the probability for this is  $\mu_3/\lambda_{23}$ . Thus the total rate for process (i) is  $\mu_2\mu_3/\lambda_{23}$ . Process (ii) consists of site 3 decaying first, followed by site 2 and makes an identical contribution to the rate. Thus, the renormalized death rate of the cluster is

$$\bar{\mu} = 2\mu_2\mu_3/\lambda_{23} . \quad (96)$$

Except for an extra factor of 2, the recursion relations (95) and (96) are completely equivalent to the recursion relations (62) and (63) in the strong disorder renormalization group analysis of the random transverse field Ising chain. Consequently, Hooyberghs et al. [41, 42] also found equivalent results. The critical point in the disordered one-dimensional contact process is of infinite-randomness type, i.e., under renormalization, the relative width of the probability distributions of  $\mu_i$  and  $\lambda_{ij}$  increase without limit.

The scaling behavior at such an infinite randomness critical point is different from that of the clean contact process. Most importantly, the dynamics is extremely slow. The power-law scaling (86) gets replaced by activated dynamical scaling

$$\ln(\xi_t) \sim \xi_{\perp}^{\psi}, \quad (97)$$

characterized by a new exponent  $\psi$ . This exponential relation between time and length scales implies that the dynamical exponent  $z$  is formally infinite. In contrast, the static scaling behavior remains of power law type.

Moreover, at an infinite-randomness fixed point the probability distributions of observables become extremely broad, so that averages are dominated by rare events such as rare spatial regions with large infection rate. In such a situation, averages and typical values of a quantity do not necessarily agree. Nonetheless, the scaling form of the *average* density is obtained by simply replacing the power-law scaling combination  $tb^{-z}$  by the activated combination  $\ln(t)b^{-\psi}$  in the argument of the scaling function:

$$\rho(r, \ln(t), L) = b^{-\beta/\nu_{\perp}} \rho(rb^{1/\nu_{\perp}}, \ln(t)b^{-\psi}, Lb^{-1}) . \quad (98)$$

Analogously, the scaling forms of the average survival probability and the average number of sites in a cluster starting from a single site are

$$P_s(r, \ln(t), L) = b^{-\beta/\nu_{\perp}} P_s(rb^{1/\nu_{\perp}}, \ln(t)b^{-\psi}, Lb^{-1}) \quad (99)$$

$$N(r, \ln(t), L) = b^{-2\beta/\nu_{\perp}+d} N(rb^{1/\nu_{\perp}}, \ln(t)b^{-\psi}, Lb^{-1}) . \quad (100)$$

These activated scaling forms lead to logarithmic time dependencies at the critical point (in the thermodynamic limit). The average density and the survival probability asymptotically decay like  $\rho(t) \sim [\ln(t)]^{-\bar{\delta}}$  and  $P_s(t) \sim [\ln(t)]^{-\bar{\delta}}$  with  $\bar{\delta} = \beta/(\nu_{\perp}\psi)$  while the average number of particles in a cluster starting from a single seed site increases like  $N(t) \sim [\ln(t)]^{\bar{\Theta}}$  with  $\bar{\Theta} = d/\psi - 2\beta/(\nu_{\perp}\psi)$ . Within the strong disorder renormalization group approach the critical exponents of the disordered one-dimensional contact process can be calculated exactly. The numerical values are  $\beta = 0.38197$ ,  $\nu_{\perp} = 2$ ,  $\psi = 0.5$ ,  $\bar{\delta} = 0.38197$ , and  $\bar{\Theta} = 1.2360$ . In spatial dimensions larger than one, the renormalization group can only be implemented numerically. As was discussed in section 5.4, this has been done for the strong-disorder renormalization group of the two-dimensional random transverse field Ising model [26]. Using the analogy between the renormalization group of the Ising model and the contact process, Hooyberghs et al. [42] therefore concluded that the disordered contact process in two dimensions will also show an infinite randomness critical point.

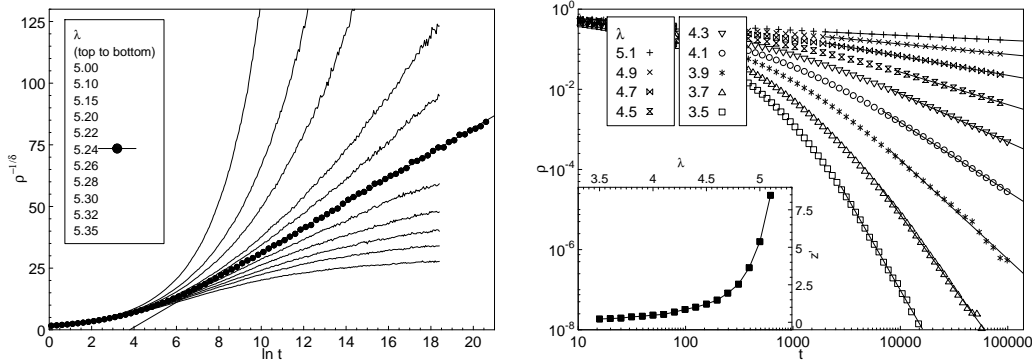


**Figure 11.** Left:  $\rho^{-1/\bar{\delta}}$  vs.  $\ln(t)$  for a system of  $10^4$  sites with  $p = 0.3$  and  $c = 0.2$ . The data are averages over 480 runs, each with a different disorder realization. The filled circles mark the critical birth rate  $\lambda_c = 5.24$ , and the straight line is a fit of the long-time behavior to eq. (101). Right: Log-log plot of the density time evolution in the Griffiths region for systems with  $p = 0.3$ ,  $c = 0.2$  and several birth rates  $\lambda$ . The system sizes are  $10^7$  sites for  $\lambda = 3.5, 3.7$  and  $10^6$  sites for the other  $\lambda$  values. The straight lines are fits to the power law  $\rho(t) \sim t^{-1/z'}$  predicted in eq. (94). Inset: Dynamical exponent  $z'$  vs. birth rate  $\lambda$  (from [43]).

In addition to the infinite-randomness behavior at the critical point, the strong-disorder renormalization group also yields strong power-law rare region effects in the Griffiths phase in agreement with the optimal fluctuation arguments presented in section 6.2.1.

*6.2.3. Computer simulations.* Early Monte-Carlo simulations of the disordered contact process [234–237] gave somewhat inconclusive results ranging from a modification of the critical exponents to logarithmical violations of scaling. This was partially due to the fact that a consistent theory was not available at that time. Hooyberghs et al. [42] performed both Monte-Carlo and density matrix renormalization group (DMRG) studies of rather small systems ( $L \leq 24$ ). They concluded that the phase transition is indeed controlled by the infinite randomness fixed point discussed in section 6.2.2, but only if the initial (bare) disorder is large enough. For weaker initial disorder they predict nonuniversal continuously varying exponents with either power-law or activated dynamical scaling.

Recently, Vojta and Dickison [43] have performed a detailed large-scale Monte-Carlo study of the one-dimensional contact process with binary disorder distribution (91). They studied system sizes up to  $L = 10^7$  and very long-times up to  $t = 10^9$  which is three orders of magnitude in  $t$  longer than previous simulations. A first set of calculations started from a full lattice and followed the time evolution of the average density. To test the strong-disorder renormalization group theory, the time dependence of the density can be plotted according to the predicted activated scaling law

$$\rho(t) \sim [\ln(t)]^{-\bar{\delta}}, \quad (101)$$

with  $\bar{\delta} = 0.38197$ . The left panel of figure 11 shows the resulting graph for a system of  $10^4$  sites with  $p = 0.3$  and  $c = 0.2$ . The evolution of the density at the critical birthrate  $\lambda = 5.24$  follows eq. (101) over almost six orders of magnitude in time. Therefore, the

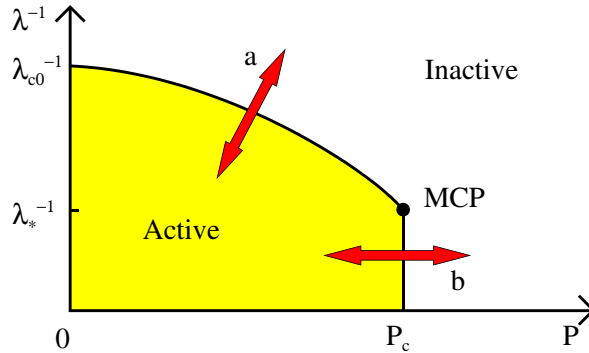


**Figure 12.** Schematic phase diagram of a site diluted contact process as function of impurity concentration  $p$  and birth rate  $\lambda$ . There is a multicritical point at  $p = p_c$  and  $\lambda = \lambda_*$  (from [243]).

critical point of the disordered contact process is indeed of infinite-randomness type. Analogous calculations were performed for two other sets of parameters ( $p = 0.3$  with  $c$  varying from 0.2 to 0.8 as well as  $c = 0.2$  with  $p$  varying from 0.2 to 0.5). For all parameters (including the cases of weak disorder), the critical point is characterized by the logarithmic density decay (101) with a universal exponent  $\bar{\delta} = 0.38197$ . In addition to the critical point, Vojta and Dickison [43] also studied the Griffiths region between the clean critical birthrate,  $\lambda_c^0 = 3.298$  and the dirty critical birthrate  $\lambda_c = 5.24$ . The right panel of figure 11 shows a double-logarithmic plot of the density time evolution for birth rates  $\lambda = 3.5 \dots 5.1$  and  $p = 0.3, c = 0.2$ . For all birth rates  $\lambda$  shown,  $\rho(t)$  follows (94) over several orders of magnitude in  $\rho$  (except for the largest  $\lambda$  where we could observe the power law only over a smaller range in  $\rho$  because the decay is too slow). The nonuniversal dynamical exponent  $z'$  can be obtained by fitting the long-time asymptotics of the curves to eq. (94). The inset of the figure shows  $z'$  as a function of the birth rate  $\lambda$ . As predicted,  $z'$  increases with increasing  $\lambda$  throughout the Griffiths region with an apparent divergence around  $\lambda = \lambda_c = 5.24$ .

These large-scale simulations of the one-dimensional contact process with point defects thus provide strong evidence that the critical point is of infinite-randomness type with universal critical exponents (even for weak bare disorder). The critical point is accompanied by strong Griffiths singularities characterized by non-universal power-law decay of the density. These results are in excellent agreement with the general classification of dirty phase transitions suggested in section 3.3.

*6.2.4. Contact process on a randomly diluted lattice.* Quenched spatial disorder can also be introduced into the contact process by site or bond dilution of the underlying lattice. In space dimensions  $d \geq 2$ , this leads to the phase diagram shown in figure 12 which is very similar to that of a diluted quantum magnet discussed in section 5.4. (In contrast, in  $d = 1$ , any dilution immediately destroys the active phase.) For small impurity concentrations below the percolation threshold of the lattice,  $p < p_c$ , the active phase survives, but the critical birth rate increases with  $p$  (to compensate for the missing neighbors). Right at the percolation threshold the active phase survives on the infinite percolation cluster for  $\lambda > \lambda_*$ . For  $p > p_c$ , no active phase can exist because the lattice consists of disconnected clusters of finite size that do not support a steady state density of active sites.

The contact process on a site-diluted lattice therefore has two nonequilibrium phase transitions, separated by a multicritical point at  $(p_c, \lambda_*)$ . For  $p < p_c$ , the transition (marked by “a” in Fig. 12) is expected to be in the universality class of the generic disordered contact process discussed in the last subsections. In contrast, the phase transition “b” across the percolation threshold of the lattice is expected to show different critical behavior.

Vojta and Lee [243] showed that the interplay of geometric criticality and dynamic fluctuations of the contact process does indeed lead to a novel universality class for this nonequilibrium phase transition. Even though the transition is driven entirely by the geometry of the lattice, the dynamical fluctuations of the contact process enhance the singularities in all quantities involving dynamic correlations. By combining results from classical percolation theory [147] with the finite-size properties of a supercritical contact process, Vojta and Lee [243] determined the critical behavior analytically. They found activated dynamical scaling  $\ln \xi_t \sim \xi_{\perp}^{\psi}$  with the critical exponent  $\psi$  being equal to the fractal dimension of the critical percolation cluster,  $\psi = D_f$ . As a result, the critical behavior is very similar to that of the infinite-randomness critical point discussed above. Specifically, the long-time decay of the density  $\rho$  of active sites at  $p = p_c$  is logarithmically slow,  $\rho(t) \sim [\ln(t/t_0)]^{-\bar{\delta}}$ . The exponent  $\bar{\delta} = \beta_c/(\nu_c D_f)$  is determined by  $D_f$  together with the order parameter and correlation length exponents,  $\beta_c$  and  $\nu_c$ , of the lattice percolation transition. In contrast to the enhanced dynamical singularities, the exponents of static quantities like the steady state density  $\rho_{st}$  and the spatial correlation length  $\xi_{\perp}$  are identical the corresponding lattice percolation exponents,  $\rho_{st}(p) \sim |r|^{\beta_c}$  and  $\xi_{\perp} \sim |r|^{\nu_c}$  where  $r = p - p_c$  measures the distance from the percolation threshold. Off criticality, i.e., away from the percolation threshold, there are strong rare region effects characterized by a non-exponential density decay  $\rho(t) \sim (t/t_0)^{-d/z'}$  for  $p > p_c$  and  $\rho(t) - \rho_{st} \sim e^{-[(d/z'') \ln(t/t_0)]^{1-1/d}}$  for  $p < p_c$ . The nonuniversal exponents  $z'$  and  $z''$  diverge as  $\xi_{\perp}^{D_f}$  for  $p \rightarrow p_c$ .

### 6.3. Contact process with extended defects

So far, our discussion of disorder effects on the phase transition in the contact process has been restricted to uncorrelated or short-range correlated disorder (i.e., point defects). In this subsection we consider spatially extended (linear or planar) defects. From the general arguments in section 3.2, we expect the disorder correlations to enhance the impurity effects.

Vojta [65] studied a contact process with quenched spatial disorder perfectly correlated in  $d_{\text{cor}} > 0$  space dimensions but uncorrelated in the remaining  $d_{\text{ran}} = d - d_{\text{cor}}$  space dimensions. In such a system, the rare regions are infinite in  $d_{\text{cor}}$  dimensions but finite in  $d_{\text{ran}}$  dimensions. This is a crucial difference from systems with uncorrelated disorder, where the rare regions are finite. Because the contact process has a phase transition in all dimensions larger than zero, an infinite rare region can undergo a real phase transition *independently* of the rest of the system. Those rare regions that are locally in the ordered phase will have a true nonzero stationary density, even if the bulk system is still in the inactive phase. The resulting global phase transition is thus smeared by the same mechanism that smears the equilibrium transition in an Ising model with planar defects discussed in section 4.6 or the itinerant Ising magnet of section 5.6. As the birth rate  $\lambda$  is increased, the order parameter develops very inhomogeneously in space with different parts of the system becoming active independently at different values of  $\lambda$ .

The leading behavior in the tail of the smeared transition can again be determined by optimal fluctuation arguments [65]. Here we summarize the results for a binary probability distribution  $P[\lambda(\mathbf{x}_{\text{ran}})] = (1-p)\delta[\lambda(\mathbf{x}_{\text{ran}}) - \lambda] + p\delta[\lambda(\mathbf{x}_{\text{ran}}) - c\lambda]$  with constants  $p$  and  $c$  between zero and one.  $\mathbf{x}_{\text{ran}}$  is the projection of the position vector  $\mathbf{x}$  on the uncorrelated directions. The probability  $w$  for finding a rare region of linear size  $L_{\text{RR}}$  devoid of impurities is, up to pre-exponential factors, given by  $w \sim \exp(-\tilde{p}L_{\text{RR}}^{d_{\text{ran}}})$  with  $\tilde{p} = -\ln(1-p)$ . According to finite-size scaling [22], such a region undergoes a true phase transition to the active phase at  $\lambda_c(L_{\text{RR}}) = \lambda_c^0 + AL_{\text{RR}}^{-\phi}$  where  $\phi$  is the clean ( $d$ -dimensional) finite-size scaling shift exponent and  $A$  is a constant. If the total dimensionality  $d = d_{\text{cor}} + d_{\text{ran}} < 4$ , hyperscaling is valid and  $\phi = 1/\nu_{\perp}$  which we assume from now on. The total (average) density  $\rho$  at a certain  $\lambda > \lambda_c^0$  is obtained by summing over all active rare regions. In this way, the stationary density develops an exponential tail,

$$\rho(\lambda) \sim \exp(-B(\lambda - \lambda_c^0)^{-d_{\text{ran}}\nu_{\perp}}), \quad (102)$$

reaching to the clean critical point  $\lambda_c^0$ . Here,  $B = \tilde{p}A^{d_{\text{ran}}\nu_{\perp}}$  is a constant. Analogous arguments can be made for the survival probability  $P(\lambda)$  of a single seed site. If the seed site is on an active rare region it will survive with a probability that depends on  $\lambda$  with a power law. If is not on an active rare region, the seed will die. To exponential accuracy the survival probability is thus also given by (102).

We now turn to the dynamics in the tail of the smeared transition. The long-time behavior of the density is dominated by the slow decay of the rare regions while the bulk contribution decays exponentially. Proceeding in analogy to section 4.8, Vojta [65] showed that the leading long-time decay of the density at the clean critical point,  $\lambda = \lambda_c^0$ , follows a stretched exponential,

$$\ln \rho(t) \sim -\tilde{p}^{z/(d_{\text{ran}}+z)} t^{d_{\text{ran}}/(d_{\text{ran}}+z)} \quad (103)$$

where  $z$  is the clean dynamical exponent of the  $d$ -dimensional bulk system. For  $\lambda > \lambda_c^0$ , the behavior changes. At times below a crossover time  $t_x \sim (\lambda - \lambda_c^0)^{-(d_{\text{ran}}+z)\nu_{\perp}}$  the density decay is still given by the stretched exponential (103). For times larger than  $t_x$  the system realizes that some of the rare regions are in the active phase and contribute to a finite steady state density. The approach of the average density to this steady state value is characterized by a nonuniversal power-law.

$$\rho(t) - \rho(\infty) \sim t^{-\zeta}. \quad (104)$$

To test the predictions of the optimal fluctuation theory, Dickison and Vojta [66] have performed large-scale Monte-Carlo simulations of a contact process on a square lattice. The disorder consists of linear defects, i.e., the local birthrate  $\lambda(\mathbf{x})$  depends only on one of the coordinates and is perfectly correlated in the other. The disorder distribution is binary.

The left panel of figure 13 shows a comparison of the stationary density  $\rho_{\text{st}}$  as a function of  $\lambda$  between the clean system and a dirty system with  $p = 0.2, c = 0.2$ . The clean system ( $p = 0$ ) has a sharp phase transition with a power-law singularity of the density,  $\rho_{\text{st}} \sim (\lambda - \lambda_c^0)^{\beta}$  at the clean critical point  $\lambda_c^0 \approx 1.65$  with  $\beta \approx 0.58$  in agreement with the literature [235]. In contrast, in the dirty system, the density increases much more slowly with  $\lambda$  after crossing the clean critical point. This suggests either a critical point with a very large exponent  $\beta$  or exponential behavior. To test the prediction (102) of the optimal fluctuation theory, the right panel of figure 13 shows  $\ln \rho_{\text{st}}$  as a function of  $(\lambda - \lambda_c^0)^{-\nu_{\perp}}$  for several impurity concentrations  $p$ . (The

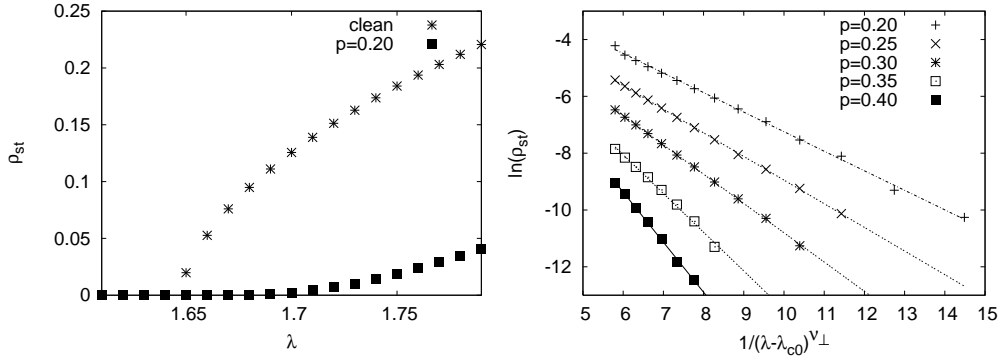


**Figure 13.** Left: Stationary density  $\rho_{st}$  as a function of birth rate  $\lambda$  for a clean system and a system with impurity concentration  $p = 0.2$  and strength  $c = 0.2$ . The data are averages over 200 disorder realizations and the system size is  $L = 1000$ . Right: Logarithm of the stationary density  $\rho_{st}$  as a function of  $(\lambda - \lambda_c^0)^{-\nu_{\perp}} = (\lambda - \lambda_c^0)^{-0.734}$  for several impurity concentrations  $p$  and  $L = 3000$ . The straight lines are fits to eq. (102) (from [66]).

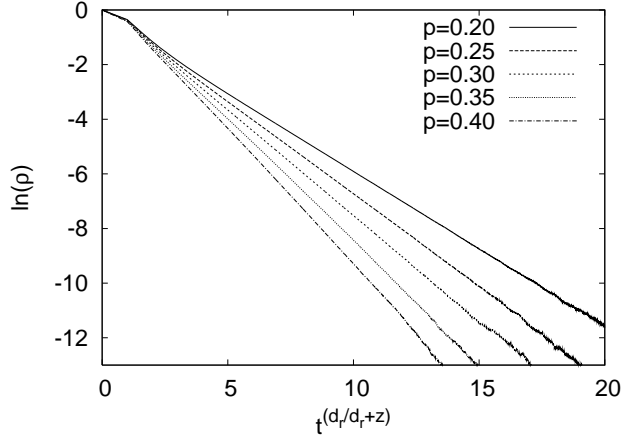


**Figure 14.** Logarithm of the density at the clean critical point  $\lambda_c^0$  as a function of  $t^{1/(1+z)} = t^{0.362}$  for  $c = 0.2$  and several impurity concentrations ( $p = 0.2, \dots, 0.4$  from top to bottom) and system size  $L = 3000$ . The long-time behavior follows a stretched exponential  $\ln \rho = -Et^{0.362}$  (from [66]).

clean two-dimensional spatial correlation length exponent is  $\nu_{\perp} = 0.734$  [244].) The data show that the density tail is indeed a stretched exponential, following the law (102) over at least two orders of magnitude in  $\rho_{st}$ . Fits of the data to eq. (102) can be used to determine the decay constants  $B$ . As predicted by extremal statistics theory, the decay constants depend linearly on  $\tilde{p} = -\ln(1 - p)$ .

In addition to the stationary density, Dickison and Vojta [66] also studied its time evolution in the tail of the smeared transition. Figure 14 shows the time dependence of the density right at the clean critical point. The data follow the predicted stretched exponential behavior (103) with  $z = 1.76$  [244] over more than three orders of magnitude in  $\rho$ . Additional calculations have been performed for  $\lambda > \lambda_c^0$ . In this parameter region, the stationary density is nonzero. The approach of the density to

this nonzero stationary value follows a nonuniversal power-law as predicted in (104).

#### 6.4. Other nonequilibrium systems

While the influence of quenched spatial disorder on the directed percolation universality class has been studied in great detail, other dirty absorbing state transitions have received much less attention. Hooyberghs et al. [42] studied disorder effects on the transition of a generalized contact process with two absorbing states [230]. This model is in the DP2 [227] or parity conserving [224] universality class (the two coincide in one space dimension [215]). According to the Harris criterion, the clean transition is unstable with respect to weak disorder because the clean correlation length exponent is  $\nu_{\perp} \approx 1.83$  (see, e.g., [215]) violating the inequality  $d\nu_{\perp} > 2$ . Hooyberghs et al. applied the strong-disorder renormalization group to a weakly disordered generalized contact process with quenched spatial disorder. They found that the renormalization group scheme does not work; the flow is *not* towards larger disorder. They concluded that the transition is unlikely to be controlled by an infinite disorder fixed point. Very recently, Odor and Menyhard [245] reported numerical simulations of a cellular automaton in the parity conserving universality class. They found that weak disorder does not change the critical exponents from their clean values. How this can be reconciled with the violation of the Harris criterion remains a question for future research.

Let us also briefly mention another important nonequilibrium model displaying rare region effects, even though it is not directly related to an order-disorder phase transition, viz. Sinai's model of diffusion with random local bias [246]. In the absence of a bias, the mean-square displacement in this model grows logarithmically slowly in time, while for small bias it grows with a nonuniversal power-law. Igloi, Turban and Rieger [119, 247] pointed out a connection between the Ising model and directed walks. Later, Igloi and Rieger [248] established an exact relation between the statistical properties of anomalous diffusion and the properties of random quantum spin chains. At about the same time Fisher, Le Doussal and Monthus used a version of the strong-disorder renormalization group to determine the exact asymptotic long-time behavior of the Sinai model [138, 139]. These papers started a stream of work on this topic. A detailed discussion is beyond the scope of this review, for more details see, e.g., reference [121].

## 7. Discussion and conclusions

In this section we summarize the main theoretical ideas presented in the review. To this end, we organize the examples presented in sections 4, 5, and 6 according to the proposed classification of rare region effects, and we relate our results to those of other methods. We also discuss the generality of the rare region classification, its limitations, the experimental situation, and some related questions.

### 7.1. Summary: Classification of rare region effects

This topical review has been devoted to rare region effects at order-disorder transitions between conventional phases. In section 3.3 we have introduced a classification of these effects according to the effective dimensionality  $d_{\text{RR}}$  of the rare regions [67]. Its basic idea is as follows: The probability  $w$  for finding a rare region of volume  $V_{\text{RR}}$  (in the



random directions) decreases exponentially with its size,  $w \sim \exp(-pV_{\text{RR}})$ . This must be compared to how rapidly the contribution of a *single* region to thermodynamic quantities increases with its size. As was explained in section 3.3, three cases can be distinguished.

*Class A:* If the effective dimensionality of the rare regions is below the lower critical dimension of the problem,  $d_{\text{RR}} < d_c^-$ , the contribution of a rare region to thermodynamic quantities only increases like a power of its size. Therefore, Griffiths effects are expected to be exponentially weak and the dirty critical point will display power-law scaling.

*Class B:* For  $d_{\text{RR}} = d_c^-$ , rare region contributions increase exponentially with the size of the rare region resulting in strong power-law Griffiths singularities. The dirty critical point is expected to be of infinite randomness type with activated scaling.

*Class C:* If  $d_{\text{RR}} > d_c^-$ , an isolated rare region can undergo the phase transition independent of bulk and develop a static order parameter. This completely destroys the global phase transition by smearing.

In the following we relate the explicit results discussed in sections 4, 5, and 6 to this classification. We start with the classical systems of section 4. The classical randomly diluted Ising model introduced in section 4.1 as well as the classical random- $T_c$  Landau-Ginzburg-Wilson theory of section 4.3 have spatially uncorrelated disorder. The rare regions are of finite size in all directions and their effective dimensionality is  $d_{\text{RR}} = 0$ . Since the lower critical dimension of the Ising model is  $d_c^- = 1$ , these systems fall into class A. In agreement with the classification, their Griffiths singularities are exponentially weak, as was discussed in sections 4.2 and 4.3. In contrast, the properties of the dirty critical point are still controversial. On the one hand, high precision numerical simulations (see, e.g., [31, 249]) yield conventional power-law critical behavior and no indications of exotic properties, in agreement with early perturbative renormalization results [250, 251]. Moreover, the exponent values are in *quantitative* agreement with re-summed high-order perturbative renormalization group calculations [252–256]. On the other hand, Dotsenko et al. [257, 258] analyzed the stability of the perturbative fixed points with respect to replica symmetry breaking and found them unstable, suggesting unconventional behavior. However, two-loop field theoretical studies [259, 260] did not find such instabilities with respect to replica-symmetry breaking. Clearly, more work is necessary to determine whether the critical point in the Ising model with uncorrelated disorder indeed follows all of the predictions of class A.

If the disorder is perfectly correlated in  $d_{\text{cor}}$  dimensions, the rare regions are infinite in the corresponding directions but finite in the remaining  $d_{\text{ran}} = d - d_{\text{cor}}$  directions. Thus, their effective dimensionality is  $d_{\text{RR}} = d_{\text{cor}}$ . The McCoy-Wu model discussed in section 4.5, a two-dimensional Ising model with linear defects, falls into class B because  $d_{\text{RR}} = d_c^- = 1$ . In agreement with the classification, this model displays strong power-law Griffiths singularities and an infinite-randomness critical point. Using Monte-Carlo simulations [40] and a numerical implementation of the strong-disorder renormalization group [26], the same behavior was also found in two dimensions. As was discussed in section 4.5, perturbative renormalization group calculations [106, 107, 261] cannot capture the nonperturbative rare region physics, they predict conventional behavior in disagreement with the exact results. In this context, an investigation of replica-symmetry breaking in systems with extended defects would be of great interest.

In an Ising model with planar defects, the rare regions have dimension  $d_{\text{RR}} = 2$ .

This is above the lower critical dimension, and the model falls into class C. The explicit results discussed in section 4.6 show that the global phase transition is indeed smeared [63] as was also confirmed by large-scale Monte Carlo simulations [64].

In the case of zero-temperature quantum phase transitions, the imaginary time direction has to be included when calculating the effective rare region dimension  $d_{\text{RR}}$ . Therefore, the rare regions in the random transverse field Ising model introduced in section 5.1 are one-dimensional,  $d_{\text{RR}} = 1$ , and the model falls into class B. The strong disorder renormalization group results [26, 34, 35] and Monte-Carlo simulations [39, 40, 116] discussed in sections 5.1 to 5.4 are in complete agreement with this classification: The critical point is of infinite-randomness type with activated scaling. It is accompanied by strong power-law Griffiths singularities.

At the quantum phase transition of the diluted bilayer Heisenberg quantum antiferromagnet discussed in section 5.5, the effective dimensionality of the rare regions in  $d_{\text{RR}} = 1$ , too. However, the lower critical dimension of the Heisenberg universality class is  $d_c^- = 2$ . Therefore, this system falls into class A. This agrees with the results of large-scale Monte-Carlo simulations [70] that show a conventional critical point with power-law scaling and universal exponents.

In systems with dissipative order parameter dynamics like the itinerant magnets of section 5.6, the behavior gets modified because the effective interaction in imaginary time direction takes a long-ranged  $1/\tau^2$  form. The rare regions therefore correspond to one-dimensional classical systems with  $1/\mathbf{x}^2$  interaction. For Ising symmetry, the rare regions can undergo the phase transition independently from the bulk, and the system is in class C. This results in a smeared global phase transition [60]. One-dimensional Heisenberg models with  $1/\mathbf{x}^2$  interaction are exactly at their lower critical dimension. Consequently, disordered itinerant Heisenberg magnets fall into class B and show power-law quantum Griffiths effects [67] (at least as long as long-range interactions between the rare regions can be neglected [73]). As is to be expected, a straight-forward perturbative analysis [179] of the transition in a disordered itinerant magnet does not predict any unconventional properties. However, Narayanan et al. [262, 263] included the rare regions in a perturbation renormalization group calculation in an approximate way. They found that the rare regions destabilize the conventional fixed points but they could not resolve the ultimate fate of the transition.

In section 6, we have demonstrated that the rare region classification also applies to nonequilibrium phase transitions in the directed percolation universality class. In the contact process with uncorrelated disorder (point defects), the effective dimension of the rare regions is  $d_{\text{RR}} = 1$  including the time dimension. This is identical to the lower critical dimension of directed percolation, and thus the system is in class B. In agreement with the classification, the strong-disorder renormalization group as well as Monte-Carlo simulations yield an infinite-randomness critical point and strong power-law Griffiths effects. If the defects are extended, the rare region dimension is  $d_{\text{RR}} > 1$  placing the system in class C. The classification thus predicts a smeared transition in agreement with the explicit results in section 6.3.

In summary, all results presented in sections 4, 5, and 6 fit into the general classification of rare region effects at weakly disordered order-disorder transitions, as introduced in section 3.3.

## 7.2. Experiments

This subsection is devoted to experimental observations of the rare region effects discussed in this review.

*7.2.1. Classical phase transitions.* As explained in section 4, the thermodynamic rare region effects at generic classical (i.e., thermal) phase transitions are exponentially weak. As was first argued by Imry [52] they are probably unobservable in experiments, because the probability for finding sufficiently large rare regions is extremely small even in a macroscopic sample of about  $10^{23}$  particles. Indeed, to the best of our knowledge, the thermodynamic Griffiths singularities derived in sections 4.1 to 4.3 have never been experimentally verified.

In contrast to the thermodynamics, the long-time dynamical behavior of generic classical systems is predicted to be dominated by the rare regions, see section 4.4. Lloyd and Mitchell [264] investigated the dynamics above the Neel temperature  $T_N = 210\text{K}$  of the dilute Heisenberg antiferromagnet  $\text{KMn}_{0.3}\text{Ni}_{0.7}\text{F}_3$  using inelastic neutron scattering. Below the transition temperature  $T_N^0 = 246\text{K}$  of pure  $\text{KNiF}_3$  they found very slow relaxation compatible with a long-time tail of stretched exponential form. However, the data were not sufficient for a quantitative confirmation of (36).

In recent years, there have been a number of systems in which experiments have revealed unusual cluster or domain structures. Many of these phenomena have been related related to Griffiths phases, at least at a qualitative level. Binek, Kleemann, and coworkers [265–267] found domain-like antiferromagnetic correlations in the Ising-type antiferromagnets  $\text{FeCl}_2$  and  $\text{FeBr}_2$  when exposed to an axial field  $H$  at temperatures below the Neel temperature on zero field. They attributed these structures to fluctuating distributions of demagnetizing fields and called the corresponding phase a *field-induced Griffiths phase*. However, it should be emphasized that the character of this domain phase is fundamentally different from the Griffiths phases discussed in this review. The latter are caused by *static* disorder fluctuations while the demagnetizing fields fluctuates in time. Later, Binek and Kleemann also studied the diluted ferromagnet  $\text{K}_2\text{Cu}_{1-x}\text{Zn}_x\text{F}_4$  and the diluted antiferromagnet  $\text{Fe}_{1-x}\text{Zn}_x\text{F}_4$  [268] by measuring the magnetic susceptibility. They found deviations from the Curie-Weiss behavior of the corresponding clean systems, but no relation to the exponential Griffiths singularities discussed in sections 4.1 to 4.3 was established. Similar results were also reported for  $\text{Rb}_2\text{Co}_{1-x}\text{Mg}_x\text{F}_4$  [269]. Colla et al. [270] studied the dielectric response of a disordered antiferroelectric,  $\text{Pb}_{0.97}\text{La}_{0.03}(\text{Zr}_{0.60}\text{Sn}_{0.30}\text{Ti}_{0.10})\text{O}_3$ . They found nonanalytic contributions compatible with a Griffiths scenario in the nonlinear dynamic susceptibility but not in the dependence on dc fields.

An important class of materials whose properties have been related to rare region effects are the manganites. They are members of a broader class of compounds where the electronic correlations play an important role. The manganites have rich phase diagrams exhibiting a variety of phases with unusual spin, charge, lattice and orbital order; for details see, e.g., the reviews [271, 272] and the references therein. They display many exotic properties, most notably unexpectedly large magnetotransport properties. Moreover, even in the best available crystals, manganites are intrinsically inhomogeneous, a phenomenon sometimes called nanoscale phase separation. Salamon and coworkers [273, 274] proposed a connection between the unusual properties of doped  $\text{LaMnO}_3$  and the Griffiths phase that arises when disorder suppresses the magnetic transition (see also reference [275] for a theoretical account). They found that

the magnetic susceptibility in  $\text{La}_{0.7}\text{Ca}_{0.3}\text{MnO}_3$  strongly increases *before* the system reaches the Curie temperature. They interpreted this upturn as a Griffiths singularity and analyzed it using the susceptibility matrix approach of Bray [55]. However, an explicit verification of the exponential classical Griffiths singularity was not found. Hartinger et al. [276] and Deisenhofer et al. [277] found inhomogeneous states in  $\text{La}_{1-x}\text{Sr}_x\text{MnO}_3$  that they attributed to Griffiths-like phases. The latter paper also pointed out that the disorder in the manganites is likely to be correlated. Because these disorder correlations enhance the rare region effects they may be responsible for making the Griffiths singularities in the manganites accessible to experiment.

A Griffiths phase has also been predicted to occur in diluted magnetic semiconductors above the ferromagnetic transition temperature [278]. Recent measurements on  $\text{Mn}_x\text{Ge}_{1-x}$  [279] are compatible with a scenario in which ferromagnetic long-range order occurs below some  $T_c$  and short-range order occurs between  $T_c$  and  $T_c^*$ . (For  $x = 0.05$ ,  $T_c \approx 12\text{K}$  and  $T_c^* \approx 112\text{K}$ ). However, the explicit form of the Griffiths singularities was not studied.

*7.2.2. Quantum phase transitions.* While thermodynamic Griffiths singularities at generic classical transitions are very weak, looking for rare region effects at zero-temperature quantum phase transitions is a-priori more promising, because quantum Griffiths effects are generically stronger than classical ones.

When the prototypical transverse-field Ising magnet  $\text{LiHoF}_4$  is diluted by randomly replacing magnetic  $\text{Ho}^{3+}$  with nonmagnetic  $\text{Y}^{3+}$ , the long-range dipolar character of the interaction leads to frustration. In a transverse magnetic field, the result is therefore a quantum spin glass rather than a random quantum ferromagnet.  $\text{LiHo}_{1-x}\text{Y}_x\text{F}_4$  has been studied extensively since the seminal work of Wu et al. [114, 115], but its complex properties are beyond the scope of this review.

In recent years, there has been a lot of interest in the possibility of quantum Griffiths effects in the so-called heavy-fermion materials. These are intermetallic compounds of rare earth or actinide elements such as Cerium, Ytterbium or Uranium. The localized magnetic moment of the  $f$ -electrons of these atoms hybridizes with the delocalized conduction electrons generating quasi-particles with effective masses of 100 to 1000 electron masses. Many of these systems can undergo magnetic quantum phase transitions as a function of pressure or doping or magnetic field. Moreover, many show non-Fermi liquid behavior, i.e., anomalous temperature dependencies of specific heat, magnetic susceptibility and resistivity, as was first shown for  $\text{Y}_{0.8}\text{U}_{0.2}\text{Pd}_3$  in 1991 [280]. Since then, similar behavior has been found in a huge number of systems (for a detailed experimental review, see reference [281]).

Castro Neto, Castilla, and Jones [183] suggested that the anomalous temperature dependencies are a manifestation of power-law quantum Griffiths effects in the vicinity of a magnetic quantum phase transition. However, this early version of the theory neglected the damping of the magnetic modes due to the itinerant electrons. As was discussed in section 5.6 of this review, this damping qualitatively changes the low-temperature behavior. For Ising symmetry, which is relevant for the heavy-Fermion systems as most of them have sizeable spin anisotropies, the damping causes the rare regions to freeze leading to a smeared transition rather than quantum Griffiths effects [60–62]. Later, Castro Neto and Jones refined their theory by including the damping [282, 283]. They found that for sufficiently weak damping there will be a crossover temperature  $T^*$ . Power-law quantum Griffiths behavior can occur in a transient temperature window *above*  $T^*$  but below a microscopic cutoff scale (like

the Fermi temperature). For the experimentally important example of the heavy fermion materials, different approaches disagree concerning the value of this crossover temperature. Castro Neto and Jones [282–284] suggest that the damping of the locally ordered rare regions is weak. Therefore, quantum Griffiths behavior should occur in a broad temperature range and can be the source of the non-Fermi liquid behavior observed in at least some of the heavy-Fermion systems. In contrast, Millis, Morr and Schmalian [62, 285] argue that the carrier-spin coupling in heavy fermions is large, restricting quantum Griffiths effects to a narrow temperature window (if any). A complete resolution of this question will likely come from experiments that give more direct access to the strength of the damping term.

Recently, Johnston et al. [286] observed slow non-exponential nuclear magnetic relaxation in NMR experiments on the  $d$ -electron heavy fermion system  $\text{LiV}_2\text{O}_4$  with a small amount of magnetic defects. One possible explanation for this observation consists in the defects inducing magnetic order in large but finite volumes around the defect site. Johnston et al. [286] described these magnetic clusters by Griffiths physics.

Let us also briefly mention some experiments on random quantum spin chains. Early examples include the organic crystals NMP-TCNQ [287],  $\text{Qn}(\text{TCNQ})_2$  [288], and copper-doped TMMC [289]. The former two systems show low-temperature susceptibilities proportional  $T^{-\alpha}$  with  $\alpha < 1$  that have been interpreted as evidence for rare region physics. The latter system, TMMC, realizes an almost classical spin chain, presumably due to the large value of the spin involved ( $S = 5/2$  for  $\text{Mn}^{2+}$ ). More recently, Payen et al. [290] reported susceptibility and magnetization for the doped  $S = 1$  Haldane spin system  $\text{Y}_2\text{BaNi}_{1-x}\text{Zn}_x\text{O}_5$ . Below 4K they observed power-law temperature dependencies with non-universal exponents suggesting a gapless phase due to the disorder. Power-law temperature dependencies have also been reported for the  $S = 5/2$  spin chain system  $\text{MnMgB}_2\text{O}_5$  above a spin glass freezing temperature of about 600mK [291]. Masuda et al. [292] reported inelastic neutron scattering on the  $S = 1/2$  spin chain compound  $\text{BaCu}_2(\text{Si}_{0.5}\text{Ge}_{0.5})_2\text{O}_7$ . They found excellent agreement with the results of a strong-disorder renormalization group [207].

*7.2.3. Nonequilibrium phase transitions.* For nonequilibrium phase transitions, the experimental situation is even less satisfactory. The (clean) directed percolation universality class is ubiquitous in theory and simulations, but experimental verifications are strangely lacking [293]. To the best of our knowledge, the only (partial) verification so far has been found in the spatio-temporal intermittency in ferrofluidic spikes [294]. While disorder is often suggested as a reason for the striking absence of clean directed percolation scaling in at least some of the experiments, a systematic search for the infinite-randomness behavior discussed in section 6.2 and the accompanying power law Griffiths effects has not been performed.

In summary, even though rare region effects have been invoked in the analysis of a variety of experiments, clearcut experimental verifications of Griffiths singularities discussed in sections 4, 5, and 6 have not yet been achieved.

### 7.3. Conclusions

Quenched spatial disorder can have dramatic consequences for the properties of continuous phase transitions and critical points. An important role is played by rare strong disorder fluctuations and the rare spatial regions where they occur. This topical

review has focused on transitions of the order-disorder type at which the quenched disorder does not qualitatively change the properties of the phases but locally modifies the tendency towards one or the other. For this random- $T_c$  or random-mass type disorder (arguably the simplest type of quenched disorder), we have set up a general framework for understanding rare region effects in the vicinity of the “dirty phase transitions”. According to the classification introduced in section 3.3, the overall phenomenology of the transition is determined by the effective dimensionality of the rare regions.

Let us briefly point out the limitations of this approach. Even for order-disorder transitions between conventional phases, the effects of long-range spatial interactions are not understood. First, the very concept of a rare region may require modifications when the order parameter of a locally ordered island generically develops power-law tails. Second, long-range interactions can significantly increase the coupling between the rare regions. As a result, the rare region effects in systems with long-range interactions are likely to be more complex than those discussed here. This is particularly important in metallic systems, where the presence of electronic soft modes often self-generates long-range order parameter interactions [14]. For instance, it has been suggested [73] that the long-range RKKY interaction in metals further enhances the rare region effects in itinerant Heisenberg magnets.

Often, the presence of quenched disorder leads to the formation of new phases, such as the spin glass phases in classical magnets or the random-singlet states of certain antiferromagnetic spin chains, as briefly mentioned in section 5.7. These states, and phase transitions between them, are beyond the rare region classification in its present form.

In recent years, there has been strong interest in “exotic” phases and phase transitions that do not follow Landau’s order parameter paradigm (for a recent pedagogical overview, see, e.g., [295]). The influence of disorder on such transitions has not been studied in any detail, and it is likely very different from the behavior discussed here.

Finally, Griffiths singularities are normally associated with continuous phase transitions, and we have also considered this case. Concerning first-order phase transitions, it has been known for a long-time that quenched disorder generally weakens the first-order nature. Building on earlier work by Imry and Wortis [296], Aizenman and Wehr [297] proved, that in dimensions  $d \leq 2$ , a first-order transition turns into a continuous one upon introduction of arbitrarily weak (random-mass type) disorder. However, for  $d > 2$ , first order transitions can persist in the presence of quenched disorder. Not much is known about pretransitional phenomena at such first-order transitions (see, however, reference [298]). Exploring this in more detail would also be important from an experimental point of view, as some of the transition mentioned in the last section (e.g., in the manganites) appear to be of first order.

## Acknowledgements

This work would have been impossible without the contributions of many friends and colleagues. In particular, I would like to thank my collaborators on some of the topics discussed in this review: D. Belitz, M. Dickison, T.R. Kirkpatrick, M.Y. Lee, J. Schmalian, R. Sknepnek, and M. Vojta. I have also benefitted from discussions with A. Castro-Neto, P. Coleman, A. Chubukov, K. Damle, V. Dobrosavljevic, P. Goldbart, M. Greven, S. Haas, J.A. Hoyos, A. Millis, D. Morr, M. Norman, P. Phillips, H. Rieger,

A. Sandvik, Q. Si, G. Steward, J. Toner, U. Täuber, and P. Young. Finally, I'd like to thank F. Igloi, J.A. Hoyos, H. Rieger, J. Schmalian, and P. Young for the critical reading of the manuscript.

This work has been supported in part by the NSF under grant nos. DMR-0339147 and PHY99-07949, by Research Corporation and by the University of Missouri Research Board. Parts of this work have been performed at the Aspen Center for Physics and the Kavli Institute for Theoretical Physics, Santa Barbara.

## References

- [1] Ma S K 1976 *Modern theory of critical phenomena* (Reading: Benjamin)
- [2] Goldenfeld N 1992 *Lectures on phase transitions and the renormalization group* (Reading: Addison-Wesley)
- [3] Landau L D 1937 *Phys. Z. Sowjetunion* **11** 26
- [4] Landau L D 1937 *Zh. Eksp. Teor. Fiz.* **7** 19
- [5] Landau L D 1937 *Phys. Z. Sowjetunion* **11** 545
- [6] Landau L D 1937 *Zh. Eksp. Teor. Fiz.* **7** 627
- [7] van der Waals J D 1873 *On the continuity of the gas and liquid state* Ph.D. thesis University of Leiden
- [8] Weiss P 1907 *J. Phys. Radium (Paris)* **6** 667
- [9] Widom B 1965 *J. Chem. Phys.* **43** 3892
- [10] Wilson K G and Kogut J 1974 *Phys. Rep.* **12** 75
- [11] Sondhi S L, Girvin S M, Carini J P and Shahar D 1997 *Rev. Mod. Phys.* **69** 315
- [12] Sachdev S 1999 *Quantum phase transitions* (Cambridge: Cambridge University Press)
- [13] Vojta T 2000 *Ann. Phys. (Leipzig)* **9** 403
- [14] Belitz D, Kirkpatrick T R and Vojta T 2005 *Rev. Mod. Phys.* **77** 579
- [15] Dorfman J R, Kirkpatrick T R and Sengers J V 1994 *Ann. Rev. Phys. Chem.* **45** 213
- [16] Law B M and Nieuwoudt J C 1989 *Phys. Rev. A* **40** 3880
- [17] Nagel S 1992 *Rev. Mod. Phys.* **64** 321
- [18] Vojta T, Belitz D, Narayanan R and Kirkpatrick T R 1996 *Europhys. Lett.* **36** 191
- [19] Vojta T, Belitz D, Narayanan R and Kirkpatrick T R 1997 *Z. Phys. B* **103** 451
- [20] Belitz D, Kirkpatrick T R and Vojta T 1997 *Phys. Rev. B* **55** 9452
- [21] Fisher M E and Barber M N 1972 *Phys. Rev. Lett.* **28** 1516
- [22] Barber M N 1983 *Phase Transitions and Critical Phenomena*, volume 8, ed C Domb and J L Lebowitz (New York: Academic) p. 145
- [23] Cardy J (ed.) 1988 *Finite-size scaling* (Amsterdam: North Holland)
- [24] Grinstein G 1985 *Fundamental Problems in Statistical Mechanics VI*, ed E G D Cohen (New York: Elsevier) p. 147
- [25] Harris A B 1974 *J. Phys. C* **7** 1671
- [26] Motrunich O, Mau S C, Huse D A and Fisher D S 2000 *Phys. Rev. B* **61** 1160
- [27] Aharony A and Harris A B 1996 *Phys. Rev. Lett.* **77** 3700
- [28] Wiseman S and Domany E 1998 *Phys. Rev. Lett.* **81** 22
- [29] Holm C and Janke W 1993 *Phys. Rev. B* **48** 936
- [30] Ferrenberg A M and Landau D P 1991 *Phys. Rev. B* **44** 5081
- [31] Ballesteros H G, Fernandez L A, Martin-Mayor V and Sudupe A M 1998 *Phys. Rev. B* **58** 2740
- [32] McCoy B M and Wu T T 1968 *Phys. Rev. Lett.* **21** 549
- [33] McCoy B M and Wu T T 1968 *Phys. Rev.* **176** 631
- [34] Fisher D S 1992 *Phys. Rev. Lett.* **69** 534
- [35] Fisher D S 1995 *Phys. Rev. B* **51** 6411
- [36] Ma S K, Dasgupta C and Hu C K 1979 *Phys. Rev. Lett.* **43** 1434
- [37] Bhatt R N and Lee P A 1982 *Phys. Rev. Lett.* **48** 344
- [38] Fisher D S 1994 *Phys. Rev. B* **50** 3799
- [39] Young A P and Rieger H 1996 *Phys. Rev. B* **53** 8486
- [40] Pich C, Young A P, Rieger H and Kawashima N 1998 *Phys. Rev. Lett.* **81** 5916
- [41] Hooyberghs J, Igloi F and Vanderzande C 2003 *Phys. Rev. Lett.* **90** 100601
- [42] Hooyberghs J, Igloi F and Vanderzande C 2004 *Phys. Rev. E* **69** 066140
- [43] Vojta T and Dickison M 2005 *Phys. Rev. E* **72** 036126
- [44] Griffiths R B 1969 *Phys. Rev. Lett.* **23** 17
- [45] Randeria M, Sethna J and Palmer R G 1985 *Phys. Rev. Lett.* **54** 1321

- [46] Lifshitz I M 1964 *Usp. Fiz. Nauk* **83** 617 [Sov. Phys.–Usp. **7**, 549 (1965)]
- [47] Lifshitz I M 1964 *Adv. Phys.* **13** 483
- [48] Schwarz J M and Middleton A 2004 *Phys Rev. E* **70** 035103
- [49] Wortis M 1974 *Phys. Rev. B* **10** 4665
- [50] Harris A B 1975 *Phys. Rev. B* **12** 203
- [51] Bray A J and Huifang D 1989 *Phys. Rev. B* **40** 6980
- [52] Imry Y 1977 *Phys. Rev. B* **15** 4448
- [53] Dhar D 1983 *Stochastic Processes: Formalism and Applications*, ed D S Argawal and S Dattagupta (Berlin: Springer)
- [54] Dhar D, Randeria M and Sethna J P 1988 *Europhys. Lett.* **5** 485
- [55] Bray A J 1987 *Phys. Rev. Lett.* **59** 586
- [56] Bray A J 1988 *Phys. Rev. Lett.* **60** 720
- [57] Thill M and Huse D 1995 *Physica A* **214** 321
- [58] Guo M, Bhatt R and Huse D 1996 *Phys. Rev. B* **54** 3336
- [59] Rieger H and Young A P 1996 *Phys. Rev. B* **54** 3328
- [60] Vojta T 2003 *Phys. Rev. Lett.* **90** 107202
- [61] Millis A J, Morr D K and Schmalian J 2001 *Phys. Rev. Lett.* **87** 167202
- [62] Millis A J, Morr D K and Schmalian J 2002 *Phys. Rev. B* **66** 174433
- [63] Vojta T 2003 *J. Phys. A* **36** 10921
- [64] Sknepnek R and Vojta T 2004 *Phys. Rev. B* **69** 174410
- [65] Vojta T 2004 *Phys. Rev. E* **70** 026108
- [66] Dickison M and Vojta T 2005 *J. Phys. A* **38** 1199
- [67] Vojta T and Schmalian J 2005 *Phys. Rev. B* **72** 045438
- [68] Sandvik A 2002 *Phys. Rev. Lett.* **89** 177201
- [69] Vajk O P and Greven M 2002 *Phys. Rev. Lett.* **89** 177202
- [70] Sknepnek R, Vojta T and Vojta M 2004 *Phys. Rev. Lett.* **93** 097201
- [71] Juhasz R and Igloi F 2002 *Phys. Rev. E* **66** 056113
- [72] Obukhov S P 1986 *Pisma Z. Eksp. Teor. Fiz* **45** 139 [Sov. Phys.– JETP Letters **45**, 172 (1987)]
- [73] Dobrosavljevic V and Miranda E 2005 *Phys. Rev. Lett.* **94** 187203
- [74] Gefen Y, Mandelbrot B B and Aharony A 1980 *Phys. Rev. Lett.* **45** 855
- [75] Bergstresser T K 1977 *J. Phys. C* **10** 3381
- [76] Stephen M J and Grest G S 1977 *Phys. Rev. Lett.* **38** 567
- [77] Yang C N and Lee T D 1952 *Phys. Rev.* **87** 404
- [78] Lee T D and Yang C N 1952 *Phys. Rev.* **87** 410
- [79] Halperin B I and Lax M 1966 *Phys. Rev.* **148** 722
- [80] Lifshitz I M 1967 *Zh. Eksp. Teor. Fiz.* **53** 743 [Sov. Phys.–JETP, **26**, 462 (1968)]
- [81] Baaslygo L A and Dobrushin R L 1986 *Theory Prob. Appl.* **31** 572
- [82] v Dreyfus H, Klein A and Perez J F 1995 *Commun. Math. Phys.* **170** 21
- [83] Gielis G and Maes C 1995 *J. Stat. Phys.* **81** 829
- [84] Dotsenko V S 2006 *J. Stat. Phys.* **122** 197
- [85] Dotsenko V S 1999 *J. Phys. A* **32** 2949
- [86] Hohenberg P C and Halperin B I 1977 *Rev. Mod. Phys.* **49** 435
- [87] Glauber R J 1963 *J. Math. Phys.* **4** 294
- [88] Metropolis N, Rosenbluth A, Rosenbluth M and Teller A 1953 *J. Chem. Phys.* **21** 1087
- [89] Bray A J 1989 *J. Phys. A* **22** L81
- [90] Cesi F, Maes C and Martinelli F 1997 *Commun. Math. Phys.* **188** 135
- [91] Cesi F, Maes C and Martinelli F 1997 *Commun. Math. Phys.* **189** 323
- [92] Jain S 1988 *J. Phys. C* **21** L1045
- [93] Colborne S G W and Bray A J 1989 *J. Phys. A* **22** 2505
- [94] Andrichenko V B, Selke W and Talapov A L 1992 *J. Phys. A* **25** L283
- [95] Jain S 1995 *Physica A* **218** 279
- [96] Bray A J and Rodgers G J 1988 *Phys. Rev. B* **38** 9252
- [97] McCoy B M and Wu T T 1969 *Phys. Rev.* **188** 982
- [98] McCoy B M 1969 *Phys. Rev. Lett.* **23** 383
- [99] McCoy B M 1969 *Phys. Rev.* **188** 1014
- [100] McCoy B M 1970 *Phys. Rev. B* **2** 2795
- [101] Shankar R and Murthy G 1987 *Phys. Rev. B* **36** 536
- [102] Griffiths R B 1967 *J. Math. Phys.* **8** 478
- [103] Lubensky T C 1975 *Phys. Rev. B* **11** 353
- [104] Rudnick J 1978 *Phys. Rev. B* **18** 1408
- [105] Andelman D and Aharony A 1985 *Phys. Rev. B* **31** 4305



- [106] Dorovgotsev S N 1980 *Fiz. Tverd. Tela (Leningrad)* **22** 321 [*Sov. Phys.– Solid State* **22**, 188 (1980)]
- [107] Boyanovsky D and Cardy J L 1982 *Phys. Rev. B* **26** 154
- [108] Cesare L D 1994 *Phys. Rev. B* **49** 11742
- [109] Berche B, Berche P E, Igloi F and Palagyi G 1998 *J. Phys. A* **31** 5193
- [110] Wolff U 1989 *Phys. Rev. Lett.* **62** 361
- [111] Fendler B, Sknepnek R and Vojta T 2005 *J. Phys. A* **38** 2349
- [112] Bitko D, Rosenbaum T F and Aeppli G 1996 *Phys. Rev. Lett.* **77** 940
- [113] Suzuki M 1976 *Progr. Theor. Phys.* **56** 1454
- [114] Wu W *et al.* 1991 *Phys. Rev. Lett.* **67** 2076
- [115] Wu W, Bitko D, Rosenbaum T F and Aeppli G 1993 *Phys. Rev. Lett.* **71** 1919
- [116] Young A P 1997 *Phys. Rev. B* **56** 11691
- [117] Rieger H 1998 *Ann. Phys. (Leipzig)* **7** 564
- [118] Senthil T and Sachdev S 1996 *Phys. Rev. Lett.* **77** 5292
- [119] Igloi F and Rieger H 1998 *Phys. Rev. B* **57** 11404
- [120] Igloi F, Juhasz R and Rieger H 1999 *Phys. Rev. B* **59** 11308
- [121] Igloi F and Monthus C 2005 *Phys. Rep.* **412** 277
- [122] Dasgupta C and Ma S K 1980 *Phys. Rev. B* **22** 1305
- [123] Hyman R A, Yang K, Bhatt R and Girvin S 1996 *Phys. Rev. Lett.* **76** 839
- [124] Hyman R A and Yang K 1997 *Phys. Rev. Lett.* **78** 1783
- [125] Westerberg E, Furusaki A, Sigrist M and Lee P A 1997 *Phys. Rev. B* **55** 12578
- [126] Monthus C, Golinelli O and Jolicoeur T 1997 *Phys. Rev. Lett.* **79** 3254
- [127] Monthus C, Golinelli O and Jolicoeur T 1998 *Phys. Rev. B* **58** 805
- [128] Damle K 2002 *Phys. Rev. B* **66** 104425
- [129] Saguia A, Boechat B and Continentino M A 2002 *Phys. Rev. Lett.* **89** 117202
- [130] Refael G, Kehrein S and Fisher D S 2002 *Phys. Rev. B* **66** 060402
- [131] Saguia A, Boechat B and Continentino M A 2003 *Phys. Rev. B* **68** 020403
- [132] Yusuf E and Yang K 2003 *Phys. Rev. B* **68** 024425
- [133] Hoyos J A and Miranda E 2004 *Phys. Rev. B* **70** 180401
- [134] Yusuf E and Yang K 2002 *Phys. Rev. B* **65** 224428
- [135] Melin R *et al.* 2002 *Phys. Rev. B* **65** 104415
- [136] Yusuf E and Yang K 2003 *Phys. Rev. B* **67** 144409
- [137] Hoyos J A and Miranda E 2004 *Phys. Rev. B* **69** 214411
- [138] Fisher D S, Le Doussal P and Monthus C 1998 *Phys. Rev. Lett.* **80** 3539
- [139] Doussal P L, Monthus C and Fisher D S 1999 *Phys. Rev. E* **59** 4795
- [140] Monthus C 2003 *Phys. Rev. E* **67** 046109
- [141] Doussal P L and Monthus C 1999 *Phys. Rev. E* **60** 1212
- [142] Fisher D S, Le Doussal P and Monthus C 2001 *Phys. Rev. E* **64** 066107
- [143] Fisher D S and Young A P 1998 *Phys. Rev. B* **58** 9131
- [144] Igloi F, Juhasz R and Lajko P 2001 *Phys. Rev. Lett.* **86** 1343
- [145] Igloi F 2002 *Phys. Rev. B* **65** 064416
- [146] Rieger H and Igloi F 1999 *Phys. Rev. Lett.* **83** 3741
- [147] Stauffer D and Aharony A 1991 *Introduction to Percolation Theory* (Boca Raton: CRC Press)
- [148] Ikegami T, Miyashita S and Rieger H 1998 *J. Phys. Soc. Jpn.* **67** 2761
- [149] Lin Y C, Kawashima N, Igloi F and Rieger H 2000 *Progr. Theor. Phys. (Suppl.)* **138** 479
- [150] Karevski D *et al.* 2001 *Eur. Phys. J. B* **20** 267
- [151] Rieger H and Kawashima N 1999 *Eur. Phys. J. B* **9** 233
- [152] Senthil T and Majumdar S N 1996 *Phys. Rev. Lett.* **76** 3001
- [153] Cheong S W *et al.* 1991 *Phys. Rev. B* **44** 9739
- [154] Ting S T *et al.* 1992 *Phys. Rev. B* **46** 11772
- [155] Corti M *et al.* 1995 *Phys. Rev. B* **52** 4226
- [156] Vajk O P *et al.* 2002 *Science* **295** 1691
- [157] Manousakis E 1991 *Rev. Mod. Phys.* **63** 1
- [158] Behre J and Miyashita S 1992 *J. Phys. A* **25** 4745
- [159] Yasuda C and Oguchi A 1997 *J. Phys. Soc. Jpn.* **66** 2836
- [160] Yasuda C and Oguchi A 1999 *J. Phys. Soc. Jpn.* **68** 2773
- [161] Chen Y C and Castro Neto A H 2000 *Phys. Rev. B* **61** R3772
- [162] Kato K *et al.* 2000 *Phys. Rev. Lett.* **84** 4204
- [163] Sandvik A 2001 *Phys. Rev. Lett.* **86** 3209
- [164] Sandvik A 2002 *Phys. Rev. B* **66** 024418
- [165] Mermin N D and Wagner H 1966 *Phys. Rev. Lett.* **17** 1133

- [166] Hida K 1990 *J. Phys. Soc. Jpn.* **59** 2230
- [167] Millis A J and Monien H 1993 *Phys. Rev. Lett.* **70** 2810
- [168] Sandvik A and Scalapino D J 1994 *Phys. Rev. Lett.* **72** 2777
- [169] Shevchenko P V, Sandvik A and Sushkov O P 2000 *Phys. Rev. B* **61** 3475
- [170] Chakravarty S, Haplerin B I and Nelson D R 1989 *Phys. Rev. B* **39** 2344
- [171] Sachdev S and Vojta M 2001 *Proceedings of the XIII International Congress on Mathematical Physics*, ed A Fokas (Boston: International Press)
- [172] Vojta T and Schmalian J 2005 *Phys. Rev. Lett.* **95** 237206
- [173] Yu R, Roscilde T and Haas S 2005 *Phys. Rev. Lett.* **94** 197204
- [174] Lin Y C, Melin R, Rieger H and Igloi F 2003 *Phys. Rev. B* **68** 024424
- [175] Laflorencie N, Wessel S, Läuchli A and Rieger H 2006 *Phys. Rev. B* **73** 060403
- [176] Hertz J 1976 *Phys. Rev. B* **14** 1165
- [177] Millis A J 1993 *Phys. Rev. B* **48** 7183
- [178] Abanov A, Chubukov A V and Schmalian J 2003 *Adv. Phys.* **52** 119
- [179] Kirkpatrick T and Belitz D 1996 *Phys. Rev. Lett.* **76** 2571
- [180] Thouless D J 1969 *Phys. Rev.* **187** 732
- [181] Cardy J 1981 *J. Phys. A* **14** 1407
- [182] Schehr G and Rieger H 2005 *cond-mat/0511608*
- [183] Castro Neto A H, Castilla G and Jones B A 1998 *Phys. Rev. Lett.* **81** 3531
- [184] Joyce G S 1969 *J. Phys. C* **2** 1531
- [185] Dyson F J 1969 *Commun. Math. Phys.* **12** 91
- [186] Bruno P 2001 *Phys. Rev. Lett.* **87** 137203
- [187] Loh Y L, Tripathi V and Turlakov M 2005 *Phys. Rev. B* **71** 024429
- [188] Haldane F D M 1983 *Phys. Lett.* **93A** 464
- [189] Haldane F D M 1983 *Phys. Rev. Lett.* **50** 1153
- [190] Henelius P and Girvin S M 1998 *Phys. Rev. B* **57** 11457
- [191] Igloi F, Juhasz R and Rieger H 2000 *Phys. Rev. B* **61** 11552
- [192] Nishiyama Y 1998 *Physica A* **252** 35
- [193] Hida K 1999 *Phys. Rev. Lett.* **83** 3297
- [194] Todo S, Kato K and Takayama H 2000 *J. Phys. Soc. Japan.* **69** 355
- [195] Bergkvist S, Henelius P and Rosengren A 2002 *Phys. Rev. B* **66** 134407
- [196] Lajko P, Carlon E, Rieger H and Igloi F 2005 *Phys. Rev. B* **72** 094205
- [197] Carlon E, Lajko P, Rieger H and Igloi F 2004 *Phys. Rev. B* **69** 144416
- [198] Yu R, Roscilde T and Haas S 2006 *Phys. Rev. B* **73** 064406
- [199] Miranda E and Dobrosavljevic V 2001 *Phys. Rev. Lett.* **86** 264
- [200] Aguiar M C O, Miranda E and Dobrosavljevic V 2003 *Phys. Rev. B* **68** 125104
- [201] Tanaskovic D, Miranda E and Dobrosavljevic V 2004 *Phys. Rev. B* **70** 205108
- [202] Miranda E and Dobrosavljevic V 2005 *Rep. Progr. Phys.* **68** 2337
- [203] Larkin A I and Ovchinnikov Y N 1971 *Zh. Eksp. Teor. Fiz.* **61** 2147 [*Sov. Phys.-JETP.* **34**, 1144 (1972)]
- [204] Balatsky A V and Trugman S 1997 *Phys. Rev. Lett.* **79** 3767
- [205] Lamcraft A and Simons B D 2000 *Phys. Rev. Lett.* **85** 4783
- [206] Meyer J S and Simons B D 2001 *Phys. Rev. B* **64** 134516
- [207] Motrunich O, Damle K and Huse D A 2001 *Phys. Rev. B* **63** 224204
- [208] Vafeek O, Beasley M R and Kivelson S A 2005 *cond-mat/0505688*
- [209] Liu Y *et al.* 2001 *Science* **294** 2332
- [210] Mildenerger A *et al.* 2006 *Phys. Rev. B* **73** 121301
- [211] Schmittmann B and Zia R K P 1995 *Phase Transitions and Critical Phenomena*, volume 17, ed C Domb and J L Lebowitz (New York: Academic) p. 1
- [212] Marro J and Dickman R 1999 *Nonequilibrium Phase Transitions in Lattice Models* (Cambridge: Cambridge University Press)
- [213] Dickman R 1997 *Nonequilibrium Statistical Mechanics in One Dimension*, ed V Privman (Cambridge: Cambridge University Press)
- [214] Chopard B and Droz M 1998 *Cellular Automaton Modeling of Physical Systems* (Cambridge: Cambridge University Press)
- [215] Hinrichsen H 2000 *Adv. Phys.* **49** 815
- [216] Odor G 2004 *Rev. Mod. Phys.* **76** 663
- [217] Tauber U C, Howard M and Vollmayr-Lee B P 2005 *J. Phys. A* **38** R79
- [218] Grassberger P and de la Torre A 1979 *Ann. Phys. (NY)* **122** 373
- [219] Janssen H K 1981 *Z. Phys. B* **42** 151
- [220] Grassberger P 1982 *Z. Phys. B* **47** 365

- [221] Ziff R M, Gulari E and Barshad Y 1986 *Phys. Rev. Lett.* **56** 2553
- [222] Tang L H and Leschhorn H 1992 *Phys. Rev. A* **45** R8309
- [223] Pomeau Y 1986 *Physica D* **23** 3
- [224] Takayasu H and Tretyakov A 1992 *Phys. Rev. Lett.* **68** 3060
- [225] Zhong D and Avraham D B 1995 *Phys. Lett. A* **209** 333
- [226] Cardy J and Tauber U C 1996 *Phys. Rev. Lett.* **77** 4780
- [227] Grassberger P, Krause F and von der Twer T 1984 *J. Phys. A* **17** L105
- [228] Kim M H and Park H 1994 *Phys. Rev. Lett.* **73** 2579
- [229] Menyhard N 1994 *J. Phys. A* **27** 6139
- [230] Hinrichsen H 1997 *Phys. Rev. E* **55** 219
- [231] Harris T E 1974 *Ann. Probab.* **2** 969
- [232] Jensen I 1999 *J. Phys. A* **32** 5233
- [233] Janssen H K 1997 *Phys. Rev. E* **55** 6253
- [234] Noest A J 1986 *Phys. Rev. Lett.* **57** 90
- [235] Moreira A G and Dickman R 1996 *Phys. Rev. E* **54** R3090
- [236] Dickman R and Moreira A G 1998 *Phys. Rev. E* **57** 1263
- [237] Noest A J 1988 *Phys. Rev. B* **38** 2715
- [238] Bramson M, Durrett R and Schonmann R H 1991 *Ann. Probab.* **19** 960
- [239] Webman I, Avraham D B, Cohen A and Havlin S 1998 *Phil. Mag. B* **77** 1401
- [240] Cafiero R, Gabrielli A and Munoz A A 1998 *Phys. Rev. E* **57** 5060
- [241] Schonmann R S 1985 *J. Stat. Phys.* **41** 445
- [242] Alcaraz F C 1994 *Ann. Phys. (NY)* **230** 250
- [243] Vojta T and Lee M Y 2006 *Phys. Rev. Lett.* **96** 035701
- [244] Voigt C A and Ziff R M 1997 *Phys. Rev. E* **56** R6241
- [245] Odor G and Menyhard N 2006 *Phys. Rev. E* **73** 036130
- [246] Sinai Y G 1982 *Theor. Probab. Its Appl.* **27** 247
- [247] Igloi F and Turban L 1996 *Phys. Rev. Lett.* **77** 1206
- [248] Igloi F and Rieger H 1998 *Phys. Rev. E* **58** 4238
- [249] Calabrese P, Martin-Mayor V, Pelissetto A and Vicari E 2003 *Phys. Rev. E* **68** 036136
- [250] Harris A B and Lubensky T C 1974 *Phys. Rev. Lett.* **33** 1540
- [251] Grinstein G and Luther A 1976 *Phys. Rev. B* **13** 1329
- [252] Mayer I O 1989 *J. Phys. A* **22** 2815
- [253] Folk R, Holovatch Y and Yavorskii T 2000 *Phys. Rev. B* **61** 15114
- [254] Pelissetto A and Vicari E 2000 *Phys. Rev. B* **62** 5843
- [255] Varnashev K B 2000 *Phys. Rev. B* **61** 14660
- [256] Pakhmin D V and Sokolov A I 2000 *Phys. Rev. B* **61** 15130
- [257] Dotsenko V, Harris A B, Sherrington D and Stinchcombe R 1995 *J. Phys. A* **28** 3093
- [258] Dotsenko V and Feldman D E 1995 *J. Phys. A* **28** 5183
- [259] Prudnikov V V, Prudnikov P V and Fedorenko A A 2001 *Phys. Rev. B* **63** 184201
- [260] Fedorenko A A 2003 *J. Phys. A* **36** 1239
- [261] Blavatska V, von Ferber C and Holovatch Y 2003 *Phys. Rev. B* **67** 094404
- [262] Narayanan R, Vojta T, Belitz D and Kirkpatrick T R 1999 *Phys. Rev. Lett.* **82** 5132
- [263] Narayanan R, Vojta T, Belitz D and Kirkpatrick T R 1999 *Phys. Rev. B* **60** 10150
- [264] Lloyd R G and Mitchell P W 1989 *J. Phys. Condens. Matter.* **1** 5013
- [265] Binek C and Kleemann W 1994 *Phys. Rev. Lett.* **72** 1287
- [266] Binek C, de Azevedo M M P, Bertrand D and Kleemann W 1995 *J. Magn. Magn. Mater.* **140-144** 1555
- [267] Binek C, Bertrand D, Regnault L P and Kleemann W 1996 *Phys. Rev. B* **54** 9015
- [268] Binek C and Kleemann W 1995 *Phys. Rev. B* **51** 12888
- [269] Binek C, Kleemann W and Belanger D P 1998 *Phys. Rev. B* **57** 7791
- [270] Colla E V, Weissman M B, Chan W H and Chen H 2004 *Phys. Rev. B* **69** 180101
- [271] Salamon M B and Jaime M 2001 *Rev. Mod. Phys.* **73** 583
- [272] Dagotto E 2003 *Nanoscale phase separation and colossal magnetoresistance* (Berlin: Springer)
- [273] Salamon M B, Lin P and Chun S H 2002 *Phys. Rev. Lett.* **88** 197203
- [274] Salamon M B and Chun S H 2003 *Phys. Rev. B* **68** 014411
- [275] Burgy J *et al.* 2001 *Phys. Rev. Lett.* **87** 277202
- [276] Hartinger C, Mayr F, Loidl A and Kopp T 2005 *Phys. Rev. B* **71** 184421
- [277] Deisenhofer J *et al.* 2005 *Phys. Rev. Lett.* **95** 257202
- [278] Galitski V M, Kaminski A and Sarma S D 2004 *Phys. Rev. Lett.* **92** 177203
- [279] Li A P, Shen J, Thompson J R and Weitering H H 2005 *Appl. Phys. Lett.* **86** 152507
- [280] Seaman C L *et al.* 1991 *Phys. Rev. Lett.* **67** 2882

- [281] Stewart G 2001 *Rev. Mod. Phys.* **73** 797
- [282] Castro Neto A H and Jones B A 2000 *Phys. Rev. B* **62** 14975
- [283] Castro Neto A H and Jones B A 2005 *Europhys. Lett.* **71** 790
- [284] Castro Neto A H and Jones B A 2005 *Europhys. Lett.* **72** 1054
- [285] Millis A J, Morr D K and Schmalian J 2005 *Europhys. Lett.* **72** 1052
- [286] Johnston D C *et al.* 2005 *Phys. Rev. Lett.* **95** 176408
- [287] Theodorou G and Cohen M H 1976 *Phys. Rev. Lett.* **37** 1014
- [288] Tippie L C and Clark W G 1981 *Phys. Rev. B* **23** 5846
- [289] Endoh Y, Shirane G, Birgeneau R J and Ajiro Y 1979 *Phys. Rev. B* **19** 1476
- [290] Payen C *et al.* 2000 *Phys. Rev. B* **62** 2998
- [291] Fernandes J C *et al.* 2004 *Phys. Rev. B* **69** 054418
- [292] Masuda T *et al.* 2004 *Phys. Rev. Lett.* **93** 077206
- [293] Hinrichsen H 2000 *Braz. J. Phys.* **30** 69
- [294] Rupp P, Richter R and Rehberg I 2003 *Phys. Rev. E* **67** 036209
- [295] Alet F, Walczak A M and Fisher M P A 2005 [cond-mat/0511516](#)
- [296] Imry Y and Wortis M 1979 *Phys. Rev. B* **19** 3580
- [297] Aizenman M and Wehr J 1989 *Phys. Rev. Lett.* **62** 2503
- [298] Timonin P N 2004 *Phys. Rev. B* **69** 212103